Calcium Signaling during Polar Body Emission in the *Xenopus laevis* Oocyte

Julie Leblanc

Thesis submitted to the

Faculty of Graduate Studies

in partial fulfillment of the requirements

for the Doctorate of Philosophy degree in Biochemistry

Department of Biochemistry, Microbiology, and Immunology

Faculty of Medicine

University of Ottawa

ABSTRACT

Polar body emission (PBE), a form of asymmetric division, occurs twice during vertebrate oocyte maturation and is required to produce a haploid egg for sexual reproduction. Our lab elucidated parts of the mechanism that regulates PBE in *Xenopus laevis* oocytes. Cdc42 and RhoA, two GTPases, were shown to mediate membrane protrusion and the contractile ring, respectively. It is believed that cdc42 is mediating the protrusion by regulating actin polymerization. However, it is not clear what upstream signaling pathway regulates cdc42 activation during PBE. One possibility is calcium signaling, which occurs at fertilization, and is required for second PBE. Interestingly, the fertilization calcium transient also regulates cortical granule exocytosis/membrane retrieval, a process that also involves cdc42-mediated actin assembly. Furthermore, active cdc42 and RhoA are found in non-overlapping concentric zones in single-cell wound healing; their activation requires calcium signaling. To determine possible calcium transients during polar body emission, we employed the calcium-binding C2 domain of PKCβ in live cell imaging. Surprisingly, the most prominent C2 signal was seen after cdc42 activation and membrane protrusion. Co-localization experiments indicated that the C2 signal appeared at the cortical area marked by the contractile ring component anillin, and after partial constriction of the ring. Injection of the calcium chelator, dibromo-BAPTA, abolished the C2 signal, suggesting that it is indeed depicting a calcium transient. Dibromo-BAPTA injection also inhibited polar body abscission, as assessed by a novel abscission assay developed in our lab. We have for the first time detected a calcium signal during PBE that is essential to the last step of cytokinesis—abscission.

ACKNOWLEDGMENTS

First and foremost, I would like to thank Rui Zhen Li, the technician in our lab, for her work and guidance throughout my graduate studies. She has contributed to some of the work in this thesis, while I was away on maternity leave. Namely, she has provided Figure 13 and 14, and contributed to developing the abscission assay.

I am also most appreciative to my supervisor, Johné, for allowing me to complete my graduate studies in his lab; and for his continuing guidance and support.

A special thank you to Geoffrey Leblond, a former graduate student of the lab, who has always graciously lent a hand, and who has always been there to listen.

I am grateful for the colleagues I have had in the Liu lab, past and present: Terri van Gulik, Yong Tao, Dandan Liu, Hua Shao, Chun Qi Ma, Hadia Arabi Katbi – Thanks for your support and faith in me.

Thanks to my family and friends. Without them, I could not have made it this far.

Un gros merci à mon mari, Jon, et ma fille Évelynne, pour leur patience et leur amour.

TABLE OF CONTENTS

LIST OF ABBREVIATIONS

APC	anaphase promoting factor
Arp	actin related protein
ATP	adenosine triphosphate
CaMKII	calcium/calmodulin-dependent kinase II
cAMP	cyclic adenosine monophosphate
Cdc2	cell division control protein 2
Cdc20	cell division control protein 20
Cdc25	cell division control protein 25
Cdc42	cell division control protein 42
CS	chromosome separation
C3 toxin	clostridium botulinum toxin
CR	contractile ring
CSF	cytostatic factor
CG	cortical granule
CGE	cortical granule exocytosis
Cdk1	cyclin-dependent kinase 1
DAG	diacylglycerol
dbBAPTA	5,5'-dibromoBAPTA
K_D	dissociation constant
Emi2	early mitotic inhibitor 2
eGFP	enhanced green fluorescent protein
Ect2	epithelial cell transforming sequence 2
ER	endoplasmic reticulum
ESCRT	endosomal sorting complex required for transport
EMTB	ensconsin microtubule binding domain
ERK	extracellular signal regulated kinase
FE	fertilization envelope
F-actin	filamentous actin
FSH	follicle stimulation hormone
GFP	green fluorescent protein
Gβγ	G protein βγ subunit
GpCR	G protein coupled receptor
GTPase	guanine triphosphate phosphohydrolase
GEF	guanine nucleotide exchange factor
GV	germinal vesicle
GVBD	germinal vesicle break down
GTP	guanosine 5'-triphosphate
H2B	histone 2B
$Ins(1,4,5)P_3$	inositol triphosphate
$Ins(1,4,5)P_3R$	inositol triphosphate receptor
LH	luteinizing hormone
MPF	maturation promoting factor
MII	metaphase II
MTOC	microtubule organization centre
MAPK	mitogen activated protein kinase

MAPKKK	mitogen activated kinase kinase kinase
MEK1	mitogen activated kinase ERK1 kinase
MAPKK	mitogen activated kinase kinase
MCAK	Mitotic centromere-associated kinesin
Mos	moloney murine sarcoma
mRFP	monomeric red fluorescent protein
N-WASP	neuronal Wiskott-Aldrich syndrome protein
NEBD	nuclear envelope break down
OCM	oocyte culture medium
OR2	oocyte ringer 2
PM	plasma membrane
PtdIns(4,5)P_2	phosphatidylinositol 4,5 biphosphate
PS	phosphatidylserine
PLCζ	phospholipase C zeta
PBE	polar body emission
PB	polar body
Plx1	polo-like kinase 1
xPlkk1	xenopus polo-like kinase kinase 1
PMSG	pregnant mare serum gonadotropin
PKA	protein kinase A
PKC	protein kinase C
PP2A	protein phosphatase 2A
rGBD	rhotekin GTPase binding domain
SAC	spindle assembly checkpoint
SNARE	soluble NSF attachment protein receptor
Sgo	shugoshin
TMA	transient microtubule array
wGBD	N-WASP GTPase binding domain

LIST OF FIGURES AND TABLES

INTRODUCTION

Polar body emission (PBE) can be considered a specialized and unique event. It is a form of extreme asymmetrical cell division, which occurs twice during female meiosis, and is required to render the oocyte haploid in sexual reproduction. It also has implications in the fields of asymmetrical division, general cytokinesis, as well as embryogenesis. Asymmetrical division is a process through which a cell produces daughter cells with differing cell fates (Gonczy, 2008; Inaba and Yamashita, 2012). The asymmetry can stem from the differing size, or from the cytoplasmic distribution of factors within the daughter cells. Stem cells undergo asymmetrical division in order to maintain its stem cell population, as well as produce more differentiated cells. Asymmetrical division requires the common molecular pathways required in general cell division. Thus, the elucidation of the events involved in asymmetrical division can facilitate our understanding of both stem-cell renewal and general cell division. In the following introduction, the important events that occur, leading up to and during PBE will be reviewed. The description will predominantly centre on the *Xenopus laevis* oocyte model and will generally consist of the mechanisms regulating oocyte maturation during meiosis, as well as polar body emission. Important attention will be brought to the regulation of these mechanisms by calcium, in anticipation of the research conducted in this thesis.

1. Oocyte Maturation in the *Xenopus laevis* Oocyte

Fully-grown oocytes (stage VI, (Dumont, 1972)) have completed oogenesis and are arrested in the diplotene stage of prophase-I. Oocyte maturation, also known as meiosis resumption, must occur before fertilization. Once the frog attains sexual maturity (about 1 year, (Ferrell,

1999), the ovaries are able to respond to the hormonal signal required to resume meiosis. Gonadotropin-releasing factors stimulate the pituitary gland, through the action of the hypothalamus, to liberate the follicle stimulation hormone (FSH) and the luteinizing hormone (LH). This results in the follicle cells secreting maturation-specific hormones that induce oocyte maturation, as well as, ovulation.

In amphibians, this maturation specific hormone is believed to be progesterone (Baulieu, 1983). Specifically, through its classical receptor (Bayaa et al., 2000), progesterone mediates transcription-independent signaling. The prophase-1 arrest is maintained by elevated levels of cAMP (cyclic adenosine monophosphate), which are produced by the G protein βγ (Gβγ) - responsive adenylcyclase (Sheng et al., 2001). Progesterone antagonizes a G protein coupled receptor (GpCR) (Wang, 2003). This GpCR is responsible for releasing the Gβγ dimer by promoting GTP exchange on the α subunit (Sheng et al., 2001; Wang, 2003). Subsequently, preventing the release of the Gβγ dimer leads to cAMP reduction (Lutz et al., 2000; Sheng et al., 2001). Further, this prevents the activation of cAMP-regulated Protein Kinase A (PKA), a kinase, which plays a critical role in the first meiotic arrest (Eyers et al., 2005; Wang and Liu, 2004). Following these events, there is an accumulation of protein kinase activity just prior to GVBD. The two protein kinase cascades are: 1) the Mitogen-Activated Protein Kinase (MAPK) cascade (Ferrell and Machleder, 1998; Ohan et al., 1999), which consists of Mos (Moloney Murine Sarcoma, a MAPKKK), MEK1 (MAP Kinase ERK Kinase 1, a MAPKK), and ERK2 (Extracellular-regulated Kinase 2, a MAPK1); and 2) the cell cycle regulators, which consist of cdc2 (cell division control protein 2; also known as cyclin dependent kinase 1 (cdk1)) , cdc25 (cell division control protein 25), Plx1 (Polo-like Kinase

1) and xPlkk1 (Polo-like Kinase 1 Kinase). The activation of these two groups of kinases produces a positive feedback loop, with the ultimate result of promoting and maintaining the activation of the Maturation Promoting Factor (MPF). MPF is a heterodimeric protein complex, which is required for progesterone induced oocyte maturation. It is made up of the kinase cdc2, and cyclin B (Ferrell, 1999; J Pines, 1987; Lohka, 1988; Nebreda et al., 1995; Roy et al., 1991; Swenson et al., 1986).

These events lead up to the first of two meiotic divisions, termed polar body emission (PBE). Although seemingly innocuous, these highly asymmetrical cell divisions are of the utmost importance, since oogenic meiosis not only reduces the chromosomal complement to form a haploid egg, but also ensures that the egg retains the factors required for subsequent embryogenesis through minimal cytoplasmic loss. The asymmetry of polar body emission (PBE) can be truly appreciated in the *Xenopus laevis* oocyte. In this model, a 1.4mm in diameter oocyte extrudes a polar body of approximately 20μm in diameter during meiosis I and meiosis II. In fact, a *Xenopus laevis* oocyte is about one million times the size of a somatic cell, and is ideal for *in vitro* handling. Furthermore, the oocyte is characterized by a visually apparent polarity. The animal pole is the pigmented half of the oocyte that contains the germinal vesicle (nucleus), and the vegetal pole is the unpigmented half.

1.1 The Assembly of the Meiotic Spindle and the Initiation of Anaphase-I

Ultimately, the asymmetry of PBE is directed by the microtubule spindle, which becomes anchored to the oocyte cortex, unlike symmetrical cell division, where the spindle remains centrally located.

The precursor to the *Xenopus laevis* meiotic acentrosomal spindle is made of the disc shaped MTOC (Microtubule Organization Center) and the TMA (Transient Microtubule Array), which emanates from the MTOC into the nucleoplasm. This complex array forms just prior to or at GVBD and translocates to the animal pole, along with the condensed chromosomes (Gard, 1992). This occurs 30-40min following GVBD (Gard, 1992; Shao et al., 2012), and at this time, the microtubule spindle, the organizing apparatus of chromosomes, begins to assemble. The fully assembled meiotic spindle is a barrel-shaped bipolar array of microtubules, made predominantly of non-kinetochore microtubules (~95%), which include polar microtubules (aster-like), as well as barrel microtubules (interpolar) (Houghtaling et al., 2009; Yang et al., 2008). Only a small fraction of microtubules account for the kinetochore microtubules (Houghtaling et al., 2009; Ohi et al., 2007). A bipolar spindle axis is first formed by producing a short spindle, which first elongates parallel to the plasma membrane (Gard, 1992). Importantly, barrel microtubules control the bipolarity, as well as the length of the spindle (Houghtaling et al., 2009; Ohi et al., 2007). The kinase, Aurora B, regulates spindle assembly, and thus bipolarity by stabilizing barrel microtubules through the inhibition MCAK-led microtubule depolymerization (Shao et al., 2012). Before entering metaphase-I, the spindle rotates to become perpendicularly positioned via the cortex. At which point, the chromosomes begin to align themselves correctly at the center of the spindle, in order to enter metaphase-I.

The chromosome homologues are arranged into the metaphase I plate in such a way that each homologue is attached to a different spindle pole (bipolar attachment) (Fig. 1). The homologue pairs remain held together by the chiasma structures (a remnant of meiotic

recombination), since the sister chromatids, involved in the chiasma from each homologue, are tied together by cohesin. The sister chromatid arm/centromere cohesion is mediated by a meiotic-specific cohesin ring complex and its role is to enable bipolar spindle attachment of the chromosomes by allowing tension at the centromeres (Ishiguro and Watanabe, 2007).

In general, the cohesin ring, and more specifically, the meiotic-specific subunit Rec8 (Kudo et al., 2006; Parisi, 1999; Wassmann, 2013; Xu et al., 2005), is protected from separase-mediated cleavage by securin. Additionally, separase is inhibited by MPF-mediated phosphorylation prior to anaphase (Gorr et al., 2005; Hagting et al., 2002; Holland and Taylor, 2006; Wassmann, 2013; Zou et al., 1999). To promote anaphase, securin and cyclin B are targeted for degradation by a ubiquitin ligase, anaphase-promoting complex (APC) (Acquaviva and Pines, 2006; Wassmann, 2013). Cyclin B degradation leads to the inactivation of cdc2, which permits mitotic exit (Pines, 2006). The activation of the APC is generally regulated by the spindle assembly checkpoint (SAC), whereby chromosome segregation does not occur until the SAC has been satisfied (Lara-Gonzalez et al., 2012; Musacchio and Salmon, 2007; Wassmann, 2013). It is thought to monitor kinetochore-microtubule attachment (Rieder et al., 1995; 1994) via the mitotic checkpoint complex localized at the kinetochore. Upon activation of this checkpoint, the complex, which includes the activator of APC, cdc20, binds to and blocks the recruitment of substrates to the APC ((Chao et al., 2012)). Once all kinetochores are properly bound to microtubules, this complex is released, activating the APC (Musacchio and Salmon, 2007). The SAC is known to regulate the spindle assembly in the mammalian oocyte (Polanski, 2012), however, it has been recently shown that the SAC does not control

Figure 1: **Chromosome segregation events and timeline during polar body emission in the *Xenopus laevis* oocyte**. Model of chromosome segregation events during meiosis (top image). The side view of the plasma membrane is displayed. Chromosomes are coloured to distinguish between the paternal and maternal (red or blue) chromosome homologue pairs. The cohesin surrounding the chromosomes is in green and the centromeres are highlighted in yellow. For reasons of simplicity, the microtubule spindle is represented by only two microtubules (pink), attached to one homologue pair, each, with the spindle poles highlighted in grey. The middle timescale is a model, which demonstrates the morphological changes of the oocyte, in relation to the meiosis timescale. The bottom images represent an oocyte with its germinal vesicle still intact (left), and an oocyte, which has undergone germinal vesicle breakdown (right), as indicated by the white spot (white arrow). PM= plasma membrane, GV= germinal vesicle, GVBD= germinal vesicle break down, PB1= first polar body, PB2= second polar body, PN= pronucleus.

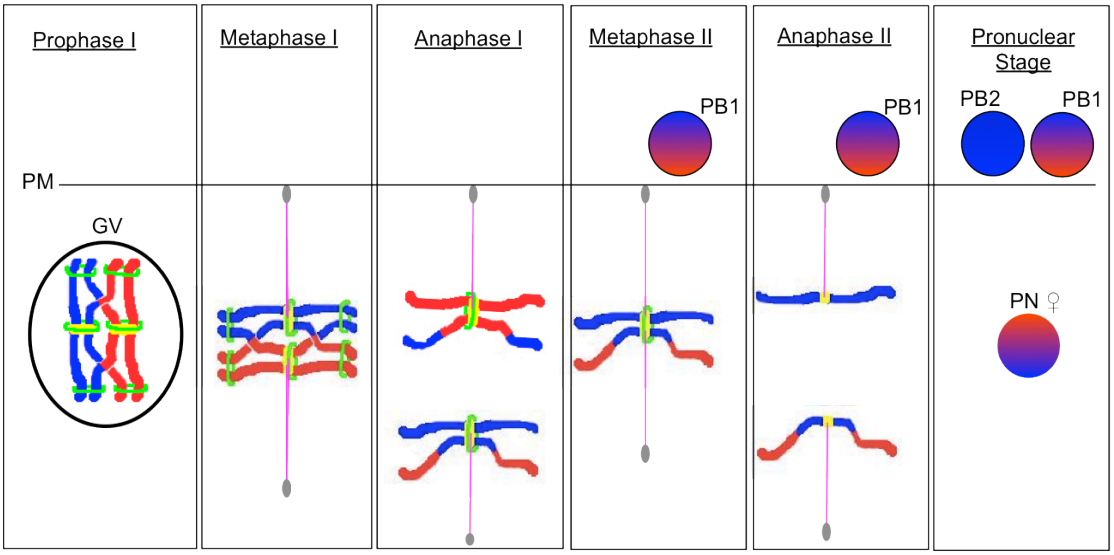
Prophase I
Metaphase I
Anaphase I
Metaphase II
Anaphase II
Pronuclear Stage
PB1
PB1
PB2
PB1
PM
GV
PN ♀

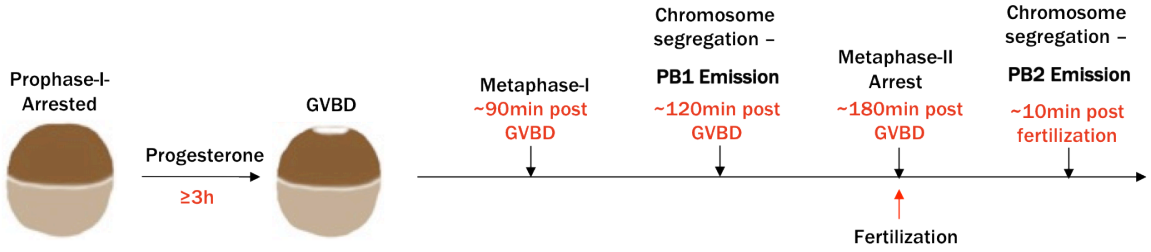
Prophase-I-Arrested
Progesterone
≥3h
GVBD
Metaphase-I ~90min post GVBD
Chromosome segregation – PB1 Emission ~120min post GVBD
Metaphase-II Arrest ~180min post GVBD
Chromosome segregation – PB2 Emission ~10min post fertilization
Fertilization

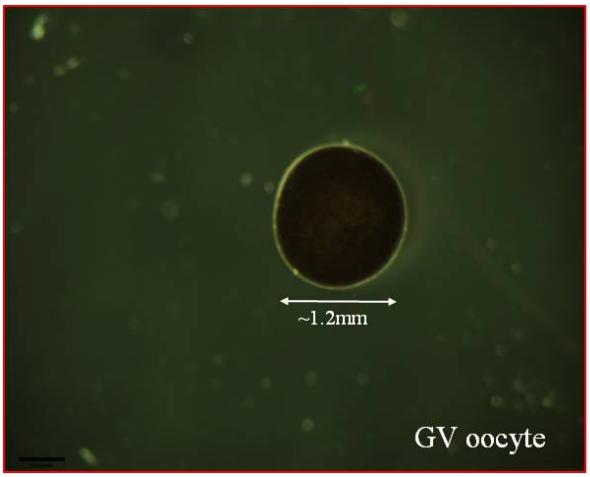
~1.2mm
GV oocyte

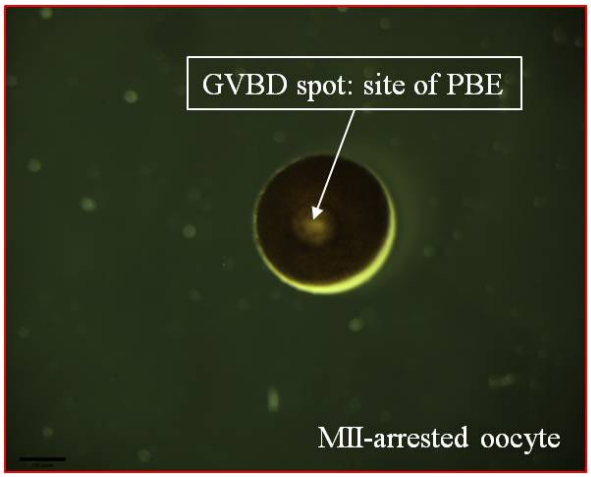
GVBD spot: site of PBE
MII-arrested oocyte

Xenopus laevis oocyte meiosis (Shao et al., 2013). In this study, they inhibited Aurora B, or the kinesin Eg5, to produce monopolar spindles. They elegantly demonstrate, by *Xenopus laevis* oocyte karyotyping, that the chromosomes still undergo the dyad to bivalent transition (Shao et al., 2013). A separase-mediated cohesin degradation pathway does control anaphase initiation in Xenopus oocytes, since inhibiting separase by a non-degradable securin mutant does not permit the resolution of bivalency (Fan et al., 2006; Shao et al., 2013; Zhang et al., 2008). While others suggest the opposite (Peter et al., 2001; Taieb et al., 2001), Shao, H. and colleagues' data indirectly suggests that the APC is required to activate chromosome segregation in *Xenopus laevis* (Shao et al., 2013).

There are also mechanisms in place to ensure that only arm cohesion is lost during anaphase I, thus promoting chromosome homologue separation, while preserving centromere cohesion. Rec8 requires phosphorylation by two kinases (in meiosis: Cdc7-dbf4 and casein kinase 1, in yeast), in order to be cleaved by separase (Ishiguro et al., 2010; Katis et al., 2010; Rumpf et al., 2010; Wassmann, 2013). In yeast, it has been shown, in order to circumvent this, Shugoshin (budding yeast/human/mouse Sgo2, *Xenopus laevis* Sgo1) recruits the phosphatase PP2A to the centromeres, thus maintaining only centromeric cohesion during meiosis I (Ishiguro et al., 2010; Katis et al., 2010; 2004; Kitajima et al., 2004; 2006; Marston et al., 2004; Rabitsch et al., 2004; Rumpf et al., 2010; Wassmann, 2013). Clearly, while not as expansive as in yeast, there is evidence for the requirement of Sgo2 and PP2A during meiosis I in the mouse oocyte (Lee et al., 2008b; Llano et al., 2008; Wassmann, 2013). Evidence for *Xenopus laevis* Shugoshin /PP2A centromeric cohesion exists in mitosis (Rivera and Losada, 2009; Rivera et al., 2012). Depletion of Sgo1 in Xenopus egg extracts leads to centromeric cohesion defects (Rivera and Losada, 2009).

Centromeric cohesion prevents the precocious separation of the sister chromatids, since arm cohesion is lost during mitotic prophase (Watanabe, 2005). Only parallels have been made for Xenopus meiosis, based on the fact that Sgo1 expression levels become elevated following GVBD (Orth et al., 2011).

During meiosis-I, once sister chromatid arm cohesion is lost, the kinetochore microtubules are responsible for the initial segregation of the chromosomes during anaphase A, when the chromosomes are pulled toward their respective poles. The barrel microtubules are arranged in such a manner that the microtubules from each pole overlap in the center of the spindle. The barrel microtubules, driven by microtubule motors, push the spindle poles apart during anaphase B. These microtubules also make up the scaffold structure called the central spindle.

1.2 Activation of cdc42 during Anaphase-I

Following chromosome separation during anaphase-I, cdc42, a GTPase, is activated in the cortical region overlaying the spindle. This region, termed the membrane protrusion or cortical cap, then encompasses the polar body chromosomes to form the polar body (Fig. 2) (Ma et al., 2006; Zhang et al., 2008). This study used an eGFP fusion protein containing the GTPase binding domain from N-WASP (Neuronal Wiskott-Aldrich syndrome protein), eGFP-wGBD, to specifically detect active (GTP-bound) cdc42 (Benink and Bement, 2005; Li et al., 2002; Ma et al., 2006; Zhang et al., 2008).

Figure 2: **Events during polar body emission in the *Xenopus laevis* oocyte.** A) During metaphase, the spindle is anchored perpendicularly to the plasma membrane. Following anaphase initiation, the membrane above the spindle begins to protrude, until it fully engulfs the polar body chromosomes. Simultaneously, the contractile ring at the polar body neck constricts, until the polar body is released from the oocyte. The side view of the plasma membrane is displayed. See Fig. 1 for figure legend. B) During anaphase, the polar body membrane protrusion and the contractile ring form simultaneously and are regulated by two different GTPases. Cdc42 activation (green), which drives the protrusion, is activated above the spindle, as active RhoA (red) drives the contractile ring constriction around the cdc42 zone (based on results in (Ma et al., 2006; Zhang et al., 2008)). Below, is the view of the plasma membrane of the nascent polar body from the side and from the top, demonstrating that RhoA encircles the cdc42 zone.

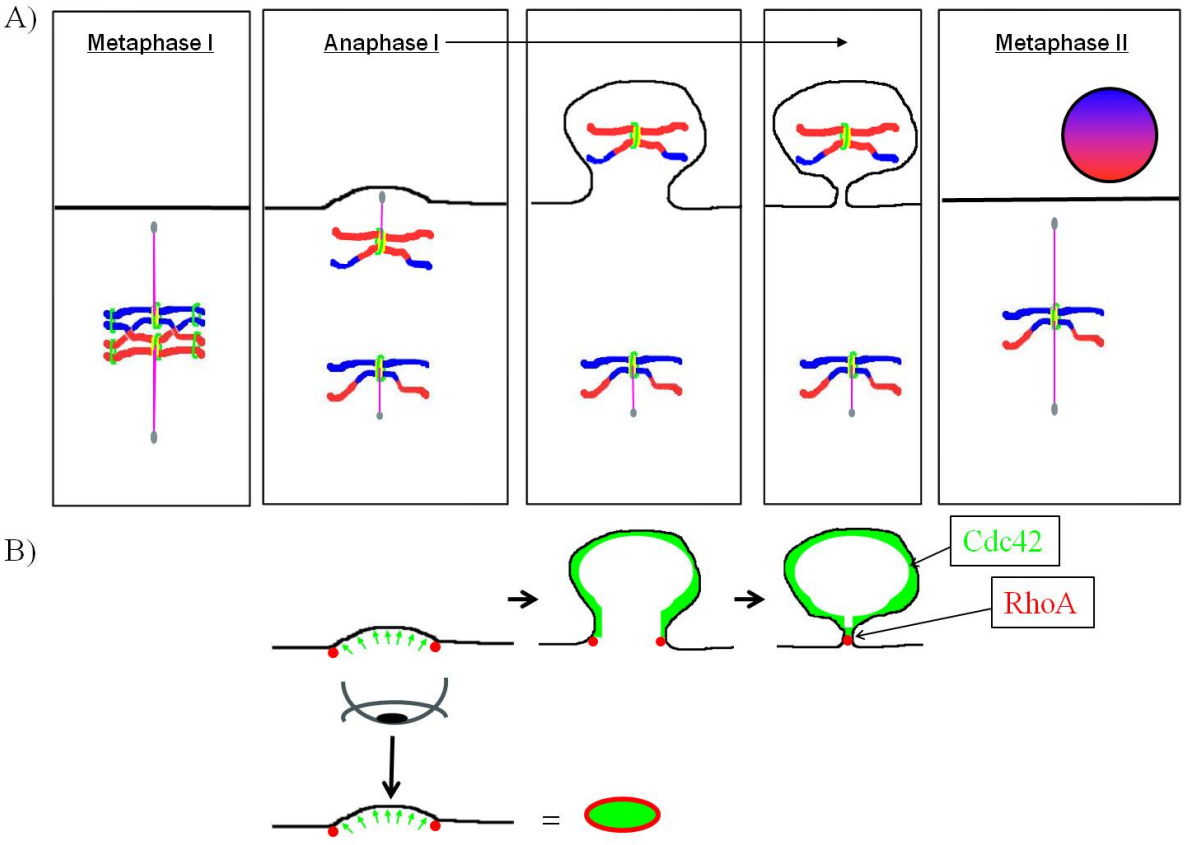
A)
Metaphase I
Anaphase I
Metaphase II
B)
Cdc42
RhoA
=

The cortex of the membrane protrusion becomes enriched with F-actin (filamentous actin), and it is thus described as an actin cap. This F-actin cap forms above the meiotic spindle in oocytes of several species, but there are temporal differences between them. In *Xenopus laevis* (Zhang et al., 2008) and *Spisula solidisima* (Pielak et al., 2004), F-actin accumulates at the cortex during anaphase, whereas, it appears at the mouse oocyte cortex as the spindle approaches it, prior to anaphase (Brunet and Verlhac, 2011). Furthermore, this kind of actin-mediated out pocketing during cell division is similar to what occurs during the budding yeast mitotic division (Adams et al., 1990), yet budding begins prior to the entry into M phase. Nevertheless, there are similarities between these examples. All except *Spisula* (although suggested) are shown to involve the action of a small GTPase from the Rho-subfamily. As in the case of *Xenopus*, cdc42 is the mediator of the actin cap in yeast (Adams et al., 1990; Johnson, 1999). Not surprisingly, cdc42 is well known for its role in regulating actin polymerization in various biological systems. It allows for actin polymerization by mediating the activation of actin nucleators, such as the Arp2/3 (Actin-related proteins 2/3) complex through the activation of N-WASP; and Formin, through direct interaction (Mattila and Lappalainen, 2008).

Inspired by the similarity between bud formation in yeast and polar body emission, our lab discovered that cdc42 is involved in the formation of the first polar body (Ma et al., 2006; Zhang et al., 2008). When cdc42 activation is abrogated by the dominant negative $cdc42^{T17N}$, anaphase is not prohibited. However, this event is futile since the membrane protrusion is not created and therefore the chromosomes destined for the PB are not extruded, and thus PBE fails. Moreover, down regulation of cdc42 leads to elimination of dynamic F-actin at the spindle pole-cortex site (Zhang et al., 2008).

Not surprisingly, the spindle itself is important for cdc42 activation during PBE. Treating oocytes with nocodazole (a microtubule-disrupting drug) leads to the disruption of the spindle (Leblanc et al., 2011). The severity of this disruption is dose-dependent. Consequently, cdc42 activity decreases with the decrease in spindle size. Cdc42 activation also depends on the spindle pole-cortex contact site. When the spindle is kept in a parallel orientation (to the PM), cdc42 is never activated and PBE is inhibited (Zhang et al., 2008). Furthermore, treatment of oocytes with taxol (a microtubule-stabilizing drug) disrupts the spindle, whereby, several spindle-like structures remain anchored to the cortex (Leblanc et al., 2011). Here, cdc42 is activated at the contact sites at the proper time, albeit at a lower level. Altogether, these results suggest that the spindle directs cdc42 activation at the cortex following anaphase initiation in *Xenopus laevis* oocytes. Cdc42, through the activation of actin polymerization, would push the membrane outward to allow for PBE (Zhang et al., 2008), which is reminiscent of its canonical role in filopodia formation (Mattila and Lappalainen, 2008).

Consistent with this model, Arp2, a protein that is part of the actin nucleator complex, Arp2/3, which is regulated by cdc42, localizes to the first PB protrusion in *Xenopus laevis* (Leblanc et al., 2011), as well as, in the mouse (Sun et al., 2011). In the case of PBE in the mouse oocyte, Halet and Carroll (Halet and Carroll, 2007) demonstrated that activated Rac, another small GTPase, localizes to the actin cap. In addition, they have recently demonstrated a role for cdc42 in promoting polar body emission (Dehapiot et al., 2013). Not surprisingly, Rac and cdc42 are very similar in structure and in function, being that they share common downstream targets, such as the Arp2/3 complex through the activation of N-

WASP (Heasman and Ridley, 2008). Nonetheless, Rac inhibition does not affect PBE in *Xenopus laevis* (Ma et al., 2006), but does in mouse oocytes (Halet and Carroll, 2007). Inhibition of Rac in mouse oocytes leads to the disruption of the spindle, and to circumvent this phenotype, they analyzed the inhibition of Rac in meiosis II, and showed that its inhibition prevents the formation of the membrane protrusion. Several other groups have inhibited cdc42 in mouse oocytes by various methods, and demonstrated, in addition to Dehapiot and colleagues' work (Dehapiot et al., 2013), the need for this GTPase in meiosis resumption (Cui et al., 2007), spindle organization (Cui et al., 2007; Na and Zernicka-Goetz, 2006) and actin localization (Bielak-Zmijewska et al., 2008; Cui et al., 2007). However, more recently, cdc42 was conditionally knocked-out in the mouse ovaries, rendering the animal infertile (Wang et al., 2013). Cdc42 was shown to be essential only to the formation of the actin cap-membrane protrusion. Very little effect was observed on the organization and migration of the spindle (Wang et al., 2013). Nevertheless, the important difference between *Xenopus laevis* and mouse cdc42-mediated PBE, is the mechanism by which cdc42 is activated. In *Xenopus laevis*, cdc42 is dependent on the perpendicular orientation of the spindle to the cortex for activation (Leblanc et al., 2011; Zhang et al., 2008), whereas, in the mouse, cdc42 activation relies on the close proximity of the chromosomes to the cortex due to the Ran-GTP gradient (Dehapiot et al., 2013) that is known to be generated by the meiotic chromosomes (Deng et al., 2007).

1.3 RhoA Activation during Anaphase-I

In addition to the abrogation of cdc42 activation, the expression of the dominant negative mutant of cdc42 ($cdc42^{T17N}$) hyperactivates RhoA, another GTPase. In this case, clusters of

RhoA activity form a ring that constricts futilely above the chromosomes, since no protrusion is formed above (Zhang et al., 2008). These clusters are reminiscent of the precursor nodes that form the contractile ring in fission yeast (Laporte et al., 2011; Pollard and Wu, 2010; Vavylonis et al., 2008).

The central spindle (Douglas and Mishima, 2010), the structure of bundled microtubules that form between the separating chromosomes, is where important molecules meet in order to establish the contractile ring (CR) (Miller, 2011), the contractile apparatus that allows the separation of one cell into two. Notably, in polar body emission, the CR is established asymmetrically, above the anchored spindle (Zhang et al., 2008), unlike in typical mitosis, where it is positioned at the equator of the cell. In other words, the division plane is specified by the orientation of the spindle (Rappaport and Rappaport, 1974). The CR is a structure predominantly composed of F-actin, as well as the motor protein myosin-II, that forms at the division plane. These components come together to provide the force required for the constriction of the ring. Myosin-II, using ATP as an energy source, can produce a contractile force by its movement across the actin filaments (Eggert et al., 2006).

RhoA is activated and forms the CR in *Xenopus laevis* oocytes (Bement et al., 2005; Ma et al., 2006; Zhang et al., 2008), as well as, forms a ring in mouse oocytes (Elbaz et al., 2013) during first PBE. In addition to RhoA, this structure consists of stable F-actin and phophorylated myosin (Zhang et al., 2008). Using a fluorescent probe to detect the active form of RhoA during anaphase I, our lab demonstrated that an active RhoA ring forms above the spindle in Xenopus (Fig. 2) (Zhang et al., 2008). The ring constricts as the eventual polar body chromosomes pass through it in order to protrude. Inhibition of RhoA by C3 toxin

(*Clostridium botulinum*) prevents spindle rotation when injected 60min following GVBD, when the spindle is typically assembling (~1hr before anaphase). However, this does not prevent chromosome segregation toward the two poles during anaphase initiation. When injected 90min following GVBD, following spindle rotation, this also permits chromosome separation. However, no polar body is formed, clearly indicating an essential role for RhoA in cytokinesis. The canonical RhoA GEF (Guanine Nucleotide Exchange Factor), Ect2, is also required for the proper regulation of RhoA during PBE in Xenopus (Zhang et al., 2008), as well as in the mouse (Elbaz et al., 2013). As in mitosis, Ect2 localizes to the central spindle during PBE. Specifically in *Xenopus laevis*, a dominant negative mutant of Ect2 (DN-Ect2) abrogates RhoA activity, thus preventing PBE, while permitting anaphase. In addition to the loss of RhoA at the CR, inhibition of Ect2 also diminishes cdc42 activity (Zhang et al., 2008). This is consistent with the finding that abrogating RhoA activity with the C3 toxin results in diminished cdc42 activity (Zhang et al., 2008). Both GTPases are therefore required to be co-regulated in order for successful PBE to occur. Specifically, where RhoA is responsible for the CR, cdc42 is required for the PB membrane protrusion during anaphase I. The co-dependence between cdc42 and RhoA demonstrates the mechanistic complexity of regulation of PBE.

In addition to the core CR components, there is a plethora of other enzymes as well as scaffolding proteins that are essential for CR structure and function. One of these, Anillin, is a scaffold protein that is key to organizing and recruiting these proteins to the CR. It binds to F-actin found in the CR, and binds to many other CR related components. Significantly, it is linked to RhoA's targets (mDia2, myosin) or effectors (Ect2, MgcRacGAP), as well as RhoA

itself (Piekny and Maddox, 2010). This is a clear demonstration of how the organization of the regulatory network is centered on the activation of RhoA.

2. The Last Step of Polar Body Emission: Abscission

Once the protrusion has formed and the CR fully constricted, one final step in cytokinesis must be completed: abscission. Our understanding of this process mostly relies on studies done in mitotic models. While the exact mechanisms regulating this crucial step are not well understood, it encompasses the disassembly of the CR, disassembly of the central spindle and the fusion/scission of membranes at the intracellular bridge. This bridge, also known as the midbody (or Fleming body or stem body), contains at its center an electron-dense structure that includes bundled microtubules of the central spindle (Flemming, 1891). The intracellular bridge is where the CR is anchored. Importantly, abscission follows the formation of secondary ingressions (Elia et al., 2011; Hu et al., 2012; Mullins and Biesele, 1977) that occur on each side of the midbody. Not surprisingly, the components that are essential to central spindle formation and function also reside at the midbody, and are equally important in this structure. They localize within specific areas of the midbody, as described by Hu, Chi-Kuo and colleagues (Hu et al., 2012). One of which, the bulge, is where RhoA and Anillin localize. More importantly, RhoA and Anillin also localize to the presumptive abscission sites (Hu et al., 2012). It is here that the abscission machinery is recruited. It includes the membrane trafficking mediators such as SNAREs (Soluble NSF attachment protein receptor), the Exocyst, and the ESCRTs (Endosomal sorting complex required for transport), as well as the microtubule severing protein, Spastin (Elia et al., 2011; Gromley et al., 2005; Guizetti et al., 2011; Lee et al., 2008a; Morita et al., 2007).

3. Fertilization and Second Polar Body Emission

During meiosis, once polar body emission is complete, the oocyte is arrested in metaphase-II (MII). Fertilization or parthenogenetic activation leads to an increase in intracellular calcium, which releases the arrest. In mammals, the increase is in the form of multiple oscillations (Miyazaki and Igusa, 1981; Swann and Ozil, 1994), whereas, in other species such as the frog, it is in the form of a single wave (Busa and Nuccitelli, 1985). A sperm factor, PLCζ (Phospholipase C zeta), was shown to mediate the calcium increase in mammals (Saunders et al., 2002) by generating inositol (1,4,5)-triphosphate ($Ins(1,4,5)P_3$) through the hydrolysis of phosphatidylinositol (4,5) biphosphate ($PtdIns(4,5)P_2$). Thus, calcium is released from the endoplasmic reticulum (ER) through the $Ins(1,4,5)P_3$ receptor ($Ins(1,4,5)P_3R$). While the sperm factor in *Xenopus laevis* is still elusive, evidence does suggest its existence (Dong et al., 2000). Nonetheless, the calcium wave in *Xenopus laevis* is indeed mediated by the $Ins(1,4,5)P_3$ pathway (Bugrim et al., 2003; El-Jouni et al., 2005; Fall et al., 2004; Nuccitelli et al., 1993; Wagner et al., 2004).

In morphological terms, the calcium increase results in cortical granule exocytosis (CGE) and CGE is known to be a part of the slow polyspermy block (Gilbert, 2000). Cortical granules are prominently distributed underneath the plasma membrane and are approximately 1.5μm in diameter in *Xenopus laevis* (Grey et al., 1974). The content of these granules is released into the perivitelline space at fertilization. Proteases expulsed by this process break down the links between the vitelline membrane (or *zona pellucida*) and the plasma membrane (Glabe and Vacquier, 1978; Vacquier et al., 1973). Mucopolysaccharides

increase water flow into the perivitelline space by creating an osmotic gradient, thus lifting the fertilization envelope (FE) (previously, vitelline) (Gilbert, 2000). Further, the FE is hardened by a peroxidase that mediates the crosslinking of tyrosines of adjacent proteins residing in the FE (Foerder and Shapiro, 1977; Mozingo and Chandler, 1991). Finally, hyalin forms a coat around the egg in order to support the blastomere during division (Hylander and Summers, 1982). The combination of these events assures the removal and prevention of additional sperm from binding to the oocyte. Naturally, these events occur in a relatively short time period, that of 1-2 minutes.

As stated previously, a calcium transient mediates CGE, which involves compensatory endocytosis, or removal of the excess membrane at the PM, as a result of CGE. Notably, cdc42-mediated actin polymerization drives the constriction of the nascent vesicle in *Xenopus laevis* eggs (Sokac et al., 2003; Yu and Bement, 2007). Precisely, it is here that the mixing of lipids from the plasma membrane with that of the cortical granule membranes leads to the anchoring of PKCβ at the site of exo/endocytosis. Diacylglycerol (DAG), a co-activator of PKCβ, is enriched at the plasma membrane following the fertilization-specific calcium elevation, before CGE. DAG, from the plasma membrane, mixes with the newly exocytosed membrane of CGs and thus targets PKCβ (via C1 domain) to these sites. Initially, PKCβ is most likely cytoplasmic, when its activators do not bind to it. In this condition, PKCβ adopts an autoinhibited conformation, which does not bind to membranes (Oancea and Meyer, 1998). PKCβ is recruited to all membranes (including plasma membrane and CG membranes) upon calcium elevation, via its C2 domain. Once its C2 domain binds to calcium, it acquires an affinity for the lipid phosphatidylserine (PS), thus translocating it to membranes. It is through DAG's interaction with PKCβ that this kinase is

able to remain at membranes. DAG becomes only enriched within the membranes of newly-exocytosed CG's and not within those that have not fused with the plasma membrane (Yu and Bement, 2007). Thus, PKCβ is only targeted to newly exocytosed CG's. These sites require compensatory endocytosis, which is mediated by PKCβ, through the activation of cdc42. Consequently, cdc42 drives actin polymerization required for endocytosis of the excess membrane. Importantly, this places calcium upstream of cdc42 during this process (Yu and Bement, 2007).

Moreover, cdc42 has also been shown to be dependent on calcium signaling during single-cell wound healing in *Xenopus laevis* eggs (Benink and Bement, 2005). In this study, a circular wound is created by focusing a laser on the oocyte plasma membrane. Using time-lapse imaging, the researchers demonstrate that concentric non-overlapping rings of active cdc42 and active RhoA are formed around the wound and promote actin polymerization at this site. RhoA localizes to the edge of the wound, whereas, cdc42 localizes outside the RhoA zone. This pattern is very much reminiscent of the localization of both these GTPases during PBE (Zhang et al., 2008). The cdc42 and RhoA rings constrict to seal the wound. Significantly, activation of cdc42 and RhoA is inhibited and thus wound healing does not occur when extracellular calcium is removed (Benink and Bement, 2005). Again, this places cdc42 downstream of calcium signaling.

Importantly, second PBE occurs several minutes following the fertilization-specific calcium increase. The high level of MPF activity, which is indicative and essential to the MII-arrest, is maintained by an activity called Cytostatic Factor (CSF) (Masui and Markert, 1971). Most of what is known about CSF was discovered in Xenopus eggs. CSF inhibits the APC (Peters,

2006), leading to the stabilization of cyclin B and thus MPF (Tunquist and Maller, 2003; Tunquist et al., 2003). This activity is promoted predominantly by the Mos-MAPK pathway (Kishimoto, 2003; Nebreda and Ferby, 2000; Sagata, 1996; Tunquist and Maller, 2003) and Emi2 (Early mitotic inhibitor 2) (or XErp1), a direct inhibitor of the APC (Schmidt et al., 2005; Shoji et al., 2006; Tung and Jackson, 2005; Tung et al., 2005). These signaling pathways interact to form an intricate network required for the MII-arrest (Hansen et al., 2006; Isoda et al., 2011). Calcium activates CaMKII (Calmodulin Kinase II) (Lorca et al., 1993; Madgwick et al., 2005) and along with Plx1 (Schmidt et al., 2005), they phosphorylate and target Emi2 for destruction, which allows for APC-directed anaphase onset.

The MII spindle, in the case of the frog, is placed perpendicular to the plasma membrane. In mammals, it is placed parallel, and moves perpendicularly during anaphase II. During anaphase II or just before, centromeric cohesin is lost, and two models explain the cause. Based on work done in mammals, one model stipulates that Sgo2 is displaced from the centromere during late MII, whereas the second proposes that a PP2A inhibitor localizes to the centromere and deprotects Rec8 from separase-mediated cleavage (Wassmann, 2013).

4. Calcium Signaling during Cell Division

Additionally, the metaphase to anaphase transition during mitosis has been shown to be regulated via a calcium mechanism. In Ptk1 cells, calcium increases within the spindle at the onset of anaphase. Calcium injections lead to anaphase initiation; chelation leads to a significant delay in chromosome segregation (Izant, 1983; Poenie et al., 1986). As well, changes in intracellular calcium in the spindle are coincident with the metaphase-anaphase

transition in PtK2 cells (Ratan and Shelanski, 1986). In the stamen hair cell of *Tradescantia*, an intracellular calcium increase occurs at the onset of anaphase (Hepler and Callaham, 1987). In the *Pelvetia fastigiata* egg, using BAPTA (1,2-bis(2-aminophenoxy)ethane-N,N,N',N'-tetraacetic acid) and its various derivatives, with different dissociation constants (K_D), Speksnijder, J. and colleagues demonstrate that tip growth, as well as, cell division is blocked when calcium is chelated (Speksnijder et al., 1989). Importantly, as in Xenopus oocyte maturation (Duesbery and Masui, 1996; Miller et al., 1993), dbBAPTA (5-5'-dibromoBAPTA, K_D= 1.5μM (Miller et al., 1993) was shown to be most efficient, suggesting that shuttle buffering is required to properly inhibit calcium transients (Speksnijder et al., 1989). Shuttle buffering stipulates that a chelator binds to calcium from within an area of high calcium, and shuttles it to an area of low calcium (and repeats), thus disrupting local high calcium signals. Furthermore, the chelator does this with greater efficiency when the K_D is approximately that of the concentration of the high calcium signal (Miller et al., 1993). Furthermore, Parry, H. et al. demonstrated that the ER encircles the nucleus and spindle during mitosis in the *Drosophila melanogaster* syncyntial embryo (Parry et al., 2005). Using ratiometric imaging, calcium signaling was probed for within the spindle area, and within the whole embryo. Importantly, they discovered that calcium increases within the spindle area during anaphase, while the levels in the embryo remain low. In addition, chelating Ins(1,4,5)P_3, led to anaphase inhibition (Parry et al., 2005).

Similarly, in the sea urchin embryo, a calcium transient has been detected during the metaphase-anaphase transition (Ciapa et al., 1994; Groigno and Whitaker, 1998; Poenie et al., 1985; Wilding et al., 1996). As well, inhibition of calcium signaling with heparin (Ins(1,4,5)P_3R antagonist) prevented chromosome segregation. Importantly, they showed

that this inhibition was reversible when Ins(1,4,5)P_3 or calcium was photoreleased. Chelating calcium using dbBAPTA or NP-EGTA (photo-releasable EGTA) resulted in the inhibition of chromosome segregation and cytokinetic defects (Groigno and Whitaker, 1998).

Calcium transients have also been detected at the cleavage furrow of Xenopus embryos. Calcium travels as a wave along the furrow at a velocity (3µm/s), slower than the fertilization-specific wave and occurs in the absence of extracellular calcium. Furthermore, heparin inhibits these waves and consequently leads to delays of the first cleavage, while subsequent cell divisions are inhibited or delayed (Muto et al., 1996). Miller, A.L. and colleagues, using a similar approach to Speksnijder and colleagues' (Speksnijder et al., 1989), were able to suppress and regress the first and second cleavage furrow when injecting the chelators at different times before and during furrowing. dbBAPTA was also the most efficient in doing so (Miller et al., 1993), suggesting that shuttle buffering is required to inhibit calcium transients in Xenopus, a conclusion also made by others (Snow and Nuccitelli, 1993). However, Noguchi, T. et al. argue that the calcium signals detected are not related to cytokinesis (Noguchi and Mabuchi, 2002). They detected two calcium waves during the first mitosis in the Xenopus egg and inhibited the two waves with EGTA or dbBAPTA, but this did not affect the first cleavage. However, only dbBAPTA prevented the second cleavage. The authors argue that this phenotype is not related to chelating calcium, but to the aberrant cortical contraction produced at the injection site. This is, however, not consistent with Muto, A. and colleagues' findings, where heparin inhibited cytokinesis (Muto et al., 1996).

Furthermore, in the mouse egg, global calcium transients have been detected just prior to or just after entry into the first mitosis (FitzHarris et al., 2005; Halet et al., 2003; Larman et al., 2004; Tombes et al., 1992) or have not been detected during the entry into the second mitosis (FitzHarris et al., 2005). Using BAPTA-AM to chelate intracellular calcium in the mouse egg, Tombes, R. et al demonstrate a partial inhibition of NEBD (Nuclear envelope breakdown), with a significant inhibition achieved by also removing extracellular calcium (Tombes et al., 1992). However, Fitzharris, G. et al. posit that calcium is sufficient but not necessary for NEBD (FitzHarris et al., 2005). NEBD can be accelerated upon photolysis of Ins(1,4,5)P_3. However, they disrupted intracellular calcium levels by different methods (3 chelators, including dbBAPTA; and depletion of Ins(1,4,5)P_3R) and this did not lead to disruption of NEBD. They suggest that BAPTA in its acid form does not affect NEBD (FitzHarris et al., 2005), while BAPTA in its acetyl ester (BAPTA-AM) form, used by others (Tombes et al., 1992), does affect NEBD by disrupting protein synthesis or by disrupting lumenal calcium levels (FitzHarris et al., 2005). In addition, they observe a calcium-independent increase during NEBD, which was due to the change in environment, by comparing the CaGr-dextran (calcium probe conjugated to dextran) signal to the rhodamine-dextran signal (calcium-independent fluorescent molecule) (FitzHarris et al., 2005). This calcium independent increase might explain why others have detected a calcium increase at this time (Halet et al., 2003; Larman et al., 2004; Tombes et al., 1992).

During second PBE in the mouse oocyte, calcium signaling maintains an important role (Miao et al., 2012). Miao, YL. et al. were able to prohibit calcium influx and efflux simultaneously, also known as “calcium insulation”, by treating the oocytes with gadolinium (Gd^{3+}). This also allows calcium oscillations to continue. In these oocytes, anaphase-II

occurs normally, however, they fail to undergo spindle rotation, and thus fail second PBE. Additionally, buffering intracellular calcium levels with BAPTA-AM, which only permitted the first transient, led to normal second PBE, as long as extracellular calcium was present (Miao et al., 2012). These results underline the importance of calcium influx for meiosis II. Furthermore, CaMKIIγ (Ca^{2+}/calmodulin-dependent protein kinase II gamma), when over-expressed in its constitutively active form, releases the metaphase-II arrest (Backs et al., 2010; Knott et al., 2006; Miao et al., 2012). Miao, YL. et al. demonstrate that calcium influx is upstream of this calcium-modulated kinase (Miao et al., 2012).

No direct evidence demonstrates the role for calcium during the late stages of PBE in *Xenopus laevis*. However, calcium is a requirement for proper spindle assembly in the frog oocyte (Sun and Machaca, 2004). In this study, thapsigargin was used to empty the intracellular calcium stores (ER); or the intracellular calcium levels were disrupted by lowering the levels of extracellular calcium, or intracellular calcium levels were buffered by BAPTA. None of these conditions did not prevent GVBD, however, spindle assembly was drastically hindered. The varieties of spindle defects were categorized according to their severity. The first group consisted of somewhat disorganized spindles, which were qualified as being prometaphase-like. The second group consisted of completely disorganized spindles, which did not have clear spindle structures, and the microtubules were either severely condensed or spread out. The third group consisted of double spindles. Not surprisingly, the majority of the oocytes from all three conditions did not emit the first polar body.

Since the disruption of calcium signaling during maturation led to these spindle assembly defects, PBE could not be analyzed. Importantly, the significance is that it is still unclear if calcium signaling also regulates PBE in the *Xenopus laevis* oocyte.

5. Hypothesis and Statement of Objectives

Hypothesis:

Polar body emission requires a spatially restricted calcium transient that is distinct from the global calcium wave induced by fertilization.

Statement of Objectives:

1- Establish an egg activation protocol applicable for live cell imaging.

2- Investigate the presence/absence of calcium signaling during first and second PBE.

3- Functionally investigate any putative calcium signal(s).

MATERIALS AND METHODS

Oocyte Collection

Sexually mature *Xenopus laevis* females were obtained from Nasco (Fort Atkinson, Wisconsin). The females were primed with 100 units of pregnant mare serum gonadotropin (PMSG) (Sigma, G4877), injected into the dorsal lymph node, three to ten days prior to sacrifice. The frog is sacrificed by decapitation following hypothermia (ice bath for thirty minutes), and the brain is pithed. Ovaries are dissected and oocytes are manually defolliculated using Dumont #5 forceps in OCM media. This removes the follicle cells surrounding the oocyte. The oocytes are kept at 18°C until required. When the media is changed daily and the dead cells are removed, oocytes can be kept for approximately one week.

Fluorescent Probes

The plasmid for eGFP-H2B was a gift from Dr. Aaron Straight (Stanford University). Plasmids for mRFP-H2B, eGFP-rGBD (rhotekin GTPase Binding Domain) (Bement et al., 2005; 2006; Benink and Bement, 2005; Li et al., 2002; Ma et al., 2006; Zhang et al., 2008), eGFP-wGBD (N-WASP GTPase Binding Domain) (Benink and Bement, 2005; Li et al., 2002; Ma et al., 2006; Sokac et al., 2003; Yu and Bement, 2007; Zhang et al., 2008), mRFP- and eGFP-C2 (PKCβ C2 domain) (Yu and Bement, 2007); 3XGFP-Anillin and EMTB-3XGFP were gifts from Dr. William Bement (University of Wisconsin, Madison). The dominant negative cdc42^{T17N} has been described previously (Ma et al., 2006; Zhang et al.,

2008). All probes are described in Table 1. All constructs were in the pcs2+ vector, used for *in vitro* transcription. All plasmids were linearized by restriction enzymes before *in vitro* transcription using Ambion SP6 mMESSAGE mMachine kit (Ambion, AM1340). The mRNA was quantified using the Qubit™ fluorometer (Invitrogen, Q32857).

Microinjections

Microinjections are conducted using glass needles (micropipettes, Drummond, cat. # 1-000-0300) formed by the micropipette puller (Sutter Instruments, Co., Model P-97). Injections are controlled using a pressurized microinjector (Medical Systems Corp., Greenvale, NY 11548, PLI-100). The needles are first calibrated by drawing-up water into the needle and adjusting the microinjector so that the needle expulses around 10nL per injection.

Time-lapse Confocal Fluorescence Imaging

Oocyte maturation is induced by incubating the oocytes in 1μM of progesterone (Sigma, P0130) in OCM. Oocytes were monitored every 10 minutes for the appearance of a "maturation spot" (Fig. 1, bottom), indicative of nuclear envelop breakdown (or GVBD). GVBD oocytes were transferred to fresh medium (OCM). Time-lapse confocal imaging commences 75-90 minutes following GVBD. Previously, it has been demonstrated that anaphase initiation commences approximately 120min following GVBD (Ma et al., 2006; Zhang et al., 2008) (Fig. 3a). Oocytes become arrested in metaphase II approximately 3 hours following GVBD. These metaphase II-arrested oocytes are prick-activated, and

Table 1: Description of the probes and mutant utilized to study polar body emission.

Probe/Mutant	Domain/Protein	Role
eGFP-/mRFP-H2B	Histone 2B	Detects Chromosomes
eGFP-rGBD	GTPase binding domain of rhotekin	Detects active RhoA
eGFP-/mRFP-wGBD	GTPase binding domain of N-WASP	Detects active cdc42
eGFP-/mRFP-C2	C2 domain of PKCbeta	Detects calcium
Anillin-3XGFP	Full length Anillin	Detects Anillin
EMTB-3XGFP	Ensconsin microtubule binding domain	Detects microtubules
$cdc42^{T17N}$	Mutant cdc42	Dominant negative of cdc42

immediately visualized. Anaphase II begins approximately 10-12min following pricking (Fig. 3b).

Imaging is acquired with a 60X oil objective (Nikon Plan Apo 60X, 1.40 oil) on a Nikon Diaphot 200 with a BioRad MRC 1024 laser scanning confocal imaging system, equipped with a krypton/argon laser (excitation: 488, 568 and 647nm). The emission filters include: 522/35nm (green) and 605/32nm (red). The typical laser intensity was 10-30%. Time-lapse imaging is taken at various time intervals and the z slices are typically 2-3um thick, with a typical scanning depth of 50um. Scanning is typically achieved in 512x512 (pixels x lines) and the pixel size is 0.3um (XY). Image series were 3D-rendered (sum projection) using Volocity software (Improvision, Ltd.). The imaging chamber is an open dish (MetTak Corporation), and at its center, is a shallow well (optical glass), where the oocyte is placed animal pole facing down. All imaging is done at room temperature (18-20ºC).

Parthenogenetic Activation

Oocytes become arrested in metaphase II approximately 3 hours following GVBD. These metaphase II-arrested oocytes are prick-activated, and immediately visualized. Activation is completed by prick-activation using a glass needle (micropipettes, Drummond, cat.# 1-000-0300) formed by the micropipette puller (Sutter Instruments, Co., Model P-97). Pricking is conducted in OR2 supplemented with calcium ([$CaCl_2$] =1mM). Typically, anaphase II begins approximately 10-12min following pricking. Less successfully, A23187 (Sigma, C7522) has been used to activate oocytes. This calcium ionophore was diluted to a final

concentration of 0.5ug/mL and oocytes were incubated in the solution for 1min, and then transferred to fresh buffer without ionophore.

Abscission Assay

Fluorescently labeled Dextran (Texas Red) (D-3328, Invitrogen) (20-30nL of 10mg/mL) is injected into the oocyte at approximately 1hr following chromosome separation, after abscission has typically occurred (Fig. 22). Open (abscission incomplete) and closed (abscission complete) states of the polar body are assessed by detection of dextran within the polar body.

Statistics and Reproducibility

In the case where statistics are not shown, experiments are repeated at least in triplicate, and oocytes from different frogs are included, in order to demonstrate reproducibility.
The Fisher's exact test was completed using the GraphPad online calculator (http://graphpad.com/quickcalcs/contingency1/).

Buffer List

OCM (Oocyte Culture Medium)

Volume ratio 3:2 of L-15 prepared medium to ddH_2O

5ml/L Gentamycin (Gibco, 10mg/mL, 15710-064)

L-15 Prepared Medium

L-15 (Leibovitz) (Invitrogen, containing L-glutamine, cat# L4386-1L)

1.07g Bovine Serum Albumin (BSA)

ddH_2O to 1L

Filter with Millipore Stericup Express^{TM} Plus 0.22um (SCGPU11RE)

Oocyte Ringer 2 (OR2)

Volume ratio 1:1:8 of Stock A: Stock B: ddH_2O

pH to 7.8

Autoclave

Stock A

48.221g NaCl

1.864g KCl

2.03g $MgCl_2$-H_2O

11.915g HEPES

1.52g NaOH

ddH_2O to 1L

Stock B

1.42g Na_2HPO_4

ddH_2O to 1L

Oocyte Ringer 2 Plus Calcium (OR2++)

100mL OR2

200uL $CaCl_2$ 0.1M

1mL Gentamycin (Gibco, 10mg/mL, 15710-064)

RESULTS

The general methods to study polar body emission, which include mRNA microinjection, progesterone stimulation and GVBD assessment, apply to all the following experiments, and are detailed in the Material and Methods section of this thesis. Typically, GV oocytes are injected with the probes, and then stimulated with progesterone to undergo maturation (GVBD). GVBD oocytes are then individually selected for time-lapse imaging experiments, based on the time they have undergone GVBD (Fig. 3). Expression of the probes does not affect oocyte maturation, and the oocytes normally enter metaphase-II (Fig. 4). The general presentation of a figure typically includes the top view (looking down onto the plasma membrane) and the side view of the chromosomes. The figures also include either 2D images taken from the 3D format, or axial images (sectional or slices). Not all time-points are included for reasons of simplicity.

1. Second Polar Body Emission: Parthenogenetic Activation

To study second polar body emission, I needed to choose a method to release the metaphase-II arrest in order to study second PBE. In nature, this is done by fertilization, but there exists a mimic of this process, parthenogenetic activation. Methods of parthenogenetic activation include the use of chemicals (Loeb, 1899), physical means (Bataillon, 1910) or by other experimental means (Pincus, 1939; Tarkowski et al., 1970; Thibault, 1949).

I first tried using A23187 (calcium ionophore) to activate the MII-arrested oocytes (Fig. 5 (Leblanc et al., 2011)). First, oocytes were injected with the probe, and then were stimulated

Figure 3: **General methods for time-lapse confocal imaging of polar body emission in the *Xenopus laevis* oocyte.** mRNAs encoding fluorescent protein probes or mutants are produced by *in vitro* transcription. mRNA-injected oocytes are incubated for a minimum of 6 hrs in order for them to express the probes before stimulation with progesterone. It takes at least 3hrs for the oocytes to undergo GVBD after progesterone stimulation. At this time, they are individually transferred into separate wells for further incubation. A) First polar body emission: The oocyte is placed animal pole facing down, into a well placed at the centre of the dish, with the GVBD spot facing the objective of an inverted microscope. Time-lapse imaging typically begins between 1h45-2h00 following GVBD, just prior to anaphase initiation. B) Second polar body emission: Prick-activation, by piercing metaphase II-arrested oocytes with a sharp glass needle, takes place a minimum of 3hrs following GVBD. The pricked oocyte is immediately placed with the GVBD spot facing the inverted microscope objective. Time-lapse imaging typically begins right away, about 10min before anaphase initiation.

A)

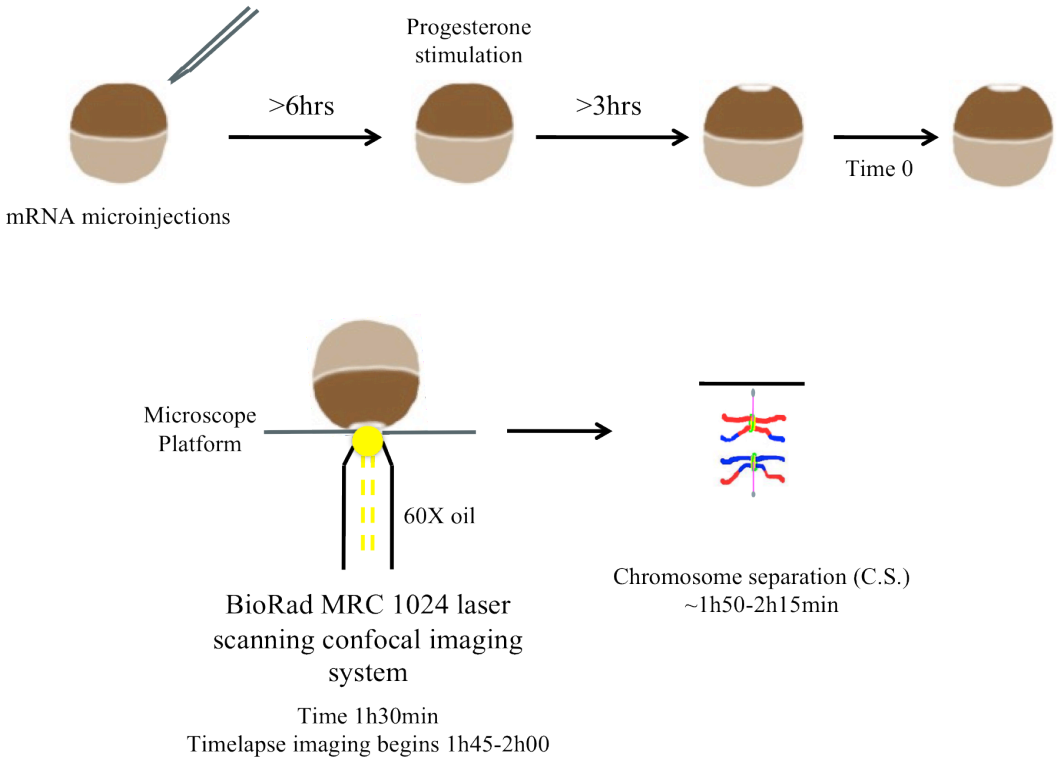
Progesterone
stimulation
>6hrs
>3hrs
Time 0
mRNA microinjections
Microscope
Platform
60X oil
Chromosome separation (C.S.)
~1h50-2h15min
BioRad MRC 1024 laser
scanning confocal imaging
system
Time 1h30min
Timelapse imaging begins 1h45-2h00

B)

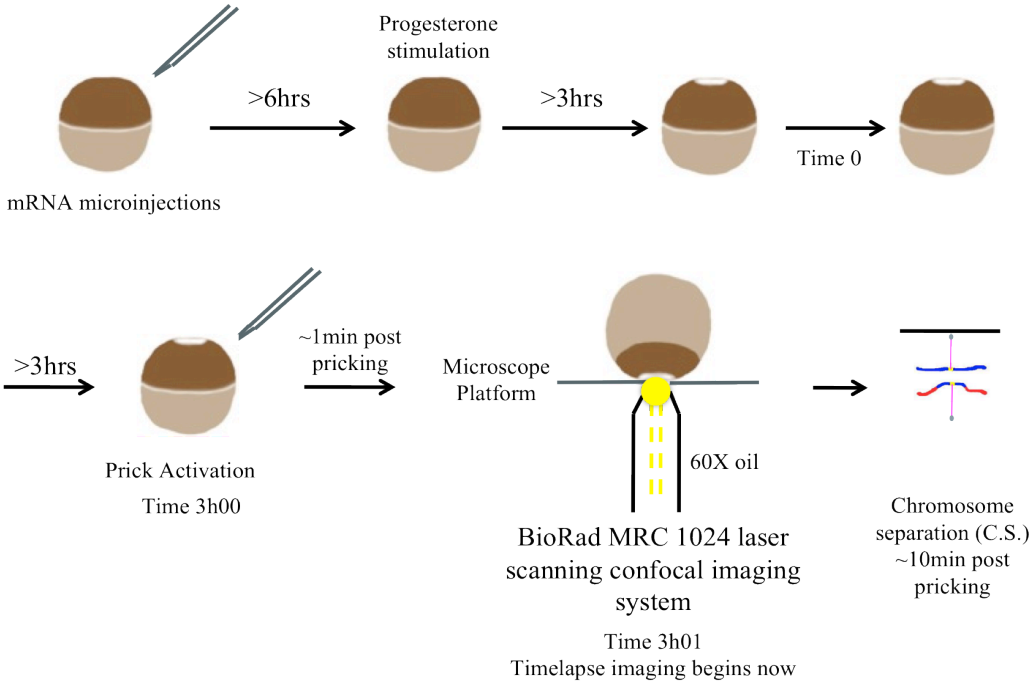
Progesterone
stimulation
>6hrs
>3hrs
Time 0
mRNA microinjections
>3hrs
~1min post
pricking
Microscope
Platform
60X oil
Prick Activation
Time 3h00
BioRad MRC 1024 laser
scanning confocal imaging
system
Time 3h01
Timelapse imaging begins now
Chromosome
separation (C.S.)
~10min post
pricking

Figure 4: **Effect of the C2 probe on *Xenopus laevis* meiosis.** No observable effects were detected in oocytes injected with eGFP-C2. Represented in the image is a metaphase-II arrested oocyte that had been injected (at GV-stage) with eGFP-C2 and mRFP-H2B. Notice the first PB (1PB) and the metaphase-II array of chromosomes. Side view of the chromosomes shown.

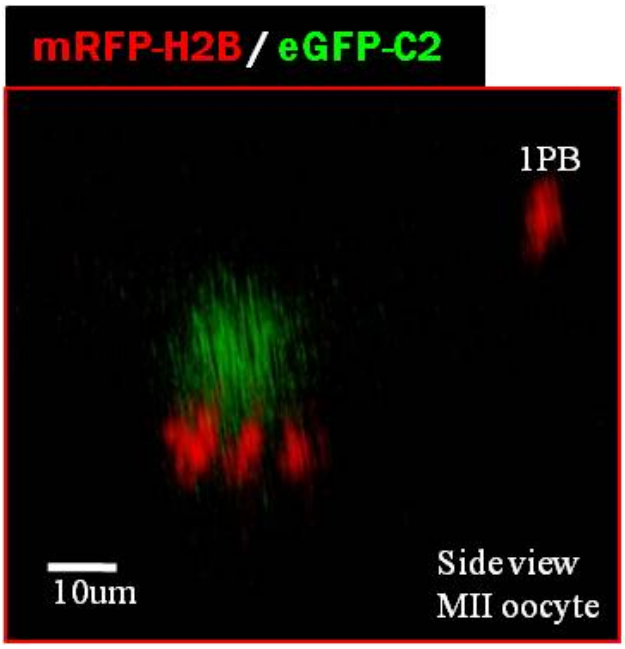
mRFP-H2B / eGFP-C2
1PB
10um
Side view
MII oocyte

Figure 5: **Parthenogenetic activation by calcium ionophore**: GV oocytes were injected with mRNA for eGFP-H2B (chromosomes). Injected oocytes were incubated overnight in OCM with 1 mM progesterone to mature to metaphase II. Metaphase II-arrested oocytes (note that in this oocyte, only metaphase II chromosomes were shown, with the first polar body either lost or not in the same view field) were incubated with the calcium ionophore A23187 (0.5 mg/ml) for 1 min, then were washed and moved to the ionophore-free buffer for confocal time-lapse imaging. This resulted in successful chromosome separation (1:00, arrows) and partial polar body protrusion (7:00, and 9:00), but the polar body eventually retracted (12:00). Time 0:00 represents 12 min after treatment. Chromosomes' localization is probed with eGFP-H2B. Dashed lines denote plasma membrane. Figure taken from ((Leblanc et al., 2011)).

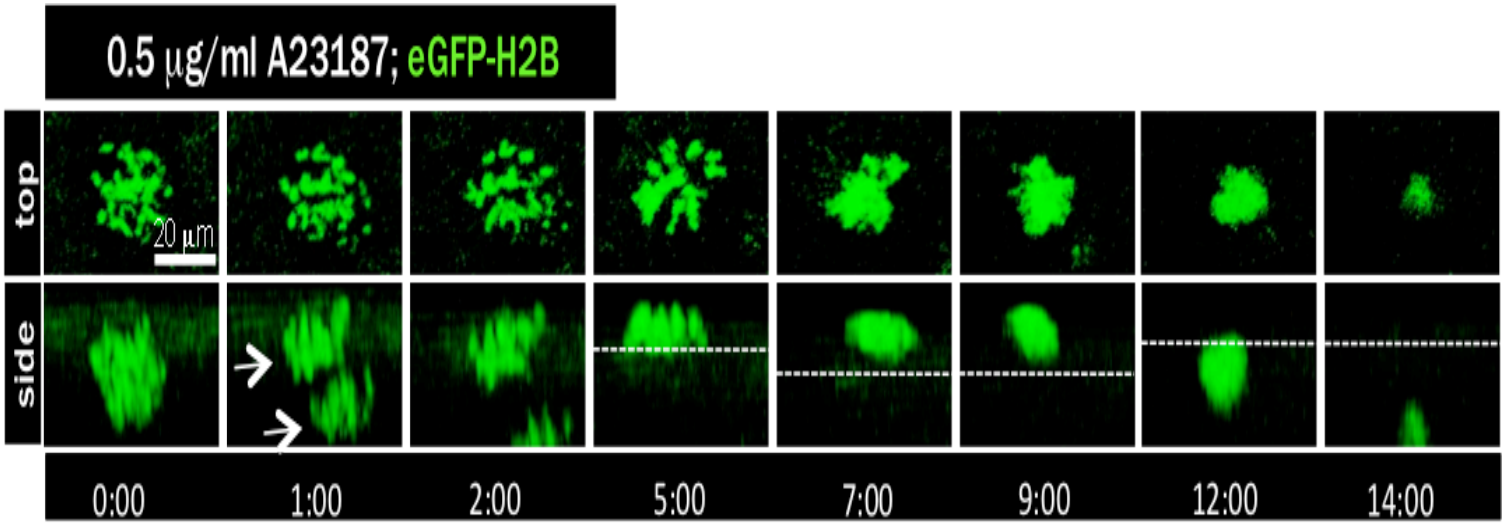
0.5 μg/ml A23187; eGFP-H2B
top
side
20 μm
0:00
1:00
2:00
5:00
7:00
9:00
12:00
14:00

with progesterone overnight. The resulting MII-arrested oocytes were subsequently incubated with A23187 and then transferred to A23187-free buffer. Confocal time-lapse imaging began almost immediately. Within the first time point (Fig. 5, side view), one can discern the approximate localization of the plasma membrane, due to the slight background (above the chromosomes). After incubation with A23187, chromosome segregation occurs normally (Fig. 5, 1:00, 13min following treatment). However, the chromosomes destined for the polar body, which had begun to extrude at the plasma membrane of the oocyte (as evident by the background fluorescence associated with the oocyte's surface) (Fig. 5, 5:00-9:00), sink back within the oocyte (Fig. 5, 12:00), indicating failure of cytokinesis (7/9 oocytes) (Leblanc et al., 2011).

Since this method was not efficient in producing successful second PBE, I then conducted pricking experiments, where a fine needle (10µm diameter tip) pierces the MII-arrested oocyte to induce activation (Bataillon, 1910). First, oocytes were injected with the probe, and then were stimulated with progesterone overnight. The resulting MII-arrested oocytes were subsequently prick-activated, and confocal time-lapse imaging began almost immediately. Indeed, pricking efficiently produced successful second PBE (Fig. 6, (Leblanc et al., 2011)). Chromosome segregation occurs normally (Fig. 6, 2:00) following prick-activation (11min following activation in this oocyte). The chromosomes destined for the polar body, begin to extrude at the plasma membrane, coincidentally reaching the height of the first polar body (Fig. 6, 9:00-17:00), and remaining outside of the plasma membrane, like the first polar body, thus, the second polar body is successfully emitted (Fig. 6, 17:00) (>50 oocytes) (Leblanc et al., 2011).

Figure 6: **Parthenogenetic activation by fine glass needle**: GV oocytes were injected with mRNA for eGFP-H2B (chromosomes). Injected oocytes were incubated overnight in OCM with 1 mM progesterone to mature to metaphase II. A metaphase-II arrested oocyte was prick-activated with a fine glass needle, then subjected to confocal time-lapse imaging. This resulted in chromosome separation (2:00, arrows) and successful second polar body (PB) emission. Time 0:00 represents 9 min after pricking. Dashed lines denote plasma membrane. Figure taken from ((Leblanc et al., 2011)).

Prick-Activated; eGFP-H2B
top
side
0:00
1:00
2:00
4:00
6:00
9:00
11:00
17:00
20μm
1st PB
2nd PB

2. Second Polar Body Emission: cdc42 is required for Second Polar Body Protrusion

After establishing the means to induce second PBE, I wanted to determine if cdc42, similarly to first PBE (Ma et al., 2006; Zhang et al., 2008), was required during second PBE. The first step was to use confocal time-lapse imaging to follow active cdc42 after prick-activation of MII-arrested oocytes. Oocytes were injected with the probes and then stimulated with progesterone overnight to reach metaphase II (Table 2, 32/43). Metaphase II oocytes were pricked followed by confocal time-lapse imaging. In Figure 7 (Leblanc et al., 2011), near the time when chromosomes segregate, active cdc42 appears directly above the segregating chromosomes (Fig. 7, 00:04), consistent with being at the spindle pole-cortex contact site. The signal becomes stronger during chromosome separation (Fig.6, 00:04-00:06); eventually enveloping the nascent polar body chromosomes (Fig.6, 00:10-00:21). Active cdc42's localization is distinctly cortical, and not cytoplasmic, as observed in the axial views of Figure 7B. Active cdc42 can be seen outlining the second polar body protrusion (Fig. 7, xz). The "hallowing" of the cdc42 signal, as seen from the top view of the polar bodies (Fig.6, xy), is consistent with this observation.

Complementary to this, the function of cdc42 during second PBE was investigated using the dominant negative mutant cdc42^{T17N}. This dominant negative inhibits endogenous cdc42 by sequestering proteins that are required for its activation (ex. Guanine nucleotide exchange factors), since the dominant negative is stabilized in its inactive form (GDP-bound) (reviewed in (Johnson, 1999)). mRNA encoding cdc42^{T17N} was injected into GV oocytes, together with mRNAs encoding fluorescent probes. Oocytes were then stimulated with progesterone overnight. While the majority of control oocytes exhibited a first polar body

and a metaphase II spindle (Fig. 7, Table 2, 32/43 oocytes), the majority of cdc42N17-injected oocytes (Fig. 8, Table 2, 36/38) had no first polar body, but had a single metaphase spindle with clearly more chromosomes, having failed to emit the first polar body (Leblanc et al., 2011).

These cdc42^{T17N} –injected "metaphase II" eggs were pricked-activated. Thirteen minutes following prick activation, chromosome separation occurs in the cdc42^{T17N} –injected oocytes (Fig. 8, 00:03). Very little active cdc42 appeared (Fig. 8, 00:06) and no membrane protrusion was seen. The polar body chromosomes remained at the cortex, but eventually disappear within the oocyte (Fig. 8, 00:24), as the egg chromosomes had done earlier. This can be better appreciated in Figure 8B. In the xz axial view, the chromosomes are observed to remain at the cortex (green background above the chromosomes), whilst barely any active cdc42 appears to accumulate above. The lack of a protrusion can also be appreciated. In this later group, the chromosomes sit under the plasma membrane without protruding (Fig. 8, cdc42^{T17N} xz axis). In the cdc42^{T17N} group, only 1/17 oocytes (~6%) is able to emit the second polar body, whereas, in the control group, 10/21 oocytes (~48%) are able to emit the second polar body (Table 3). The 11 control oocytes that did not emit the second polar body were not successfully parthenogenetically activated. Altogether, these results demonstrate that cdc42 is activated during second PBE and is functionally required to produce the polar body membrane protrusion. Thus, both first and second PBE share this mechanism.

3. Second Polar Body Emission: RhoA Activation

Figure 7: **Cdc42 activation during second polar body emission.** GV oocytes were injected with mRNAs for mRFP-H2B (chromosomes) and eGFP-wGBD (cdc42-GTP). Injected oocytes were incubated overnight in OCM with 1 mM progesterone to mature to metaphase II, and then prick-activated. A) Represented is a time series of a typical control metaphase II oocyte following prick activation, depicting cdc42 activation during second polar body emission. Note: chromosome separation at anaphase II (00:08, arrows) and the emission of the second polar body. The haploid egg chromosomes typically moved quickly inside the egg and become invisible (00:21). B) Sectional view of top (XY) and side (XZ or YZ) views of the control oocyte (00:12) depicts active cdc42 at the cortex of the protruding second polar body (arrows). Figure taken from ((Leblanc et al., 2011)).

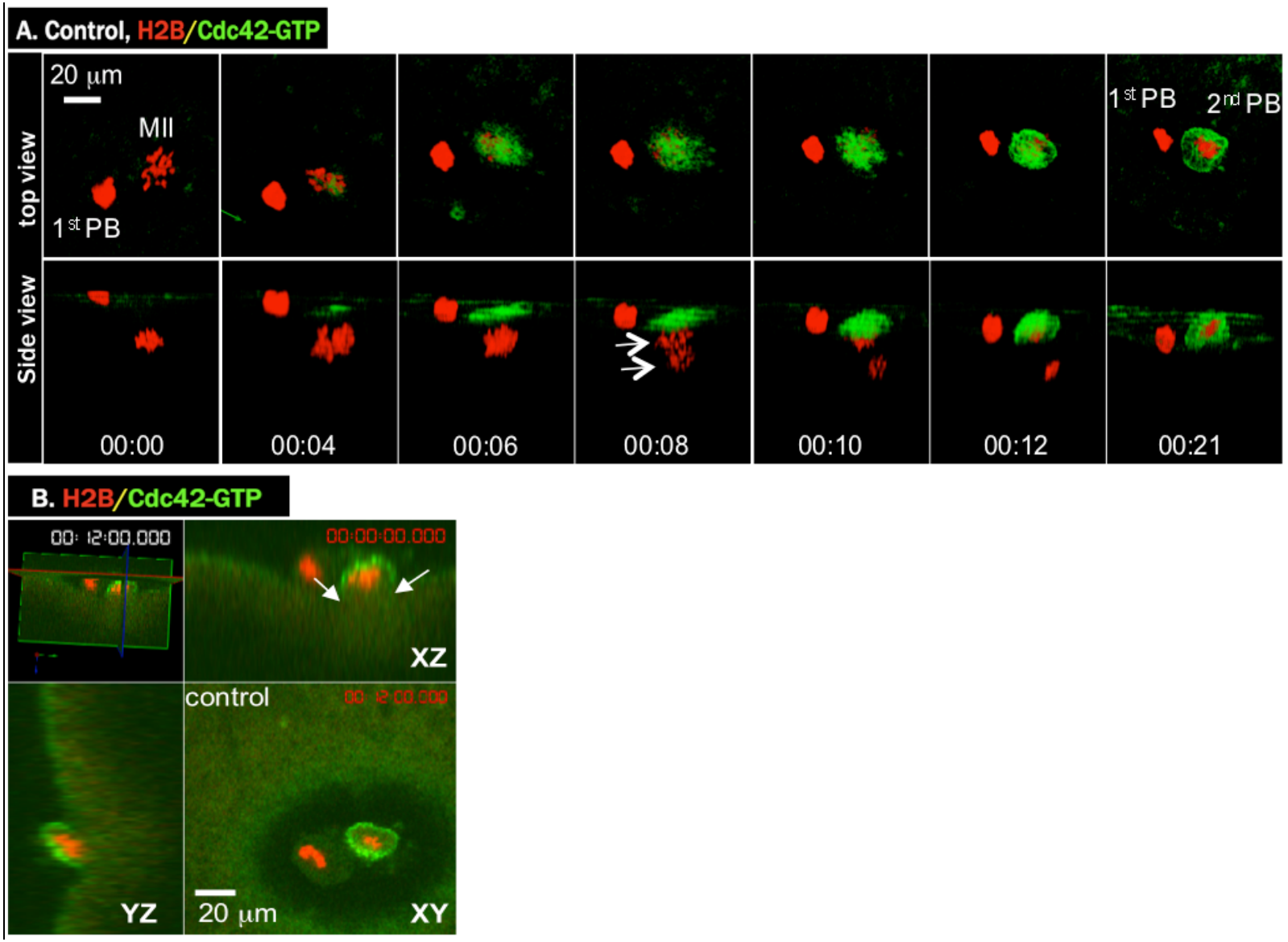
A. Control, H2B/Cdc42-GTP
top view
Side view
20 μm
MII
1st PB
1st PB
2nd PB
00:00
00:04
00:06
00:08
00:10
00:12
00:21
B. H2B/Cdc42-GTP
XZ
control
YZ
20 μm
XY

Table 2: **Over-expression of cdc42^{T17N} inhibits the formation of the first polar body protrusion.** Table summarizes results from Figure 6 and 7 and these are consistent with X. Zhang and colleagues' study (Zhang et al., 2008).

** $p<0.0001$, Fisher's exact test. Total of 5 experiments.

	1st PBE	No 1st PBE	Total
Control	32	11	43
Cdc42N17	2	36	38
Total	34	47	81

Figure 8: **Over-expression of cdc42^{T17N} inhibits the formation of the second polar body protrusion.** GV oocytes were injected with mRNAs for mRFP-H2B (chromosomes) and eGFP-wGBD (cdc42-GTP). Half of the oocytes were used as control (Fig. 6) and the other half were further injected with mRNA for cdc42N17 (10 ng per oocyte). Injected oocytes were incubated overnight in OCM with 1 mM progesterone to mature to metaphase II, and then prick-activated. A) Represented in the figure is a time series of a typical cdc42^{T17N} oocyte following prick activation. The presence of roughly twice as many chromosomes in the single metaphase array (00:00) indicated cytokinesis failure during first polar body emission. Note: the synchronous segregation of all chromosomes (00:03, arrows), indicating anaphase II and the failure of polar body protrusion. Eventually, all chromosomes moved inside the cytoplasm and became too deep to be detected (00:24). 00:00 represents 10 min after pricking in this oocyte. B) Sectional view of top (XY) and side (XZ or YZ) views of the cdc42^{T17N} oocyte depicts the lack of active cdc42 at the cortex, or protrusion of the second polar body (00:13). Figure taken from ((Leblanc et al., 2011)).

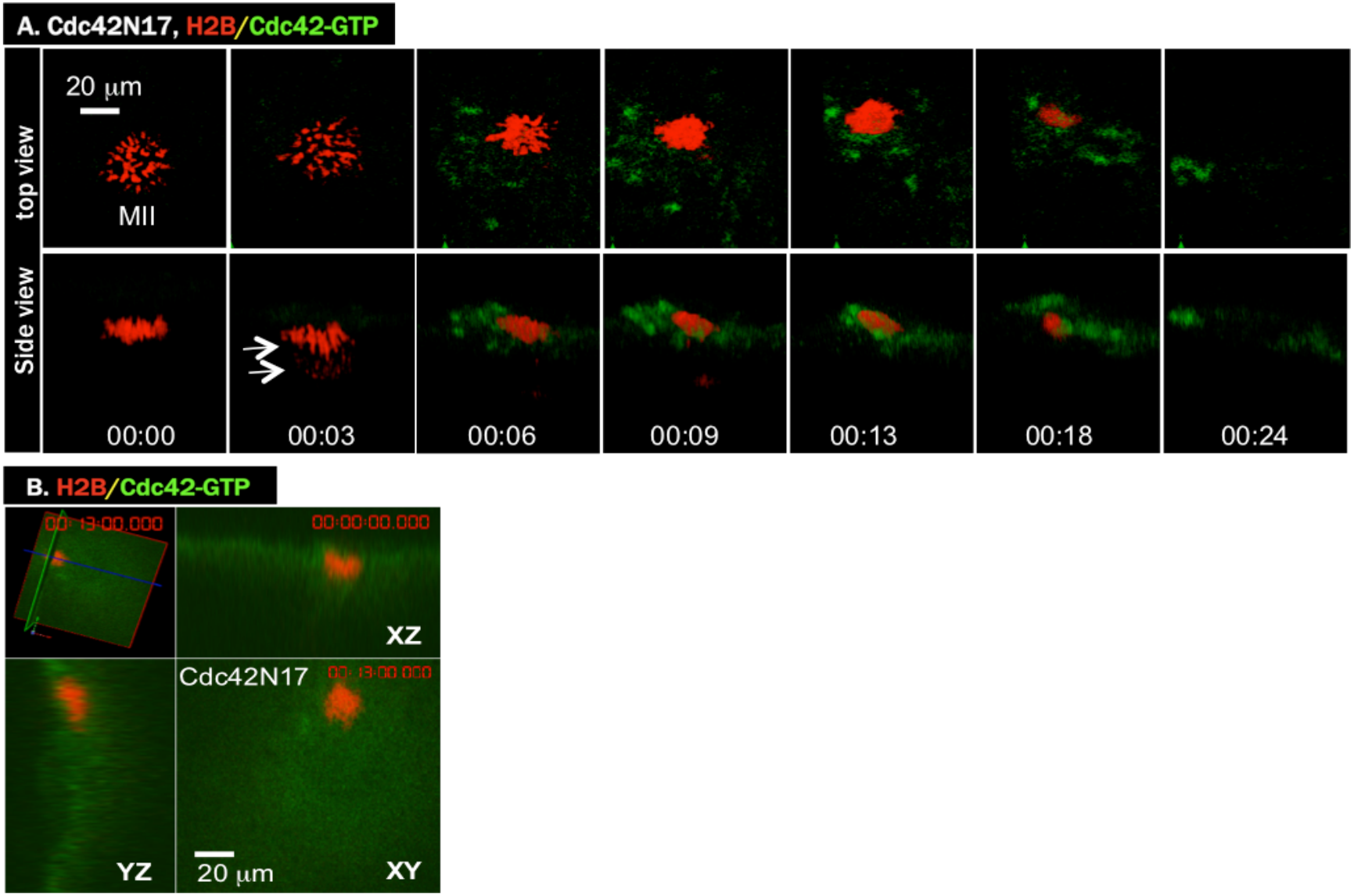
A. Cdc42N17, H2B/Cdc42-GTP
top view
Side view
20 μm
MII
00:00
00:03
00:06
00:09
00:13
00:18
00:24
B. H2B/Cdc42-GTP
00:13:00.000
00:00:00.000
XZ
Cdc42N17
00:13:00.000
YZ
20 μm
XY

Table 3: **Over-expression of cdc42^{T17N} inhibits the formation of the second polar body protrusion.** Table summarizes results from Figure 6 and 7. Note: 11/21 control oocytes did not emit the second polar body since they did not respond to prick-activation. Total of 4 experiments.

	2nd PBE	No 2nd PBE	Total
Control	10	11	21
Cdc42N17	1	16	17
Total	11	27	38

Since first and second PBE share the cdc42 mechanism, they likely share other known aspects of first PBE. RhoA also has been shown to be required for the proper function of the contractile ring and, consequently, first PBE (Zhang et al., 2008). I therefore tested whether RhoA localizes to the contractile ring during second PBE. First, oocytes were injected with the probes, and then were stimulated with progesterone overnight. The resulting MII-arrested oocytes were subsequently prick-activated, and confocal time-lapse imaging began almost immediately. Chromosome separation occurs following 6min after prick-activation (Fig. 9, 0min). Active RhoA begins to accumulate under the polar body chromosomes (Fig. 9, 8min), in the form of a ring that begins to constrict under the nascent polar body (Fig. 9, 9-21min, top view).

Furthermore, our co-localization experiment of active RhoA and active cdc42 during second PBE (Fig. 10 (Leblanc et al., 2011)) highlights the spatial similarities seen during first PBE (Zhang et al., 2008). First, oocytes were injected with the probes, and then were stimulated with progesterone overnight. The resulting MII-arrested oocytes were subsequently prick-activated, and confocal time-lapse imaging began almost immediately. In this time-lapse experiment, an active cdc42 cap is detected just above the active RhoA contractile ring (Fig. 10, 00:12, side view), thus forming mutually exclusive zones, as seen during first PBE. The active RhoA ring begins to constrict under the active cdc42 cap (Fig. 10, 00:12-00:18), which represents the polar body membrane protrusion (Fig. 10, 00:14). These results demonstrate that RhoA is activated at the contractile ring during second PBE and that its localization is distinct from that of active cdc42, in a spatial arrangement indistinguishable from that found in first PBE.

Figure 9: **RhoA is activated within the polar body neck during second PBE.** GV oocytes were injected with mRNAs for mRFP-H2B (chromosomes) and eGFP-rGBD (RhoA-GTP), followed by incubation overnight in OCM with 1 mM progesterone to mature to metaphase II. The metaphase II oocytes were pricked with a glass needle followed by time-lapse confocal imaging. Shown is a time series of a typical oocyte depicting the active RhoA ring (green) constricting under the nascent second polar body (red). Top row views the side of the chromosomes and the bottom row shows the top view of the active RhoA ring. Time is relative to chromosome separation (arrowhead, 0min).

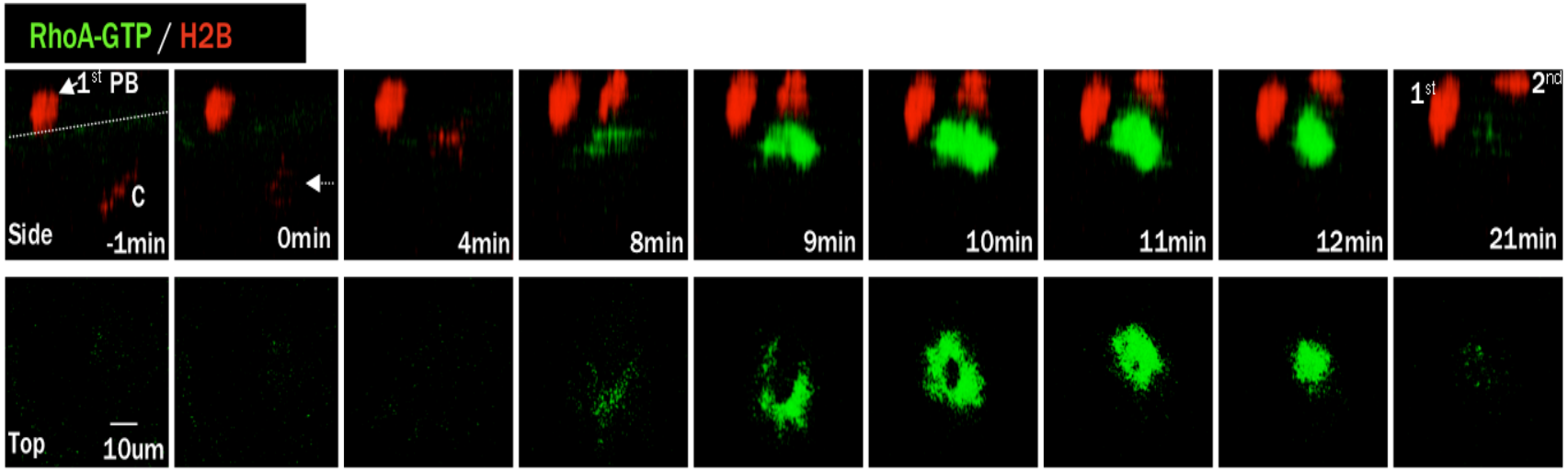
RhoA-GTP / H2B
1st PB
C
Side
-1min
0min
4min
8min
9min
10min
11min
12min
1st
2nd
21min
Top
10um

Figure 10: **Cdc42 and RhoA activity zones during second polar body emission.** GV oocytes were injected with mRNAs for mRFP-wGBD (cdc42-GTP) and eGFP-rGBD (RhoA-GTP), followed by incubation overnight in OCM with 1 mM progesterone to mature to metaphase II (00:00, showing single plane top view of a metaphase II oocyte depicting the raised polar body surface; 10/10). The metaphase II oocytes were pricked with a glass needle followed by time-lapse confocal imaging. Shown is a time series of a typical oocyte depicting the dynamic and complementary activity zones of the two GTPases. Active cdc42 (red) defines the polar body cortex and active RhoA (green) represents the contractile ring. Time denotes hh:mm from pricking. Figure taken from (Leblanc et al., 2011).

Cdc42-GTP/RhoA-GTP
Side view
Top view
20 µm
00:08
00:12
00:14
00:16
00:18
00:20
2nd pb

4. Calcium Signaling during Polar Body Emission

4.1 Detection of Calcium Signals during Polar Body Emission

Having established that cdc42 is similarly required for second polar body emission (Fig. 7 and 8), as it is for first polar body emission (Zhang et al., 2008), I wanted to determine if cdc42 activation during polar body emission is regulated by calcium signaling, as demonstrated in compensatory endocytosis and wound healing in the Xenopus eggs (Benink and Bement, 2005; Sokac et al., 2003; Yu and Bement, 2007). To address this, I conducted confocal time-lapse imaging experiments using the fluorescent probe eGFP-C2 to detect potential calcium signals. This probe is made up of the calcium-binding domain (C2) of protein kinase C beta (PKCβ) and has been used by others to study CGE in Xenopus eggs (Yu and Bement, 2007). What is significant about this probe is that upon binding to calcium, the C2 domain acquires an affinity for the lipid phosphatidylserine (PS), thus targeting it to membranes. To first test that the eGFP-C2 faithfully detects calcium transients in our system, I decided to use it to examine the well-characterized calcium wave during fertilization and parthenogenetic activation (Busa and Nuccitelli, 1985; Busa et al., 1985; Nuccitelli et al., 1993). I microinjected the probe in GV oocytes, along with the chromosome probe (mRFP-H2B). The oocytes were stimulated with progesterone overnight to reach metaphase II arrest. I then conducted a confocal time-lapse imaging experiment following prick activation of metaphase II eggs (Fig. 11). Figure 11 demonstrates axial views of the polar body emission site, specifically, side and top views of the plasma membrane. Indeed, we are able to detect the calcium wave with eGFP-C2. Within the first scan, about one minute after activation, the wave is detected (Fig. 11, 1min07s). The eGFP-C2 signal nicely delineates the plasma

Figure 11: **The eGFP-C2 probe faithfully probes for calcium.** GV oocytes were injected with mRNAs for mRFP-H2B (chromosomes) and eGFP-C2 (calcium), followed by incubation overnight in OCM with 1 mM progesterone to mature to metaphase II. The metaphase II oocytes were pricked with a glass needle followed by time-lapse confocal imaging. The fertilization-specific calcium wave (green) is detected during the first time-point of the series (1min07s), throughout the cortex. Note: the ring-like pattern around the PB is due to the curvature of the membrane. See side view for more accurate reflection. The wave is no longer detected in the second time-point. Sectional views of the first and second time-points are shown (side and top of polar body sections). Times are relative to prick-activation. White arrow points to a possible exocytosing cortical granule.

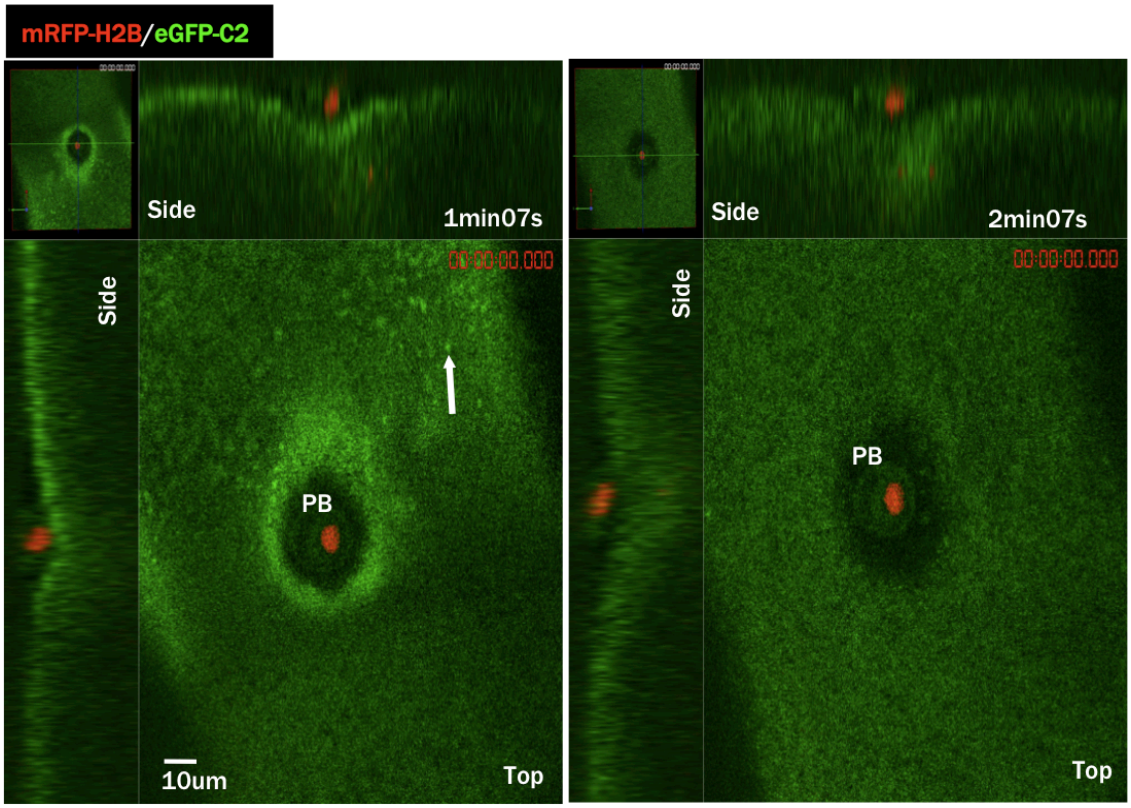
mRFP-H2B/eGFP-C2
Side
1min07s
Side
2min07s
Side
PB
10um
Top
Side
PB
Top

Figure 12: **A localized calcium transient is detected during first PBE.** GV oocytes were injected with mRNAs for mRFP-H2B (chromosomes) and eGFP-C2 (calcium), followed by incubation in OCM with 1 mM progesterone to induce maturation (GVBD). GVBD oocytes are then followed by time-lapse confocal imaging approximately 1h45min following GVBD. A calcium signal is detected as a ring within the polar body neck approximately 12min following chromosome separation. A) The two rows show the top and side views of the chromosomes (of the 3D compilation). B) The calcium transient is detected at the neck of the polar body at 00:22, which can be distinguished in the sectional views because of the background delineating the plasma membrane/cortex. The two rows show the sectional views (xz=side, xy=top) of the calcium transient.

A. mRFP-H2B / eGFP-C2
00:09
00:12
00:21
00:22
00:23
00:26
00:27
3D top
3D side
10 μm
B. mRFP-H2B / eGFP-C2
00:09
00:12
00:21
00:22
00:23
00:26
00:27
XY
XZ
10 μm

membrane (Fig. 11, 1min07s, side view). Looking down onto the plasma membrane (top view), a strong eGFP-C2 signal is detected (Fig. 11, 1min07s). The "spots" (white arrow) are consistent with the exocytosing cortical granules that have been detected by others using the C2 probe (Yu and Bement, 2007). More importantly, this plasma membrane signal disappears one minute later (Fig. 11, 2min07s), which is consistent with the signal being the fertilization induced calcium wave. This result indicates that eGFP-C2 detects the fertilization-specific calcium wave in *Xenopus laevis* eggs.

Having confirmed the utility of the C2 probe to detect calcium signals, I decided to first determine if first polar body emission is associated with any calcium signals (Fig. 12). First, the oocytes were injected with probes and then stimulated with progesterone, followed by monitoring of GVBD. GVBD oocytes were subjected to time-lapse imaging prior to the metaphase-anaphase transition. While in metaphase-I (Fig. 12A, 00:09) and anaphase (Fig. 12A, 00:12), there is a local enrichment of the eGFP-C2 within the spindle. The significance of this spindle associated C2 signal remains unknown. The most prominent C2 signal was seen 12 minutes following the initial "stretching" of the separating chromosomes (24/66 oocytes). This initial "stretch" is followed by the visually apparent separation of chromosomes into two groups (Fig. 12A, 00:12). The C2 signal first appears between the polar body and oocyte chromosomes (Fig. 12A, 00:22) and is transient, being that the signal dissipates within 4 minutes (Fig. 12A, 00:22-00:27). On average, this increase occurs at 13.1 +/- 2.6min (S.D.) (n=27) following chromosome separation, after cdc42 is activated. The side and top axial views of the plasma membrane of the same oocyte, underlines the relative localization of this C2 signal (Fig. 12B). At 00:22, the C2 signal appears at the border of the polar body and oocyte, as indicated by the green background delineating the plasma

membrane (Fig. 12B, xz). From the top, it can be seen that the signal forms a ring (Fig. 12B, 00:22, xy), consistent with its placement within the narrow polar body neck.

I also tested if the C2 signal was similarly associated with second PBE. First, oocytes were injected with the probes, and then were stimulated with progesterone overnight. The resulting MII-arrested oocytes were subsequently prick-activated, and confocal time-lapse imaging began almost immediately. Following prick-activation, a C2 increase is detected within the first few minutes of prick-activation (1min55s post pricking) (Fig. 13, 00:00), consistent with the fertilization-specific wave (Yu and Bement, 2007). Following chromosome separation (Fig. 13, 00:15, white arrows), another C2 increase occurs (Fig. 13, 00:26) at a location similar to that found during first PBE, and dissipates within a similar time frame (4min, Fig. 13, 00:25-00:29,). However, unlike the fertilization wave, which covers the whole cortex (Fig. 13, 00:00), the second C2 increase, is a local signal. Similarly to first PBE, this increase occurs between the polar body and oocyte chromosomes, ~ 10 minutes after the initiation of chromosomes segregation (Fig. 13, 00:25). The axial views in Fig. 13B compare the wave to the later C2 signal. The wave is found all along the plasma membrane (Fig. 13B, 0:00, 1min50s following prick-activation), while the later C2 signal is found locally, at the border of the polar body and oocyte (Fig. 13B, 00:26). Altogether, these results suggest that calcium increases following chromosome separation during PBE, between the polar body and oocyte chromosomes. I will subsequently refer to this "second C2 increase" as the calcium transient, for both the first and second PBE, for reasons of simplicity.

4.2 Association of the Calcium Transient with the Contractile Ring

Figure 13: **A localized calcium transient is detected during second PBE.** GV oocytes were injected with mRNAs for mRFP-H2B (chromosomes) and eGFP-C2 (calcium), followed by incubation in OCM with 1 mM progesterone to mature to metaphase II. The metaphase II oocytes were pricked with a glass needle followed by time-lapse confocal imaging. The fertilization/activation specific calcium wave is detected (00:00), followed by a localized calcium transient, ~10min following chromosome separation. A) The side view of the chromosomes is shown (of the 3D compilation). B) The sectional views (xz=side, xy=top) of the wave and calcium transient are shown.

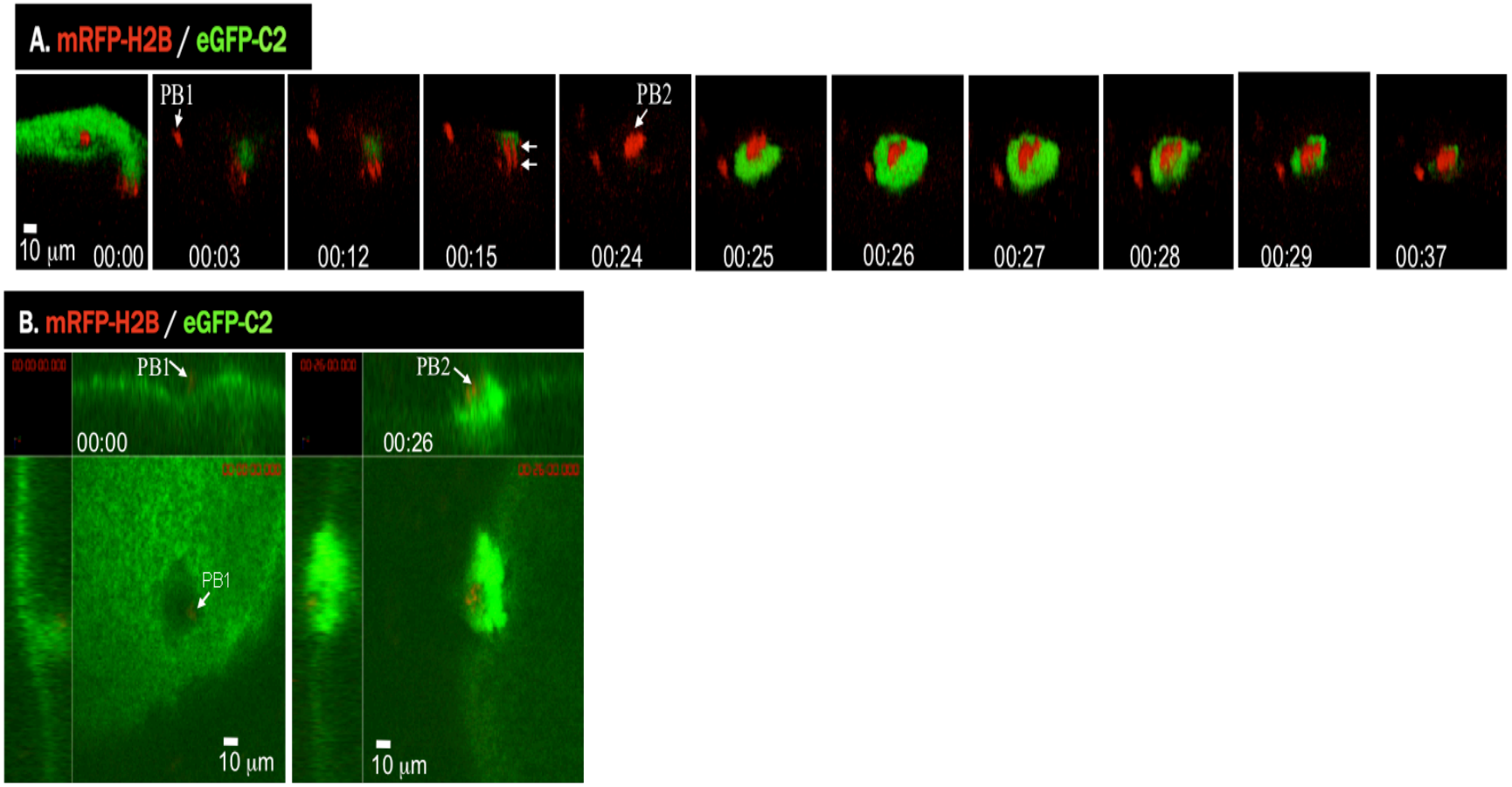
A. mRFP-H2B / eGFP-C2
PB1
PB2
10 μm
00:00
00:03
00:12
00:15
00:24
00:25
00:26
00:27
00:28
00:29
00:37
B. mRFP-H2B / eGFP-C2
PB1
00:00
PB1
10 μm
PB2
00:26
10 μm

The location of the calcium transient, at the border of the polar body and the oocyte, suggested that it might be closely associated with the contractile ring. Therefore, co-localization experiments were conducted using a probe of a contractile ring component, Anillin. First, the oocytes were injected with probes and then stimulated with progesterone, followed by monitoring of GVBD. GVBD oocytes were subjected to time-lapse imaging prior to the metaphase-anaphase transition. Following anaphase, Anillin forms a ring surrounding the protruding polar body (Fig. 14, 00:30) that begins to constrict (Fig. 14, 02:30). The Anillin ring then resides at the border of the newly extruded polar body, and the oocyte (Fig. 14, 06:00, side view). Next, the calcium transient appears, and overlaps with the Anillin ring (Fig. 14, 06:30), which has already begun to constrict. This result confirms that the calcium transient is first detected at the contractile ring and that it is probably not involved in the constriction of the contractile ring.

Given our initial impetus of determining if cdc42 activation during polar body emission is regulated by calcium signaling, we carried out co-localization experiments using the active cdc42 probe to depict the polar body membrane protrusion. First, the oocytes were injected with probes and then stimulated with progesterone, followed by monitoring of GVBD. GVBD oocytes were subjected to time-lapse imaging prior to the metaphase-anaphase transition. When the calcium transient occurs (Fig. 15a, 7:00), it is clear that it does so at the base of this protrusion. In Fig. 15b, the sectional views of 7:00 better demonstrate this configuration. This result further confirms that the calcium transient is first detected within the contractile ring, under the polar body protrusion.

4.3 Functional Investigation of Calcium Signaling during Polar Body Emission

Figure 14: **The calcium transient is first detected at the contractile ring.** GV oocytes were injected with mRNAs for mRFP-C2 (calcium) and Anillin-3XGFP (contractile ring = Anillin), followed by incubation in OCM with 1 mM progesterone to induce maturation (GVBD). GVBD oocytes are then followed by time-lapse confocal imaging approximately 1h45min following GVBD. Note: in this oocyte scanning began later (after protrusion began). The calcium transient overlaps with the Anillin ring, after the contractile ring has already begun to constrict. Each image shows the side and top sectional views of the ring. Time is relative to the first scan.

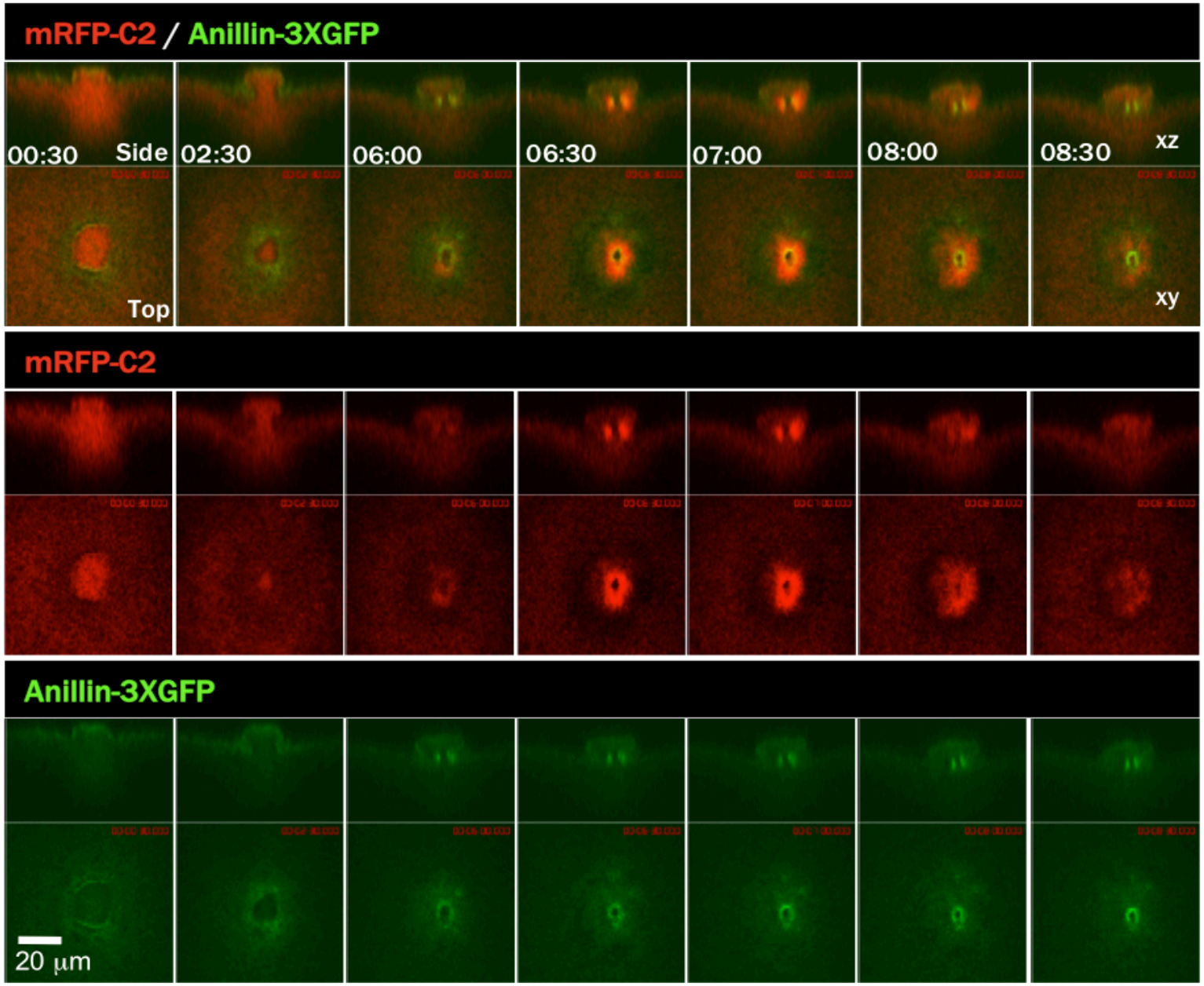
mRFP-C2 / Anillin-3XGFP
00:30
Side
02:30
06:00
06:30
07:00
08:00
08:30
xz
Top
xy
mRFP-C2
Anillin-3XGFP
20 μm

Figure 15: **The calcium transient occurs under the polar body membrane protrusion.** GV oocytes were injected with mRNAs for mRFP-C2 (calcium) and eGFP-wGBD (cdc42-GTP), followed by incubation in OCM with 1 mM progesterone to induce maturation (GVBD). GVBD oocytes are then followed by time-lapse confocal imaging approximately 1h45min following GVBD. Note: in this oocyte scanning began later (after protrusion began). Active cdc42 (eGFP-wGBD) localizes to the membrane protrusion during first PBE while the calcium transient (mRFP-C2) localizes beneath it, at the contractile ring. Times are relative to the first scan. A) Side view of the polar body emission site is presented, where the calcium transient occurs at 07:00. B) Sectional views of 07:00 demonstrating that the "transient" ring is devoid of active cdc42 signal.

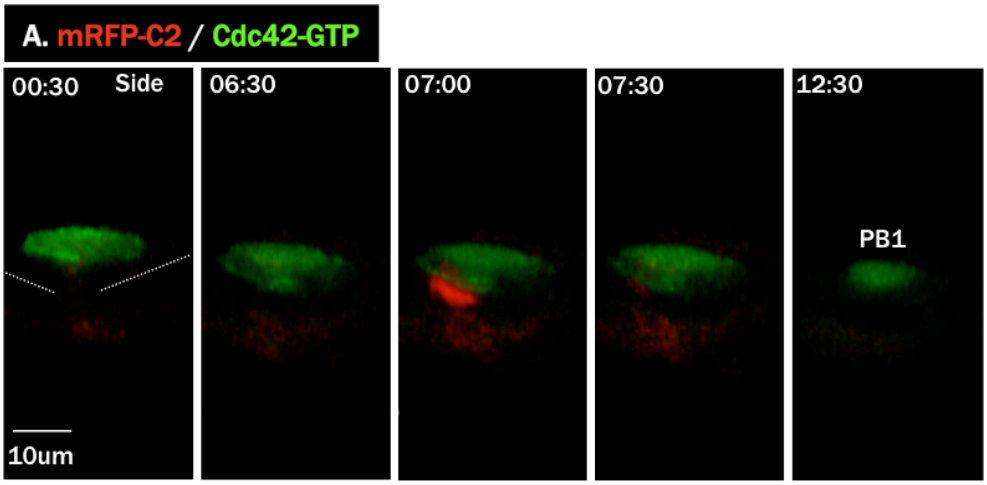
A. mRFP-C2 / Cdc42-GTP
00:30
Side
06:30
07:00
07:30
12:30
PB1
10um

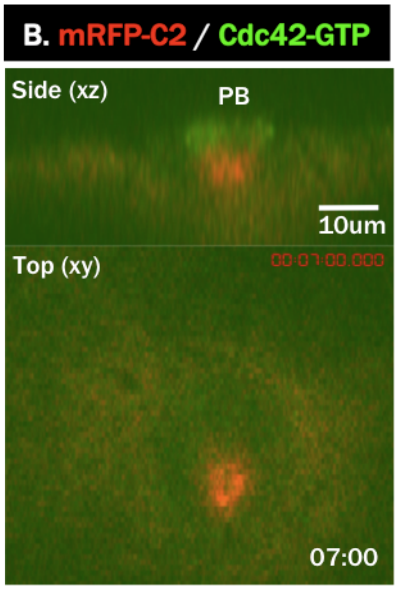
B. mRFP-C2 / Cdc42-GTP
Side (xz)
PB
10um
Top (xy)
00:07:00.000
07:00

To determine what role calcium signaling might hold during PBE, we next conducted calcium chelation experiments. We decided to employ a well-characterized weak calcium chelator, 5,5'-Dibromo BAPTA (dbBAPTA, K_D=1.5μM). dbBAPTA has been used in *Xenopus laevis* eggs to inhibit cleavage furrowing (Miller et al., 1993; Snow and Nuccitelli, 1993). First, the oocytes were injected with probes and then stimulated with progesterone, followed by monitoring of GVBD. dbBAPTA (20nL 33.3mM) was injected into oocytes 1 hour following GVBD. GVBD oocytes were subjected to time-lapse imaging prior to the metaphase-anaphase transition or they were scanned once they had achieved metaphase II-arrest (>3hrs following GVBD) (Fig. 16A). In the control group (probes only), all oocytes had completed first polar body emission successfully (Fig. 17, 20/20 oocytes), and entered metaphase II-arrest with one polar body, and a metaphase II spindle (Fig. 17, control image). However, the oocytes that were injected with dbBAPTA did not successful complete first polar body emission (Fig. 17, 0/27 oocytes). The exact cause is unclear. Most dbBAPTA-injected oocytes were scanned only after 3hrs following GVBD and appeared to have oddly organized chromosomes and/or simply the chromosomes could not be detected. In the oocytes where the chromosomes could no longer be detected, it seems that they had sank slowly back into the oocyte without chromosome separation, before imaging. Figure 17 represents a dbBAPTA-injected oocyte in which the chromosomes, along with its spindle, become disorganized. Furthermore, this oocyte was scanned much later, and the chromosomes were no longer observed (not shown), suggesting that its spindle also sank into the oocyte. Although not all spindles sank back into their respective oocytes, no oocyte emitted the first polar body. This suggests that calcium signaling is required for first polar

Figure 16: **Methods -- The effects of dbBAPTA on PBE or the calcium transient.** GV oocytes were injected with mRNAs, followed by incubation in OCM with 1 mM progesterone to induce maturation (GVBD). A) dbBAPTA was injected 1hr following GVBD, and time-lapse imaging began soon after, or one scan was taken once the oocyte achieved MII-arrest (>3hrs following GVBD). B) dbBAPTA was injected 2-5min from the start of chromosome segregation, which was determined by time-lapse confocal imaging. Time-lapse imaging resumed following the injection to assess the calcium transient (eGFP-C2).

A)

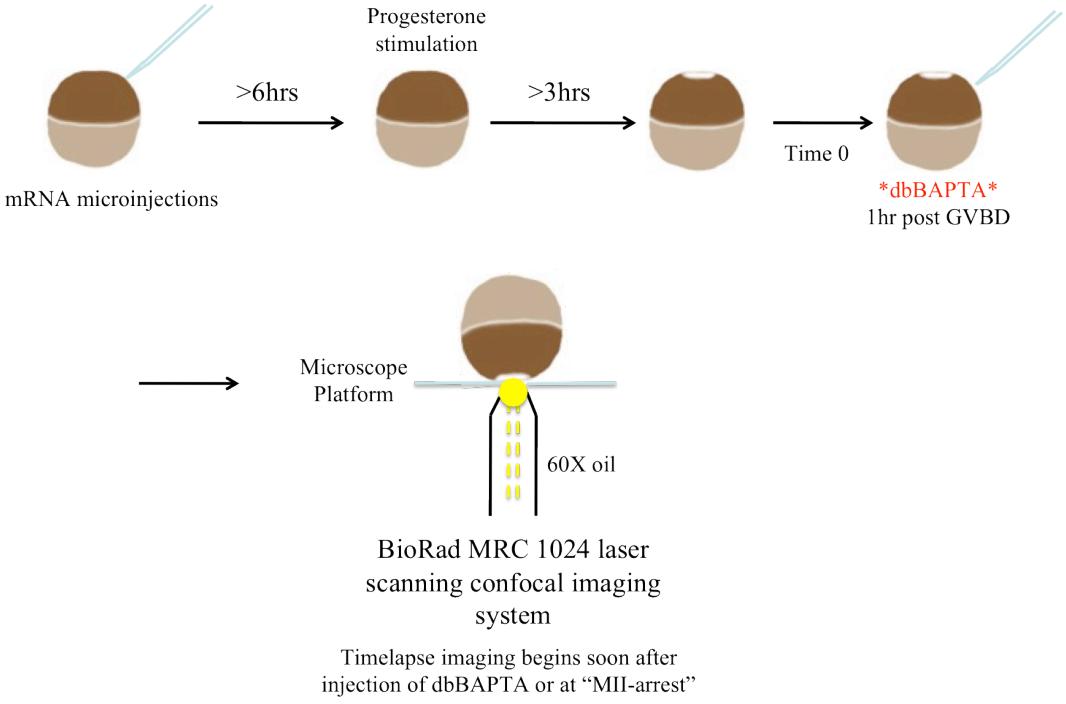
Progesterone
stimulation
>6hrs
>3hrs
Time 0
mRNA microinjections
dbBAPTA
1hr post GVBD
Microscope
Platform
60X oil
BioRad MRC 1024 laser
scanning confocal imaging
system
Timelapse imaging begins soon after
injection of dbBAPTA or at "MII-arrest"

B)

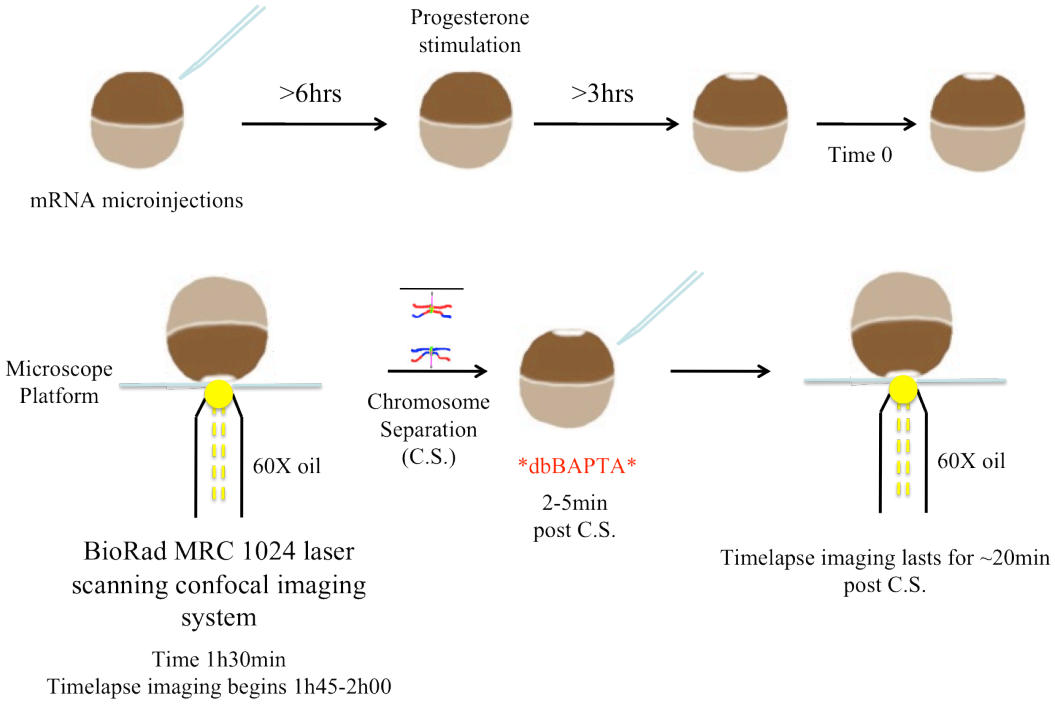
Progesterone
stimulation
>6hrs
>3hrs
Time 0
mRNA microinjections
Microscope
Platform
60X oil
Chromosome
Separation
(C.S.)
dbBAPTA
2-5min
post C.S.
60X oil
BioRad MRC 1024 laser
scanning confocal imaging
system
Time 1h30min
Timelapse imaging begins 1h45-2h00
Timelapse imaging lasts for ~20min
post C.S.

Figure 17: **dbBAPTA injected 1h following GVBD inhibits PBE.** GV oocytes were injected with mRNAs for mRFP-H2B (chromosomes) and EMTB-3XGFP (microtubules), followed by incubation in OCM with 1 mM progesterone to induce maturation (GVBD). dbBAPTA is then injected 1h following GVBD, and time-lapse imaging begins soon after. The side view of the chromosomes is shown. Times of the dbBAPTA images are relative to the dbBAPTA injection.

Control: 20/20 oocytes emitted the first polar body.

dbBAPTA: 0/27 oocytes emitted the first polar body.

**$p<0.0001$, Fisher's exact test. Total of 3 experiments.

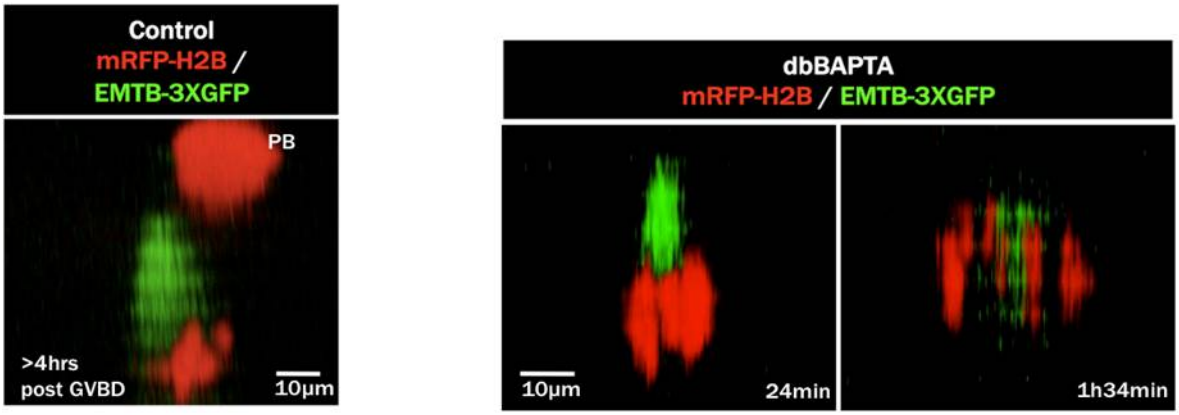
Control
mRFP-H2B /
EMTB-3XGFP
PB
>4hrs
post GVBD
10μm
dbBAPTA
mRFP-H2B / EMTB-3XGFP
10μm
24min
1h34min

body emission. Chelation leads to prohibition of chromosome separation in the majority of oocytes, most likely by disrupting spindle assembly. These results show that the integrity of the spindle, as well as first polar body emission, are sensitive to calcium chelation by dbBAPTA, consistent with an earlier study in which various calcium inhibitors were used (Sun and Machaca, 2004).

To bypass these early events and to specifically examine the possible effect of inhibiting the calcium transient around the contractile ring, I injected dbBAPTA much later to avoid possible inhibition of spindle assembly and furrowing. First, the oocytes were injected with probes and then stimulated with progesterone, followed by monitoring of GVBD. GVBD oocytes were subjected to time-lapse confocal imaging to monitor chromosome segregation (anaphase). Water (10-20nL) or dbBAPTA (10-20nL 16.7mM or 10nL 25mM) was injected into oocytes 2-5min after the first sign of chromosome separation ("stretching", as shown in Fig. 13A, 00:15). Time-lapse imaging resumed immediately afterwards. In the control group (water injection), the calcium transient occurred at the proper time (11min post chromosome separation), between the polar body and oocyte chromosomes (Fig. 18, top panel) (Table 4, 6/18 oocytes). The far right images (Fig. 18, red arrows) shows the sectional view (side and transectional top) of the calcium transient (control), where the spatial configuration can be better observed. It is worth noting that generally, only approximately 36% of control-uninjected oocytes elicit the calcium transient (24/66 oocytes with "transient"). Therefore the percentage of water-injected oocytes exhibiting the calcium transient indicated that water injection did not affect the appearance of the calcium transient at the contractile ring. However, injecting dbBAPTA following chromosome separation resulted in complete inhibition of the calcium transient (Fig. 18, Table 4, 0/18 oocytes). These results indicated

Figure 18: **The calcium transient is inhibited by the weak chelator, dbBAPTA, when injected 2-5min following chromosome separation.** GV oocytes were injected with mRNAs for mRFP-H2B (chromosomes) and eGFP-C2 (calcium), followed by incubation in OCM with 1 mM progesterone to induce maturation (GVBD). GVBD oocytes are then followed by time-lapse confocal imaging approximately 1h45min following GVBD. The images shown are of the time-point 11min following chromosome separation. Water is injected in the control oocyte 2-5min following chromosome separation, and the calcium transient is detected by eGFP-C2 (on the left: side view of the chromosomes; on the right: top view of green channel only). dbBAPTA is injected 2-5min following chromosome separation, and the calcium transient is probed for by eGFP-C2 (on the left: side view of the spindle; on the right: top view of green channel only). The side panel highlights the spatial relationship between the calcium transient, the PB and the PM (dashed line; approximate) (sectional view). The oocyte chromosomes of the control (C with arrow) are not present in the image since they were outside the scanning volume. The time-lapse imaging series typically lasts until 20min following chromosome separation.

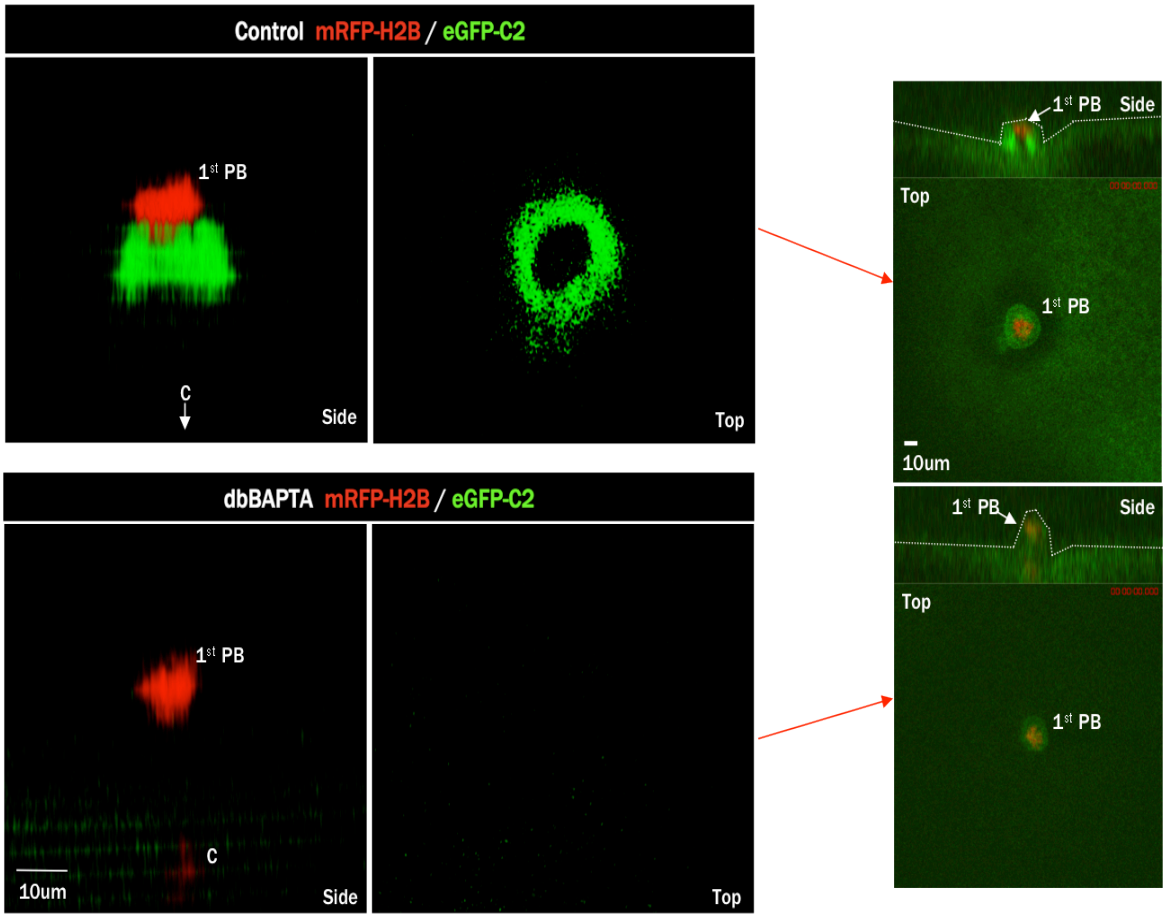
Control mRFP-H2B / eGFP-C2
1st PB
C
Side
Top
dbBAPTA mRFP-H2B / eGFP-C2
1st PB
C
10um
Side
Top
1st PB
Side
Top
1st PB
10um
1st PB
Side
Top
1st PB

Table 4: **The calcium transient is inhibited by the weak chelator, dbBAPTA, when injected 2-5min following chromosome separation.** Table summarizes the results of Figure 17.

*p=0.0191, Fisher's exact test. Total of 6 experiments.

	No transient	**Transient**	**Total**
Control (water)	12	6	**18**
dbBAPTA	17	0	**17**
Total	**29**	**6**	**35**

that dbBAPTA injected at the equator area required only a few minutes to reach the site of the calcium transient (as depicted by the C2 accumulation), consistent with an earlier estimate (Miller et al., 1993). The ability of dbBAPTA to inhibit the C2 accumulation further confirmed that the C2 accumulation depicted is a calcium transient.

To address the potential that dbBAPTA is, somehow, obstructing events during cytokinesis, I conducted confocal time-lapse imaging to confirm the localization of known PBE components under these conditions. First, the oocytes were injected with probes and then stimulated with progesterone, followed by monitoring of GVBD. GVBD oocytes were subjected to time-lapse confocal imaging to monitor chromosome segregation (anaphase). Water (10nL) or dbBAPTA (10nL 25mM) was injected into oocytes 2-5min following chromosome separation. Time-lapse imaging resumed immediately afterwards. Images shown in Figure 19 were taken several minutes after water (control) or dbBAPTA injection. In the control oocyte, active cdc42 can be seen encompassing the polar body chromosomes (Fig. 19, first column). Identically, in the dbBAPTA oocyte, active cdc42 surrounds the protruded polar body (Fig. 19, second column). These results demonstrate that dbBAPTA does not affect cdc42 activation and therefore does not affect polar body protrusion when injected following chromosome separation.

Next, I probed for Anillin to assess any effects dbBAPTA might have on the contractile ring. First, the oocytes were injected with probes and then stimulated with progesterone, followed by monitoring of GVBD. GVBD oocytes were subjected to time-lapse confocal imaging to monitor chromosome segregation (anaphase). Water (10nL) or dbBAPTA (10nL 25mM) was injected into oocytes 2-5min following chromosome separation. Time-lapse imaging

Figure 19: **dbBAPTA does not affect active cdc42 localization or the polar body membrane protrusion, when injected following chromosome separation.** GV oocytes were injected with mRNAs for mRFP-H2B (chromosomes) and eGFP-wGBD (cdc42-GTP), followed by incubation in OCM with 1 mM progesterone to induce maturation (GVBD). GVBD oocytes are then followed by time-lapse confocal imaging approximately 1h45min following GVBD. Water or dbBAPTA is injected 2-5min following chromosome separation. Time-lapse imaging reveals that cdc42 is properly activated at the site of the membrane protrusion (one post-injection time-point shown). Side view of the chromosomes is shown.

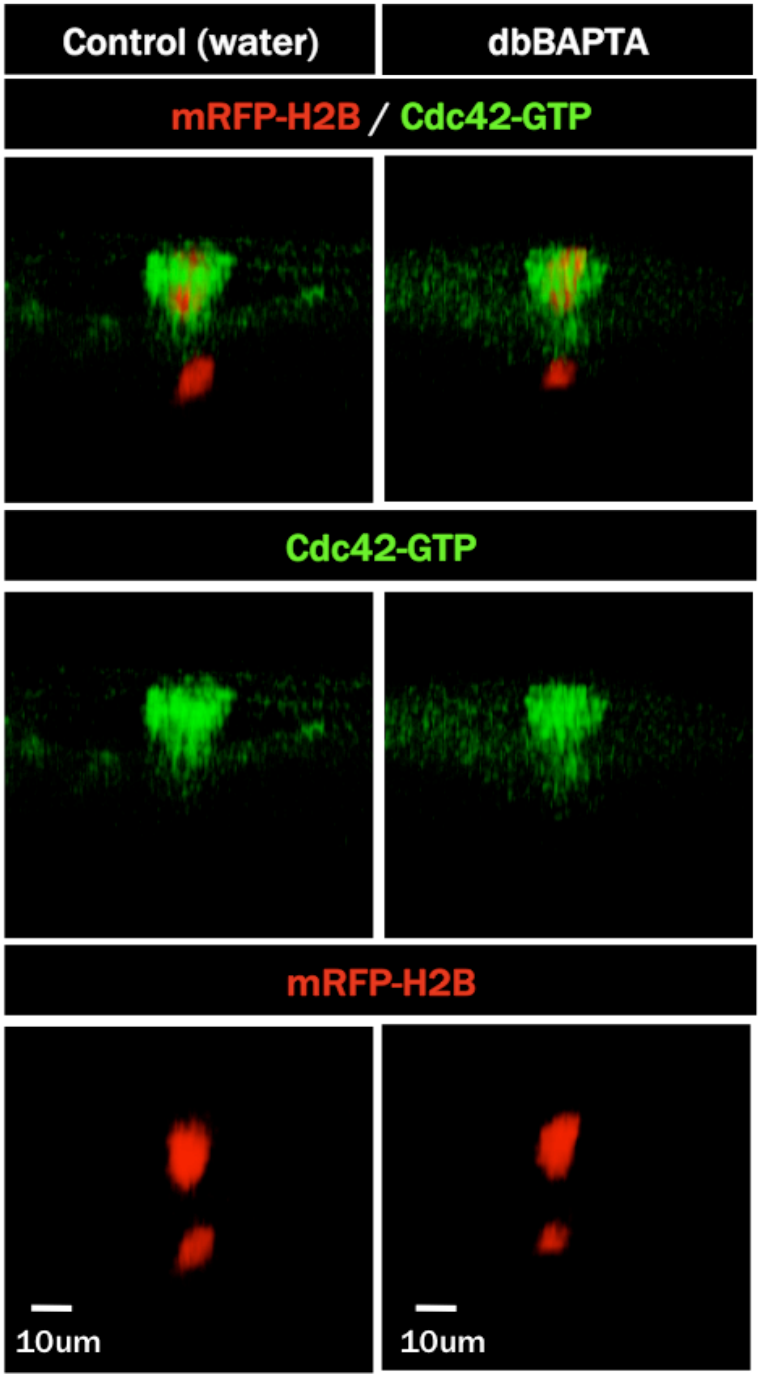
Control (water)
dbBAPTA
mRFP-H2B / Cdc42-GTP
Cdc42-GTP
mRFP-H2B
10um
10um

resumed immediately afterwards. In the control oocyte, Anillin forms a ring around the protruding polar body (Fig. 20, top panel, 00:09). This ring begins to constrict under the polar body (Fig. 20, top panel, 00:09-00:15) until it forms a fully constricted ring (Fig. 20, top panel, 00:17-00:21). Anillin's behavior is identical in the dbBAPTA-injected oocyte (Fig. 20, bottom panel). Anillin forms a ring surrounding the protruding polar body (Fig. 20, bottom panel, 00:08) and begins to constrict under the polar body (Fig. 20, bottom panel, 00:08-00:13) until its maximum is achieved (Fig. 20, bottom panel, 00:15-00:19). These results also demonstrate that dbBAPTA does not affect the constriction of the contractile ring. This conclusion can also be inferred by the fact that dbBAPTA injection following chromosome separation does not lead to polar body retraction (falling back into the oocyte).

4.4 Polar Body Abscission Assay

The last step in cytokinesis, following the constriction of the contractile ring, is abscission. The time course of polar body abscission is not known. Furthermore, there is no simple way to determine the completion of abscission because the polar body is typically wedged tightly between the plasma membrane and the overlaying vitelline membrane. To determine if dbBAPTA prevented abscission, we first developed an assay to determine whether the polar body was closed (abscission complete) or open (abscission incomplete). By injecting fluorescent red Dextran into the oocyte when abscission is typically completed, Dextran will not be able to enter the closed polar body. However, if abscission has failed, the Dextran will make its way into the polar body. Thus, by determining presence or absence of Dextran within the polar body, abscission can be assessed (Fig. 21, *ii*). Since most control oocytes

Figure 20: **dbBAPTA does not affect Anillin localization or constriction of the contractile ring, when injected following chromosome separation.** GV oocytes were injected with mRNAs for mRFP-H2B (chromosomes) and Anillin-3XGFP (contractile ring = Anillin), followed by incubation in OCM with 1 mM progesterone to induce maturation (GVBD). GVBD oocytes are then followed by time-lapse confocal imaging approximately 1h45min following GVBD. Water or dbBAPTA is injected 2-5min following chromosome separation. Time-lapse imaging reveals that Anillin forms a ring, which constricts under the nascent polar body in both the control and dbBAPTA oocyte. For the control oocyte, time 0:00 represents 3min following chromosome separation, prior to water injection. The next time-point (00:09) is approximately 7min following injection. For the dbBAPTA-injected oocyte, time 0:00 represents 1min following chromosome separation, prior to dbBAPTA injection. The next time-point (00:08) represents 6min following the injection.

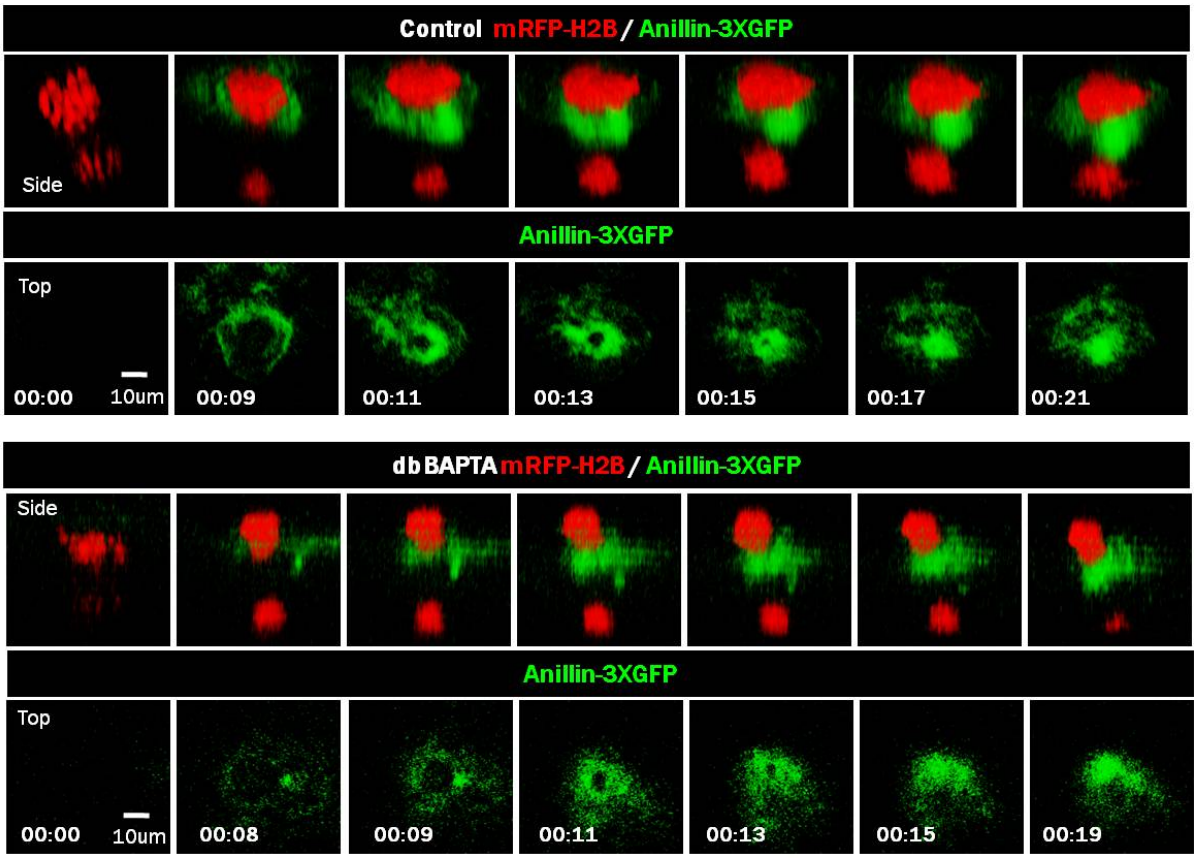
Control mRFP-H2B / Anillin-3XGFP
Side
Anillin-3XGFP
Top
00:00
10um
00:09
00:11
00:13
00:15
00:17
00:21
dbBAPTA mRFP-H2B / Anillin-3XGFP
Side
Anillin-3XGFP
Top
00:00
10um
00:08
00:09
00:11
00:13
00:15
00:19

Figure 21: **Methods – First polar body emission chelation and abscission assay.** GV oocytes were injected with mRNA, followed by incubation in OCM with 1 mM progesterone to induce maturation (GVBD). GVBD oocytes are then followed by time-lapse confocal imaging approximately 1h45min following GVBD. *i*) The first polar body abscission assay was conducted following water or dbBAPTA injection (2-5min from the start of chromosome separation), by injecting fluorescently-labeled Dextran, 1hr following chromosome separation. The oocyte was imaged again at least 15 min after Dextran injection to determine the status of abscission. *ii*) Outcomes of the first polar body abscission assay.

i)

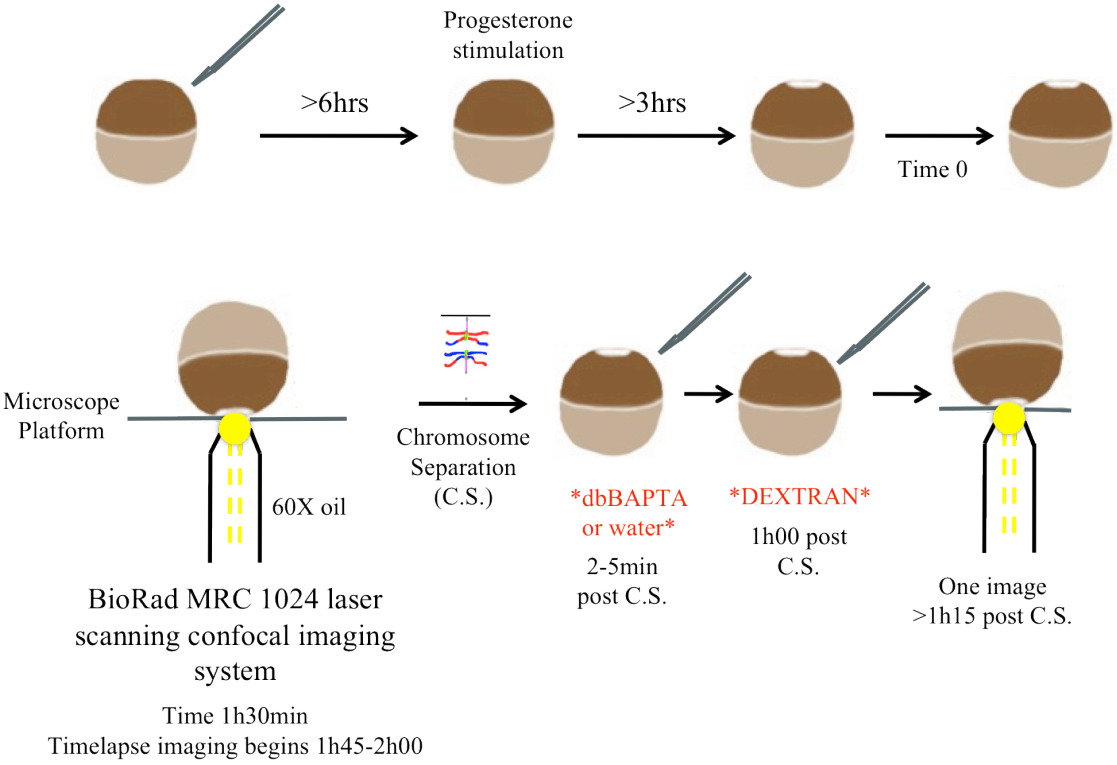
Progesterone
stimulation
>6hrs
>3hrs
Time 0
Microscope
Platform
60X oil
Chromosome
Separation
(C.S.)
*dbBAPTA
or water*
2-5min
post C.S.
DEXTRAN
1h00 post
C.S.
One image
>1h15 post C.S.
BioRad MRC 1024 laser
scanning confocal imaging
system
Time 1h30min
Timelapse imaging begins 1h45-2h00

ii)

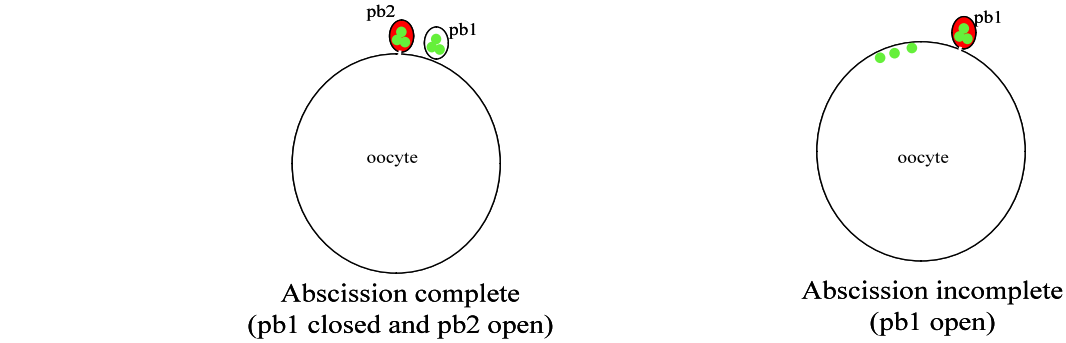
pb2
pb1
oocyte
Abscission complete
(pb1 closed and pb2 open)
pb1
oocyte
Abscission incomplete
(pb1 open)

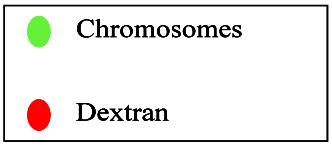
Chromosomes
Dextran

have completed first and second PB abscission one hour following chromosome separation (Fig. 22) (chromosome separation determined by time-lapse imaging, not shown), Dextran injections are conducted at this time. Confocal imaging is used to capture an image at least 15min following the Dextran injection.

To determine if dbBAPTA injections 2-5min following chromosome separation disrupted abscission, the abscission assay was conducted for these oocytes. First, the oocytes were injected with a chromosome probe and then stimulated with progesterone, followed by monitoring of GVBD. GVBD oocytes were subjected to time-lapse confocal imaging to monitor chromosome segregation (anaphase). Water (10nL) or dbBAPTA (10nL 25mM) was injected into oocytes 2-5min following chromosome separation. Dextran was then injected 1hour later, and the oocyte imaged at least 15min later (Fig. 21*ii*). Figure 23 shows sectional views of a first polar body abscission assay. The control group typically contains 2 polar bodies (Fig. 23, left image and bottom cartoon), since the Dextran injection involves piercing the metaphase II oocyte, which causes parthenogenetic activation. For the first polar body abscission assay, this second polar body serves as an internal positive control since it is always filled with Dextran (Fig. 23, PB filled with red signal, left image and bottom cartoon). In the majority of the control oocytes (Table 5, 22/30, ~73%), the other polar body (1^{st} polar body) did not contain dextran and was therefore closed (Fig. 23, PB devoid of red signal, left image and bottom cartoon). In contrast, oocytes in the dbBAPTA-injected group exhibited only one polar body (1^{st} polar body). These oocytes failed to emit a second PB upon dextran injection, presumably because dbBAPTA inhibited egg activation (Fig. 23, right image, PB filled with red signal). Furthermore, the majority of the oocytes (Table 5, 16/21, ~76%) had an open first polar body filled with Dextran, demonstrating that abscission

Figure 22: **Abscission Assay determines that most oocytes have completed abscission by 1hr following chromosome separation.** GV oocytes were injected with mRNA, followed by incubation in OCM with 1 mM progesterone to induce maturation (GVBD). GVBD oocytes are then followed by time-lapse confocal imaging approximately 1h45min following GVBD. Water was injected into oocytes 2-5min following chromosome separation during both first and second polar body emission. Dextran was subsequently injected 1hr following chromosome separation. The oocyte was imaged again at least 15 min after Dextran injection to determine the status of abscission. Abscission is complete when polar bodies are deemed closed (no dextran in PB), or incomplete when polar bodies are deemed open (dextran in PB). The majority of oocytes have completed abscission by 1hr following chromosome separation.

First PBE: 49/65 oocytes completed abscission (5 experiments).

Second PBE: 25/31 oocytes completed abscission (3 experiments).

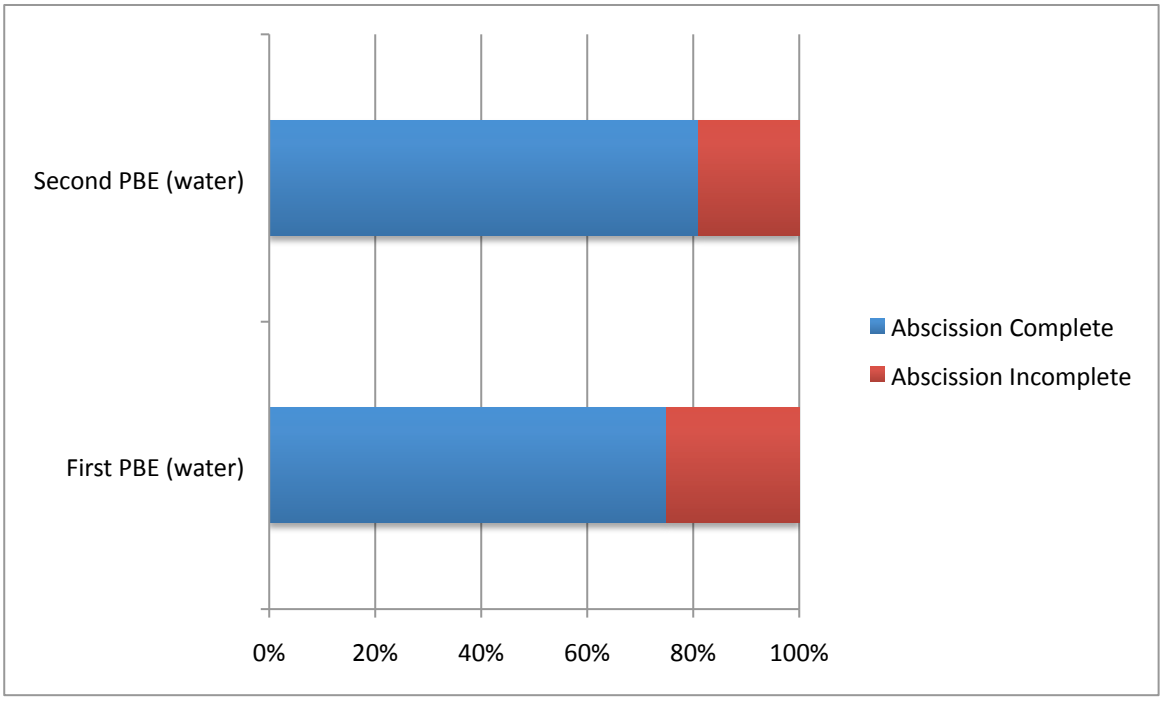
Second PBE (water)
First PBE (water)
0%
20%
40%
60%
80%
100%
Abscission Complete
Abscission Incomplete

Figure 23: **dbBAPTA inhibits abscission during first PBE.** GV oocytes were injected with mRNA for eGFP-H2B (chromosomes), followed by incubation in OCM with 1 mM progesterone to induce maturation (GVBD). GVBD oocytes are then followed by time-lapse confocal imaging approximately 1h45min following GVBD. Water or dbBAPTA was injected 2-5min following chromosome separation, then Dextran (Texas Red) was injected 1hr following chromosome separation. The oocyte was imaged again at least 15 min after Dextran injection to determine the status of abscission. Sectional views shown. The Volocity line tool acts as a scale bar. The fluorescence profiles presented in the bottom insets, as well as the scale, are magnified in the side panels. dbBAPTA also disrupts the normal formation of the metaphase II spindle (C= MII chromosomes cluster at the cortex). Below are cartoon models of the results, in which the first PB is closed in the control oocyte, and the first PB is open (red, dextran) in the dbBAPTA oocyte. The second PB in the control oocyte acts as a positive Dextran control (activation due to Dextran injection).

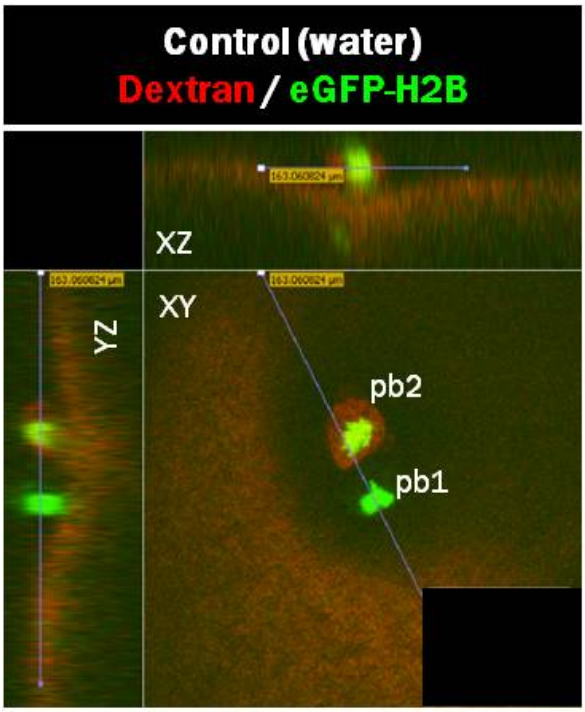

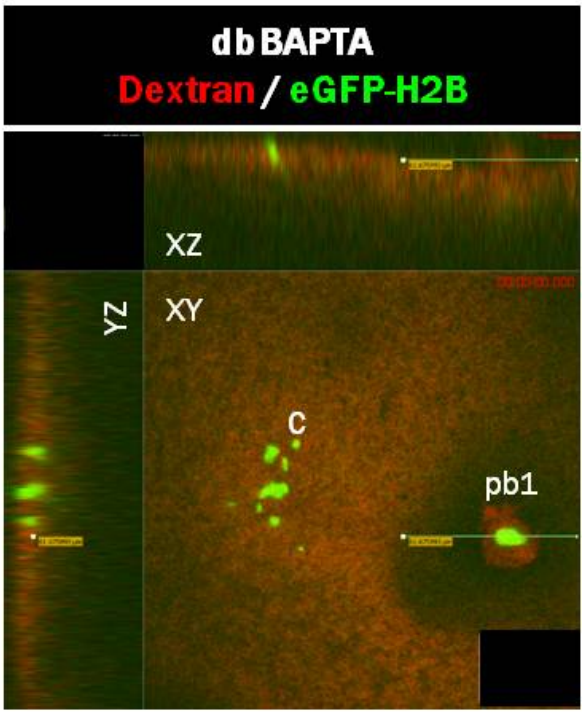

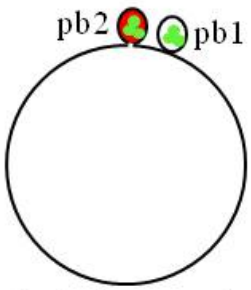

Abscission complete
(pb1 closed and pb2 open)

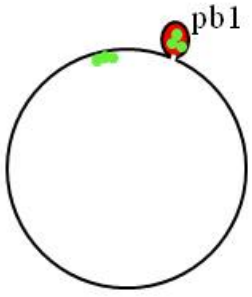

Abscission incomplete
(pb1 open)

Table 5: **dbBAPTA inhibits abscission during first PBE.** Table summarizes the results from Figure 22.
**p=0.0007, Fisher's exact test. Total of 2 experiments.

	Complete	**Incomplete**	**Total**
Control	22	8	**30**
dbBAPTA	5	16	**21**
Total	**27**	**24**	**51**

fails upon dbBAPTA injection (Fig. 23, right image and bottom cartoon). In addition, we also observed in these oocytes that the metaphase II spindle assembly was disrupted, as seen by the clusters of chromosomes laying at the cortex (Fig. 23, right image, marked as "C"). The spindle phenotype is consistent with our results (Fig. 17), as well as an earlier study that indicated the importance of calcium signaling in the meiotic spindle assembly in Xenopus oocytes (Sun and Machaca, 2004).

We also wanted to determine if dbBAPTA also inhibits second polar body abscission. First, oocytes were injected with the chromosome probe, and then were stimulated with progesterone overnight. The resulting MII-arrested oocytes were subsequently prick-activated, and confocal time-lapse imaging began in order to monitor for chromosome separation, and were injected with either water (10nL) or dbBAPTA (10nL 25mM) within 2-5min of the first sign of chromosome separation. The Dextran injection was done one hour following chromosome separation (Fig. 24). Figure 25 shows sectional views of a second polar body abscission assay. The control group possessed two closed polar bodies, indicated by the lack of red signal within them (Table 6, 25 second PB closed/31 oocytes, ~81%) (Fig. 25, left image and bottom cartoon). However, the majority of the oocytes in the dbBAPTA group possessed a closed first polar body and an open second polar body (Fig. 25, right image and bottom cartoon), demonstrating that second polar body abscission has failed in these oocytes. These results (Fig. 23 and 25) suggest that the calcium transient, as detected by the C2 accumulation, is required for polar body abscission.

The above results suggested that the calcium transient depicted by the C2 accumulation was required for polar body abscission. To support this notion, I carried out similar abscission

Figure 24: **Methods – Second polar body emission chelation and abscission assay.** GV oocytes were injected with mRNA, followed by incubation in OCM with 1 mM progesterone to induce maturation and enter MII-arrest. MII-arrested oocytes are then prick-activated and followed by time-lapse confocal imaging. *i*) The second polar body abscission assay was conducted following water or dbBAPTA injection (2-5min from the start of chromosome separation), by injecting fluorescently-labeled Dextran, 1hr following chromosome separation. The oocyte was imaged again at least 15 min after Dextran injection to determine the status of abscission. *ii*) Outcomes of the second polar body abscission assay.

i)

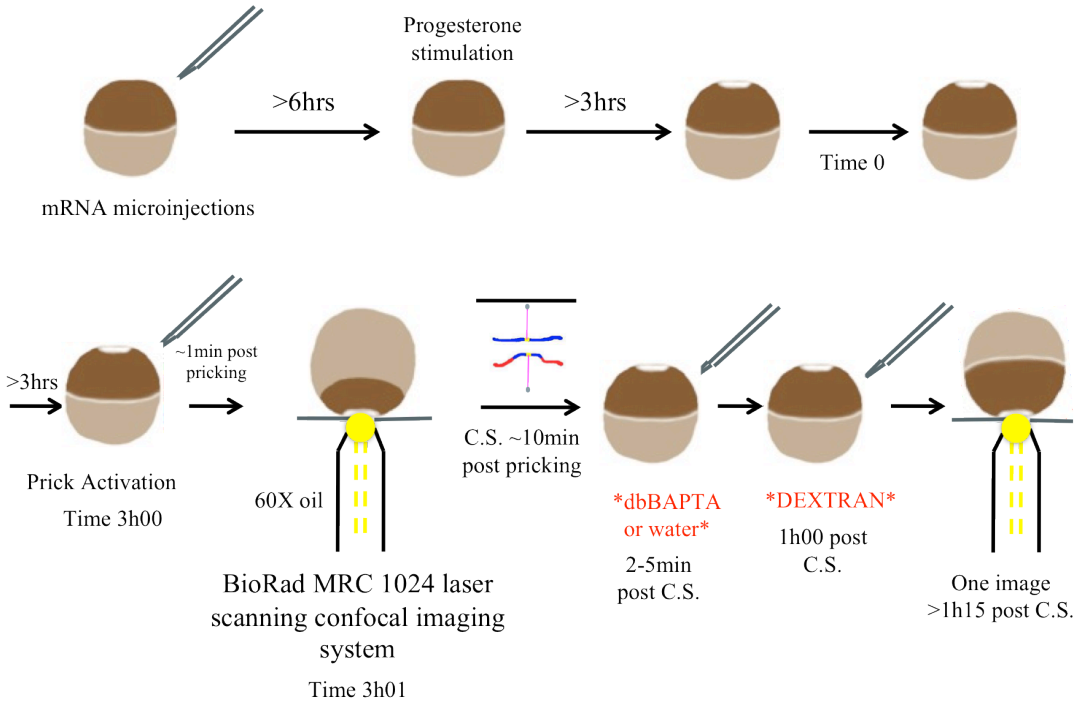
Progesterone stimulation
>6hrs
>3hrs
Time 0
mRNA microinjections
>3hrs
~1min post pricking
Prick Activation
Time 3h00
60X oil
C.S. ~10min post pricking
dbBAPTA or water
2-5min post C.S.
DEXTRAN
1h00 post C.S.
One image >1h15 post C.S.
BioRad MRC 1024 laser scanning confocal imaging system
Time 3h01

ii)

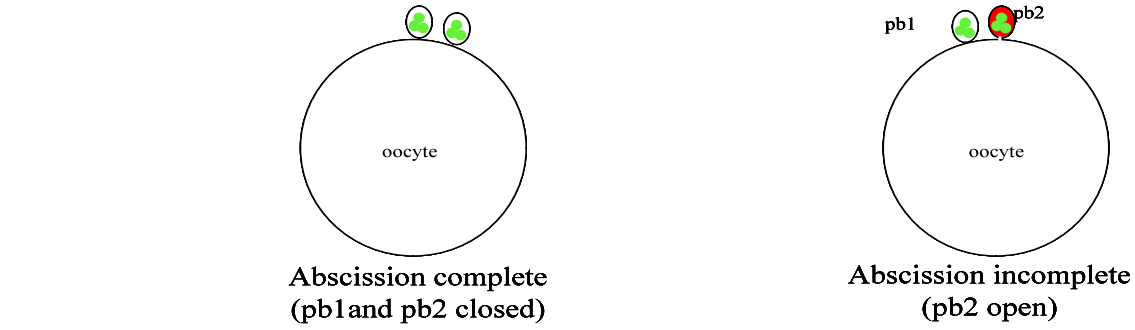
oocyte
Abscission complete (pb1and pb2 closed)
pb1
pb2
oocyte
Abscission incomplete (pb2 open)

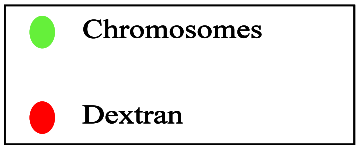
Chromosomes
Dextran

Figure 25: **dbBAPTA inhibits abscission during second PBE.** GV oocytes were injected with mRNA for eGFP-H2B (chromosomes), followed by incubation in OCM with 1 mM progesterone to induce maturation and enter MII-arrest. MII-arrested oocytes are then prick-activated and followed by time-lapse confocal imaging. Water or dbBAPTA was injected 2-5min following chromosome separation, then Dextran (Texas Red) was injected 1hr following chromosome separation. The images (sectional views) were taken following the abscission assay. The Volocity line tool acts as a scale bar. The fluorescence profiles presented in the bottom insets, as well as the scale, are magnified in the side panels. Below are cartoon models of the results, in which the first and second PBs are closed in the control oocyte, whereas the first PB is closed and the second polar body is open (red, Dextran) in the dbBAPTA oocyte.

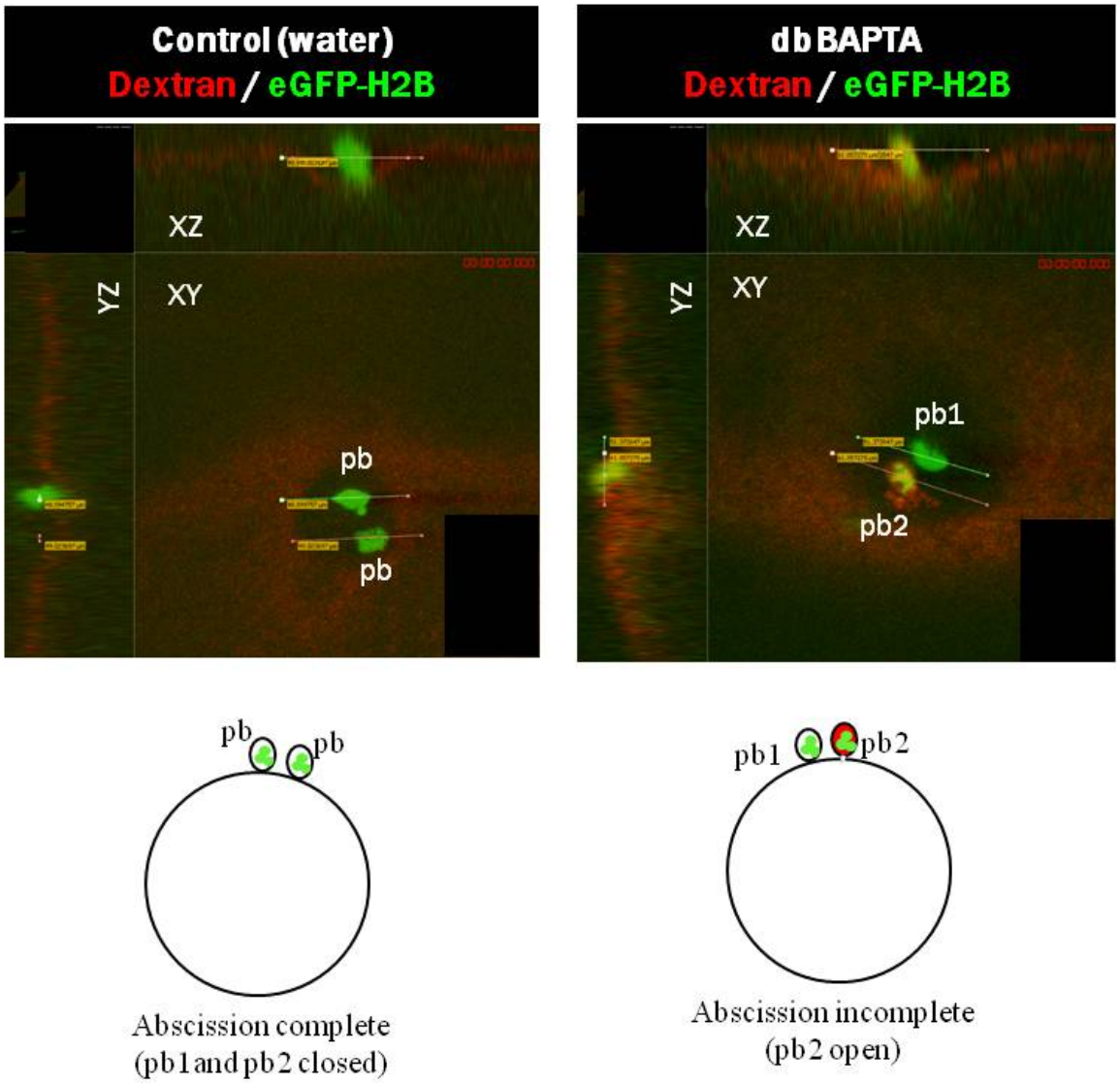
Control (water)
Dextran / eGFP-H2B
XZ
YZ
XY
pb
pb
db BAPTA
Dextran / eGFP-H2B
XZ
YZ
XY
pb1
pb2
pb
pb
Abscission complete
(pb1 and pb2 closed)
pb1
pb2
Abscission incomplete
(pb2 open)

Table 6: **dbBAPTA inhibits abscission during second PBE.** Table summarizes the results from Figure 24.
**p<0.0001, Fisher's exact test. Total of 3 experiments.

	Complete	**Incomplete**	**Total**
Control	25	6	**31**
dbBAPTA	6	26	**32**
Total	**31**	**32**	**63**

Figure 26: **Methods – First polar body emission late chelation and abscission assay.** GV oocytes were injected with mRNA, followed by incubation in OCM with 1 mM progesterone to induce maturation (GVBD). GVBD oocytes are then followed by time-lapse confocal imaging approximately 1h45min following GVBD. *i*) The first polar body abscission assay was conducted following water or dbBAPTA injection (20min following chromosome separation), by injecting fluorescently labeled Dextran, 1hr following chromosome separation. The oocyte was imaged again at least 15 min after Dextran injection to determine the status of abscission. *ii*) Outcomes of the first polar body abscission assay.

i)

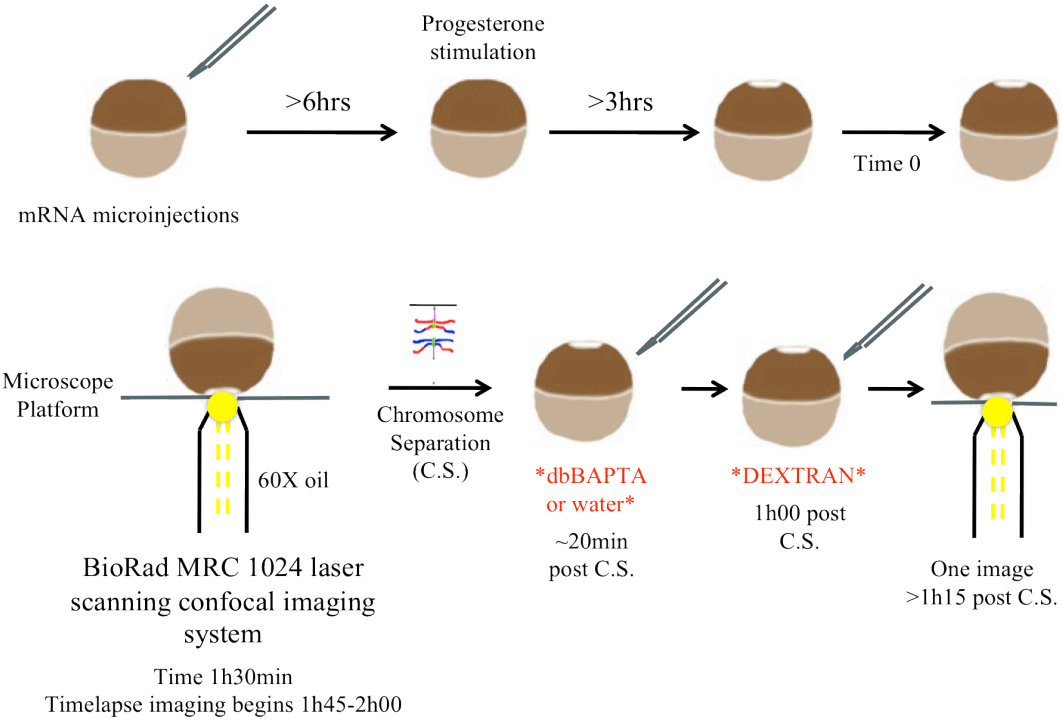
Progesterone
stimulation
>6hrs
>3hrs
Time 0
mRNA microinjections
Microscope
Platform
60X oil
Chromosome
Separation
(C.S.)
*dbBAPTA
or water*
~20min
post C.S.
DEXTRAN
1h00 post
C.S.
One image
>1h15 post C.S.
BioRad MRC 1024 laser
scanning confocal imaging
system
Time 1h30min
Timelapse imaging begins 1h45-2h00

ii)

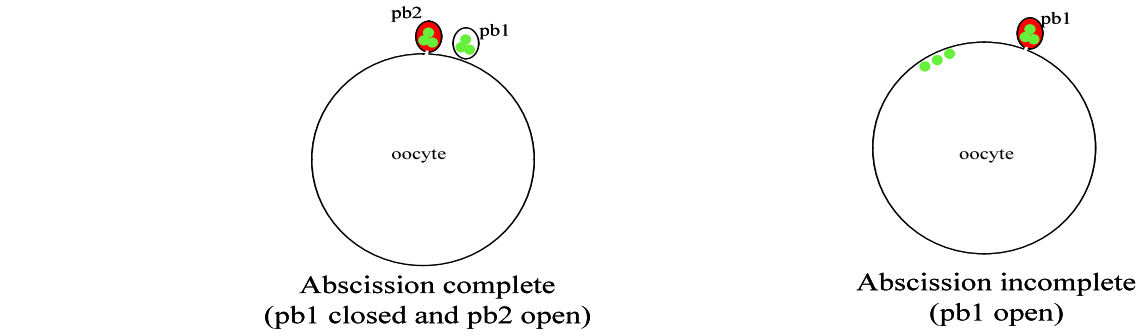
pb2
pb1
oocyte
Abscission complete
(pb1 closed and pb2 open)
pb1
oocyte
Abscission incomplete
(pb1 open)

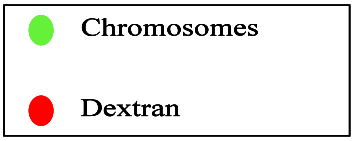
Chromosomes
Dextran

assays in oocytes in which dbBAPTA was injected after this calcium transient (Fig. 26). First, the oocytes were injected with the chromosome probe and then stimulated with progesterone, followed by monitoring of GVBD. GVBD oocytes were subjected to time-lapse confocal imaging to monitor chromosome segregation (anaphase). Water (10nL) or dbBAPTA (10nL 25mM) was injected into oocytes 20min following chromosome separation. Dextran was then injected 1hour later, and the oocyte imaged at least 15min later. The control group went on to complete first polar body abscission (Fig. 27, left image and bottom cartoon, PB devoid of red signal) (Table 7, 27 closed first PB/35 oocytes, ~77%), and subsequently form the second polar body (Fig. 27, left image and bottom cartoon, PB filled with red signal). Surprisingly, the dbBAPTA group failed first polar body abscission (Fig. 27, right image and bottom cartoon, PB filled with red signal) (Table 7, 8 closed first PB/34 (~24%)). This group also failed to properly assemble the second meiotic spindle, as observed by chromosomal clustering at the cortex (Fig. 27, right image, marked by "C"). Thus, second PBE does not occur in these oocytes. Importantly, these results suggest that continuing calcium signaling, one not detected by the C2 probe, is essential for successful completion of polar body abscission.

Figure 27: **dbBAPTA inhibits abscission during first PBE when injected 20min following chromosome separation**. GV oocytes were injected with mRNA for eGFP-H2B (chromosomes), followed by incubation in OCM with 1 mM progesterone to induce maturation (GVBD). GVBD oocytes are then followed by time-lapse confocal imaging approximately 1h45min following GVBD. Water or dbBAPTA was injected 20min following chromosome separation, then Dextran (Texas Red) was injected 1hr following chromosome separation. The oocyte was imaged again at least 15 min after Dextran injection to determine the status of abscission. Sectional views shown. The Volocity line tool acts as a scale bar. The fluorescence profiles presented in the bottom insets, as well as the scale, are magnified in the side panels. dbBAPTA also disrupts the normal formation of the metaphase II spindle (C= MII chromosomes cluster at the cortex). Below are cartoon models of the results, in which the first PB is closed and the second PB is open (red, Dextran) in the control oocyte, whereas the first PB is open (red, Dextran) in the dbBAPTA oocyte.

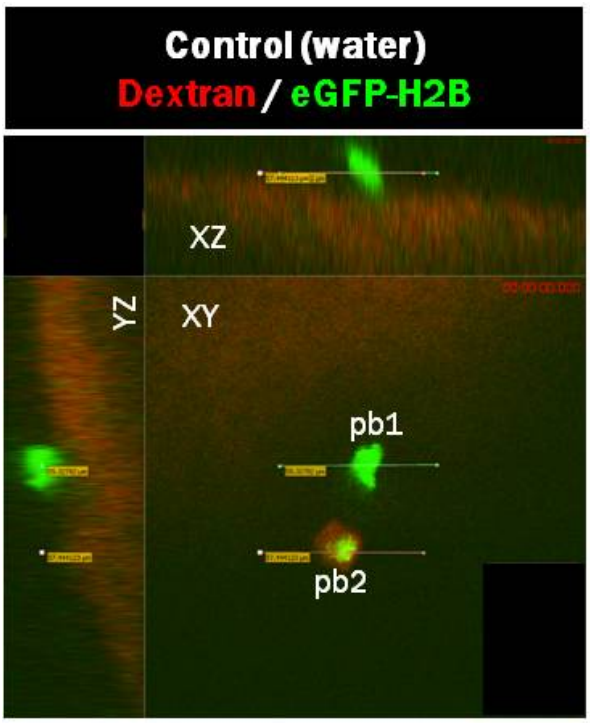

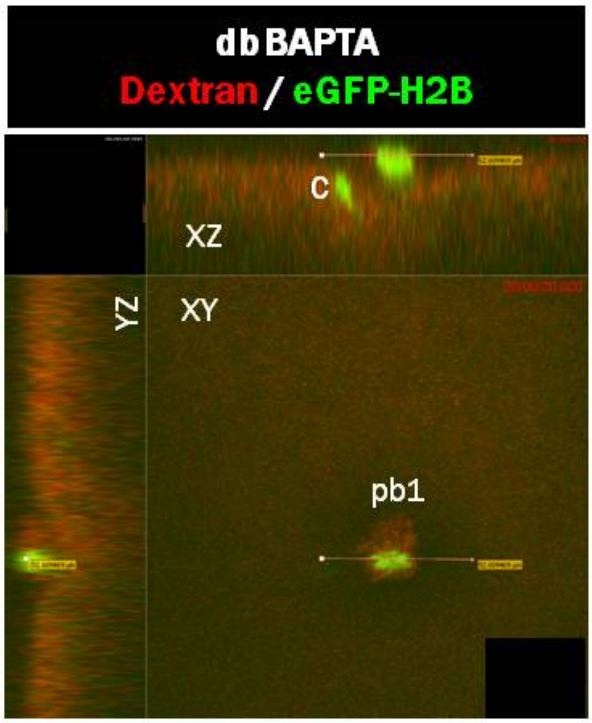

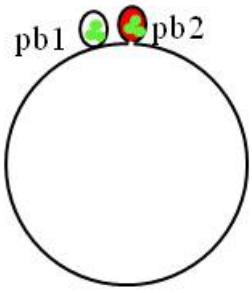

Abscission complete
(pb1 closed and pb2 open)

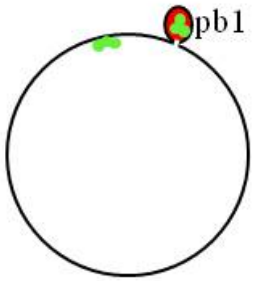

Abscission incomplete
(pb1 open)

Table 7: **dbBAPTA inhibits abscission during first PBE when injected 20min following chromosome separation.** Table summarizes the results from Figure 26.
**p<0.0001, Fisher's exact test. Total of 3 experiments.

	Closed	**Open**	**Total**
Control	27	8	**35**
dbBAPTA	8	26	**34**
Total	**35**	**34**	**69**

DISCUSSION

Cdc42 Activation during Second Polar Body Emission

In this thesis, parallels have been made with cdc42 and RhoA activation in PBE and in single-cell wound healing (Benink and Bement, 2005), as well as cdc42 activation in PBE and in cortical granule exocytosis membrane retrieval (Sokac et al., 2003; Yu and Bement, 2007). Similar to PBE, these two processes involve localized activation of cdc42 that mediates F-actin polymerization. Furthermore, PBE and single-cell wound healing both involve temporally and spatially coordinated activation of cdc42 and RhoA. Importantly, calcium signaling is required upstream of the two GTPases in wound healing and CGE membrane retrieval. Therefore, the central scheme of my thesis is to determine if calcium signaling is also required for PBE.

Before delving into the calcium research, I wished to determine if the interplay between cdc42 and RhoA is restricted to first PBE, or if it is similarly required for second PBE. We chose parthenogenetic activation by piercing the MII-arrested oocyte with a glass needle, over activation by a calcium ionophore (A23187) (Fig. 5), because not only is it more consistent in promoting complete PBE (Fig. 6), but also because it promotes the propagation of the wave through one entry point, similar to that of the sperm-induced propagation.

Similarly to first PBE, cdc42 is activated during anaphase II at the cortical region overlaying the spindle. Activated cdc42 encompasses the cortex of the protruding polar body. Furthermore, over-expression of $cdc42^{T17N}$ diminished cdc42 activation, abolished

membrane protrusion, and inhibited second PBE (Fig. 7 and 8). It is important to note that in experiments depicted in Figure 8, cdc42^{T17N} is present prior to oocyte maturation (meiosis I). These oocytes did not emit the first polar body, and therefore contained a metaphase II spindle with twice as many chromosomes as a normal metaphase II oocyte (Fig. 8, (Ma et al., 2006; Zhang et al., 2008)). More importantly, the presence of cdc42^{T17N} did not inhibit parthenogenetic activation (Fig. 8, chromosome separation at 00:03), implying that cdc42 is not involved in calcium-mediated egg activation (not including CGE).

As in *Xenopus laevis*, active cdc42 in the mouse oocyte accumulates around the nascent polar body (1st and 2nd), within the actin cap. Using the dominant negative cdc42^{T17N}, Dehapiot, B. et al. concluded that inhibition of cdc42 prevents second polar body emission and produces central spindle defects. However, they argue that cdc42 during meiosis-I is dispensable for first polar body emission, since 34% of oocytes are still able to emit a first, albeit small polar body. More importantly a recent study using conditional knock-out of cdc42 in the mouse ovaries has highlighted the role of cdc42 in polar body emission (Wang et al., 2013). In these mice, which are infertile, the oocytes where not able to form the polar body F-actin cap, while the spindle and anaphase initiation remained intact. In contrast, earlier studies, using *in vitro* oocyte maturation and various dominant negative strategies, have concluded that cdc42 is involved in the formation of the spindle and in asymmetrical spindle localization, in mouse oocytes (Bielak-Zmijewska et al., 2008; Cui et al., 2007; Dehapiot et al., 2013; Na and Zernicka-Goetz, 2006).

Furthermore, active cdc42's spatial arrangement relative to active RhoA's localization during second PBE (Fig. 9, 10) is reminiscent of their arrangement during first PBE (Zhang et al.,

2008). Active RhoA's association with second PBE further suggests that PBE uses the canonical contractile ring pathway, which includes an actomyosin ring, but also important mediators such as RhoA (Fig. 9 and 10) and Anillin (Fig. 14 and 19). While RhoA is required for promoting both the meiotic (Zhang et al., 2008) and the mitotic contractile ring (Drechsel et al., 1997) in *Xenopus laevis*, cdc42's role is enigmatic. While cdc42 is certainly required for the formation of the polar body membrane protrusion and hence essential to this form of asymmetrical cell division ((Zhang et al., 2008), Fig. 7, 8 (Leblanc et al., 2011)), cdc42's role in Xenopus mitosis is uncertain. In contrast to the clear demonstration of active cdc42 during polar body emission (Ma, Zhang, and here), no similar cdc42 activation has been reported during mitosis. Depletion of the maternal stockpile of cdc42 mRNA in Xenopus oocytes using antisense oligonucleotides (up to 90%), permits the egg to enter through embryogenesis (at least until late blastulae or early gastrulae) (Kofron, 2002). Thus, it seems that cdc42 might not be essential to cytokinesis. An alternative interpretation might be that, since at least 10% of maternal cdc42 mRNA still remains, and that there is also the maternal cdc42 protein remaining in these embryos, the residual cdc42 may support cytokinesis. This interpretation would be more in line with another study suggesting that cdc42 is in fact important during Xenopus mitosis (Drechsel et al., 1997). Abrogation of cdc42 activation by the dominant negative $cdc42^{T17N}$ in Xenopus embryos, led to partial cleavage furrowing, while specification and early ingression of the furrow were not affected. It is suggested that cdc42 may be involved in the precise targeting of membranes to the cleavage furrow (Drechsel et al., 1997). Altogether, unlike RhoA's direct role in cytokinesis, cdc42 may possess different, but essential roles in the regulation of this process. In meiosis, cdc42 is not only essential to the creation of the membrane protrusion during first and second PBE, but also to the proper regulation of the contractile ring (Zhang et al., 2008). While in

mitosis, there is no "membrane protrusion", membrane dynamics are an important part of the process, and it remains to be seen what roles cdc42 may have in the regulation of them, or, in general, cytokinesis.

Calcium Signaling during Polar Body Emission

Our quest in the understanding of the regulation of both cdc42 and RhoA during PBE led us to evaluate calcium signaling throughout PBE. Specifically, we have demonstrated a role for calcium during PBE. Indeed, we have shown that our strategy (C2 probe) was not only capable of detecting the global fertilization/activation calcium increase ((Yu and Bement, 2007), Fig. 11 and 13), but also capable of detecting a localized calcium transient during PBE (Fig. 12 and 13).

While the calcium transient detection rate varies between individual groups of oocytes, it does consistently occur ~13min (average: 13.1 +/- 2.6min S.D.) following chromosome separation of both first and second PBE (Fig. 12, 13). More importantly, it is inhibited by the calcium chelator, dbBAPTA (Fig. 18), indicating that it is a calcium-driven event. The relative low calcium affinity of the C2 probe is most likely the cause of the low detection rate. The calcium transients that are being detected are above the required calcium threshold and most likely detected at the peak of the calcium transient. This is consistent with work done on PKCα association with the plasma membrane in fertilized mouse eggs (Halet et al., 2004). PKCα association with the plasma membrane oscillates with the peak of the calcium oscillations following fertilization. Its translocation (through its C2 domain) is dependent

upon the amplitude and frequency of these oscillations, and therefore, only when intracellular calcium reaches 1-3μM, does it reach the plasma membrane (Halet et al., 2004). During PBE, it is also possible that a similar high amplitude calcium transient (Fig. 12, 13), is targeting PKCβ to the future site of abscission. Specifically, it is possible that the C2 increase may indirectly reflect the translocation of full-length PKCβ. PKCβ could be a mediator of abscission, as suggested by others (Saurin et al., 2008), as a result of being targeted by the calcium transient (Fig. 28B). This remains to be investigated.

If what we are detecting with the C2 probe is only the highest amplitude signals, this also suggests there might be the potential for detecting calcium earlier and later than the ~13min following chromosome separation calcium transient (Fig. 28). Indeed, this is consistent with our observation that chelating calcium prior to anaphase initiation (1h following GVBD) prevented the formation of the first polar body (Fig. 17), although the exact cause of PBE failure is not yet clear. To note, calcium signaling has been implicated in the spindle assembly during oocyte maturation in the frog (Sun and Machaca, 2004). Further, when calcium is chelated 20min following chromosome separation (Fig. 27), abscission also fails, indicating that calcium signals later than the detected calcium transient are required for abscission. This underlines the limitations of using the C2 domain as the calcium sensor. In the future, other higher affinity calcium sensors, particularly genetically encoded calcium indicators (Mank and Griesbeck, 2008), should be exploited to determine if this hypothesis is correct.

Figure 28: **A model -- the calcium transient is required for abscission during PBE.** A putative model describing our observations. A) Side view of the PM is depicted. Activation of cdc42 and RhoA occur at anaphase I and II. This is followed by a calcium signal detected 13min later. To be detected, this C2 signal must achieve the threshold calcium concentration for translocation (graph; red dotted line = threshold calcium concentration, grey dotted line = hypothetical calcium increase in the oocyte). B) Calcium is required for the completion of abscission. PKCβ may be a target of this signal to regulate the last step of cytokinesis (see discussion) within the contractile ring (C.R.). Calcium and diacylglycerol (DAG) are activators of conventional PKCs. Time represents minutes following chromosome separation. See Fig. 1 and 2 for a complete figure legend.

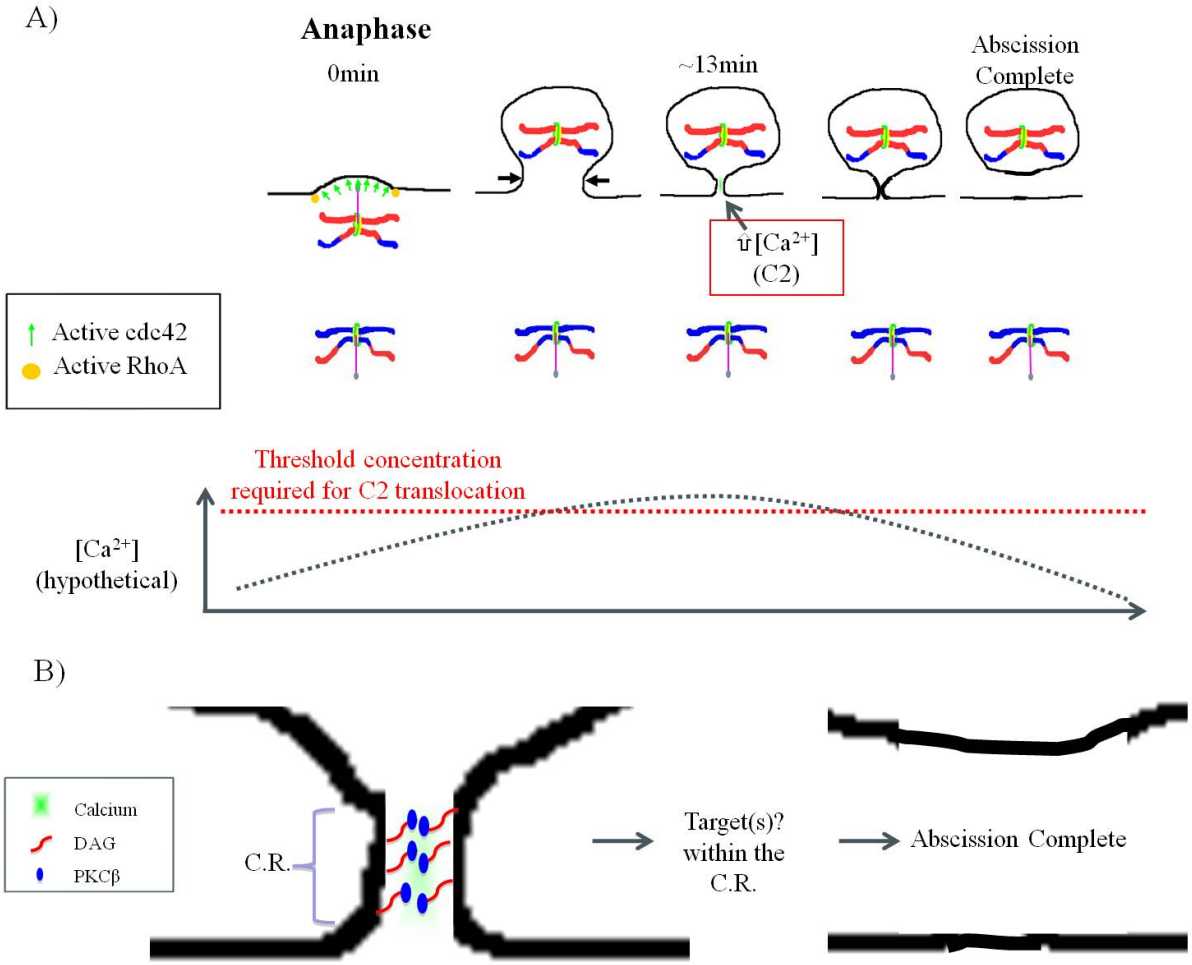
A)
Anaphase
0min
~13min
Abscission
Complete
↑[Ca2+]
(C2)
Active cdc42
Active RhoA
Threshold concentration
required for C2 translocation
[Ca2+]
(hypothetical)
B)
Calcium
DAG
PKCβ
C.R.
Target(s)?
within the
C.R.
Abscission Complete

Nevertheless, first and second PBE abscission is inhibited when intracellular calcium is chelated (Fig. 23, 25). Injection of dbBAPTA, the chelator, was conducted following chromosome separation in order to prevent possible spindle defects associated with the inhibition of calcium signaling. dbBAPTA is known to inhibit calcium gradients by shuttling calcium from the high calcium concentration end to the lowest, due to its relatively low affinity for calcium (K_D= 1.5μM (Miller et al., 1993)) (Duesbery and Masui, 1996; Miller et al., 1993; Snow and Nuccitelli, 1993; Speksnijder et al., 1989). This would suggest that abscission is also being inhibited by this mechanism. "Shuttle buffering", as it is known, makes the chelator dbBAPTA a more efficient buffer, compared to other chelators with higher affinity for calcium (i.e. EGTA, K_D= 0.01μM, (Miller et al., 1993)), which more likely will cause non-specific effects due to changes to calcium homeostasis. I have further shown that closing of the contractile ring was not prevented in oocytes injected with dbBAPTA following chromosome separation (Fig. 20), nor was the membrane protrusion (Fig. 19). This indicates that the inhibition of abscission was a direct result of targeting abscission and not other processes (membrane protrusion and constriction) required prior to its completion. I propose that the calcium transient detected with the C2 probe is in fact essential for the completion of abscission. This is also consistent with the observation that the transient occurs within the contractile ring (Fig. 14), the site for abscission.

Similarly, calcium signaling may also be involved in anaphase initiation, as suggested in mouse oocytes (Tombes et al., 1992) and in sea urchin embryos (Ciapa et al., 1994; Groigno and Whitaker, 1998; Poenie et al., 1985; Wilding et al., 1996). Confocal time-lapse imaging using the C2 probe detects enrichment of fluorescence within the spindle (Fig. 12). However,

there is no consistent increase of C2 signal prior to or just at the time of anaphase initiation (Fig. 12). Therefore the significance of the spindle associated C2 is currently uncertain. Furthermore, due to the effect of dbBAPTA on the spindle structure, it is very difficult, if at all possible, to specifically determine its effect on anaphase initiation. Ratiometric imaging might improve the resolution of putative calcium signals emanating from the spindle, but this, however, has not been approached for PBE.

Conclusion

We have for the first time detected a distinct calcium signal during polar body emission in the *Xenopus laevis* oocyte. My work also clearly indicates that this calcium transient is novel and distinct from the well-known fertilization specific calcium transient. First, it occurs during first polar body emission. Second, this transient, during second polar body emission, is temporally and spatially distinct from the fertilization wave. Temporally, it occurs 12 min after anaphase initiation while the fertilization calcium wave is complete before anaphase initiation. Spatially, this transient is restricted to the cortical region near the contractile ring, in contrast to the fertilization calcium wave, which is over the entire cortex. We have also developed a novel assay to determine the status of abscission during polar body emission. By combining the abscission assay and timely dbBAPTA injections, we have shown that this calcium transient is required for the last step of cytokinesis, abscission.

REFERENCES

Acquaviva, C., and Pines, J. (2006). The anaphase-promoting complex/cyclosome: APC/C. J Cell Sci *119*, 2401–2404.

Adams, A.E., Johnson, D.I., Longnecker, R.M., Sloat, B.F., and Pringle, J.R. (1990). CDC42 and CDC43, two additional genes involved in budding and the establishment of cell polarity in the yeast Saccharomyces cerevisiae. J Cell Biol *111*, 131–142.

Backs, J., Stein, P., Backs, T., Duncan, F.E., Grueter, C.E., McAnally, J., Qi, X., Schultz, R.M., and Olson, E.N. (2010). The isoform of CaM kinase II controls mouse egg activation by regulating cell cycle resumption. Pnas *107*, 81–86.

Bataillon, E. (1910). L"embryogenese complete provoquee chez les amphibiens par piqure de l"oeuf vierge, larve parthenogenetiques de Rana Fusca. Compt Rend Acad Sci.

Baulieu, E.E. (1983). Steroid-Membrane-Adenylate Cyclase Interactions during Xenopus laevis Oocyte Meiosis Reinitiation: A New Mechanism of Steroid Hormone Action. Experimental and Clinical Endocrinology & Diabetes *81*, 3–16.

Bayaa, M., Booth, R.A., Sheng, Y., and Liu, X.J. (2000). The classical progesterone receptor mediates Xenopus oocyte maturation through a nongenomic mechanism. Pnas *97*, 12607–12612.

Bement, W.M., Benink, H.A., and Dassow, von, G. (2005). A microtubule-dependent zone of active RhoA during cleavage plane specification. J Cell Biol *170*, 91–101.

Bement, W.M., Miller, A.L., and Dassow, von, G. (2006). Rho GTPase activity zones and transient contractile arrays. BioEssays *28*, 983–993.

Benink, H.A., and Bement, W.M. (2005). Concentric zones of active RhoA and Cdc42 around single cell wounds. J Cell Biol *168*, 429–439.

Bielak-Zmijewska, A., Kolano, A., Szczepanska, K., Maleszewski, M., and Borsuk, E. (2008). Cdc42 protein acts upstream of IQGAP1 and regulates cytokinesis in mouse oocytes and embryos. Developmental Biology *322*, 21–32.

Brunet, S., and Verlhac, M.H. (2011). Positioning to get out of meiosis: the asymmetry of division. Hum. Reprod. Update *17*, 68–75.

Bugrim, A., Fontanilla, R., Eutenier, B.B., Keizer, J., and Nuccitelli, R. (2003). Sperm Initiate a Ca2+ Wave in Frog Eggs that is More Similar to Ca2+ Waves Initiated by IP3 than by Ca2. Biophysical Journal *84*, 1580–1590.

Busa, W.B., and Nuccitelli, R. (1985). An elevated free cytosolic Ca2+ wave follows fertilization in eggs of the frog, Xenopus laevis. J Cell Biol *100*, 1325–1329.

Busa, W.B., Ferguson, J.E., Joseph, S.K., Williamson, J.R., and Nuccitelli, R. (1985).

Activation of frog (Xenopus laevis) eggs by inositol trisphosphate. I. Characterization of Ca2+ release from intracellular stores. J Cell Biol *101*, 677–682.

Chao, W.C.H., Kulkarni, K., Zhang, Z., Kong, E.H., and Barford, D. (2012). Structure of the mitotic checkpoint complex. Nature *484*, 208–213.

Ciapa, B., Pesando, D., Wilding, M., and Whitaker, M. (1994). Cell-cycle calcium transients driven by cyclic changes in inositol trisphosphate levels. , Published Online: 18 November 1993; | Doi:10.1038/366270a0 *368*, 875–878.

Cui, X.-S., Li, X.Y., and Kim, N.-H. (2007). Cdc42 is implicated in polarity during meiotic resumption and blastocyst formation in the mouse. Molecular Reproduction and Development *74*, 785–794.

Dehapiot, B., Carrière, V., Carroll, J., and Halet, G. (2013). Polarized Cdc42 activation promotes polar body protrusion and asymmetric division in mouse oocytes. Developmental Biology *377*, 202–212.

Deng, M., Suraneni, P., Schultz, R.M., and Li, R. (2007). The Ran GTPase Mediates Chromatin Signaling to Control Cortical Polarity during Polar Body Extrusion in Mouse Oocytes. Developmental Cell *12*, 301–308.

Dong, J.-B., Tang, T.-S., and Sun, F.-Z. (2000). Xenopus and Chicken Sperm Contain a Cytosolic Soluble Protein Factor Which Can Trigger Calcium Oscillations in Mouse Eggs. Biochemical and Biophysical Research Communications *268*, 947–951.

Douglas, M.E., and Mishima, M. (2010). Still entangled: Assembly of the central spindle by multiple microtubule modulators. Seminars in Cell & Developmental Biology *21*, 899–908.

Drechsel, D.N., Hyman, A.A., Hall, A., and Glotzer, M. (1997). A requirement for Rho and Cdc42 during cytokinesis in Xenopus embryos. Current Biology *7*, 12–23.

Duesbery, N.S., and Masui, Y. (1996). The role of Ca2+ in progesterone-induced germinal vesicle breakdown of Xenopus laevis oocytes: the synergic effects of microtubule depolymerization and Ca2. Dev Gene Evol *206*, 110–124.

Dumont, J.N. (1972). Oogenesis in Xenopus laevis (Daudin). I. Stages of oocyte development in laboratory maintained animals. Journal of Morphology *136*, 153–179.

Eggert, U.S., Mitchison, T.J., and Field, C.M. (2006). Animal Cytokinesis: From Parts List to Mechanisms. Http://Dx.Doi.org/10.1146/Annurev.Biochem.74.082803.133425 *75*, 543–566.

El-Jouni, W., Jang, B., Haun, S., and Machaca, K. (2005). Calcium signaling differentiation during Xenopus oocyte maturation. Developmental Biology *288*, 514–525.

Elbaz, J., Reizel, Y., Nevo, N., Galiani, D., and Dekel, N. (2013). Epithelial Cell Transforming Protein 2 (ECT2) Depletion Blocks Polar Body Extrusion and Generates

Mouse Oocytes Containing Two Metaphase II Spindles. Http://Dx.Doi.org/10.1210/en.2009-0830 *151*, 755–765.

Elia, N., Sougrat, R., Spurlin, T.A., Hurley, J.H., and Lippincott-Schwartz, J. (2011). Dynamics of endosomal sorting complex required for transport (ESCRT) machinery during cytokinesis and its role in abscission. Pnas *108*, 4846–4851.

Eyers, P.A., Liu, J., Hayashi, N.R., Lewellyn, A.L., Gautier, J., and Maller, J.L. (2005). Regulation of the G2/M Transition in Xenopus Oocytes by the cAMP-dependent Protein Kinase. J. Biol. Chem. *280*, 24339–24346.

Fall, C.P., Wagner, J.M., Loew, L.M., and Nuccitelli, R. (2004). Cortically restricted production of leads to propagation of the fertilization wave along the cell surface in a model of the Xenopus egg. Journal of Theoretical Biology *231*, 487–496.

Fan, H.-Y., Sun, Q.-Y., and Zou, H. (2006). Regulation of Separase in Meiosis: Separase is Activated at the Metaphase I-II Transition in Xenopus Oocytes during Meiosis. Cell Cycle *5*, 198–204.

Ferrell, J.E., and Machleder, E.M. (1998). The biochemical basis of an all-or-none cell fate switch in Xenopus oocytes. Science *280*, 895–898.

Ferrell, J.E. (1999). Xenopus oocyte maturation: new lessons from a good egg. BioEssays *21*, 833–842.

FitzHarris, G., Larman, M.G., Richards, C., and Carroll, J. (2005). An increase in [Ca2+]i is sufficient but not necessary for driving mitosis in early mouse embryos. J Cell Sci *118*, 4563–4575.

Flemming, W. (1891). Neue Beiträge zur Kenntnis der Zelle. Arch Mikrosk Anat *37*, 685–751.

Foerder, C.A., and Shapiro, B.M. (1977). Release of ovoperoxidase from sea urchin eggs hardens the fertilization membrane with tyrosine crosslinks. Proc. Natl. Acad. Sci. U.S.a. *74*, 4214–4218.

Gard, D.L. (1992). Microtubule organization during maturation of Xenopus oocytes: Assembly and rotation of the meiotic spindles. Developmental Biology *151*, 516–530.

Gilbert, S.F. (2000). Gamete Fusion and the Prevention of Polyspermy.

Glabe, C.G., and Vacquier, V.D. (1978). Egg surface glycoprotein receptor for sea urchin sperm binding. Proc. Natl. Acad. Sci. U.S.a. *75*, 881–885.

Gonczy, P. (2008). Mechanisms of asymmetric cell division: flies and worms pave the way. Nature Reviews Molecular Cell Biology *9*, 355–366.

Gorr, I.H., Boos, D., and Stemmann, O. (2005). Mutual Inhibition of Separase and Cdk1 by

Two-Step Complex Formation. Molecular Cell *19*, 135–141.

Grey, R.D., Wolf, D.P., and Hedrick, J.L. (1974). Formation and structure of the fertilization envelope in Xenopus laevis. Developmental Biology.

Groigno, L., and Whitaker, M. (1998). An anaphase calcium signal controls chromosome disjunction in early sea urchin embryos. Cell.

Gromley, A., Yeaman, C., Rosa, J., Redick, S., Chen, C.-T., Mirabelle, S., Guha, M., Sillibourne, J., and Doxsey, S.J. (2005). Centriolin Anchoring of Exocyst and SNARE Complexes at the Midbody Is Required for Secretory-Vesicle-Mediated Abscission. Cell *123*, 75–87.

Guizetti, J., Schermelleh, L., Mäntler, J., Maar, S., Poser, I., Leonhardt, H., Müller-Reichert, T., and Gerlich, D.W. (2011). Cortical Constriction During Abscission Involves Helices of ESCRT-III–Dependent Filaments. Science *331*, 1616–1620.

Hagting, A., Elzen, den, N., Vodermaier, H.C., Waizenegger, I.C., Peters, J.-M., and Pines, J. (2002). Human securin proteolysis is controlled by the spindle checkpoint and reveals when the APC/C switches from activation by Cdc20 to Cdh1. J Cell Biol *157*, 1125–1137.

Halet, G., and Carroll, J. (2007). Rac Activity Is Polarized and Regulates Meiotic Spindle Stability and Anchoring in Mammalian Oocytes. Developmental Cell *12*, 309–317.

Halet, G., Marangos, P., FitzHarris, G., and Carroll, J. (2003). Ca2+ oscillations at fertilization in mammals. Biochem. Soc. Trans. *31*, 907–911.

Halet, G., Tunwell, R., Parkinson, S.J., and Carroll, J. (2004). Conventional PKCs regulate the temporal pattern of Ca2+ oscillations at fertilization in mouse eggs. J Cell Biol *164*, 1033–1044.

Hansen, D.V., Tung, J.J., and Jackson, P.K. (2006). CaMKII and polo-like kinase 1 sequentially phosphorylate the cytostatic factor Emi2/XErp1 to trigger its destruction and meiotic exit. Proc. Natl. Acad. Sci. U.S.a. *103*, 608–613.

Heasman, S.J., and Ridley, A.J. (2008). Mammalian Rho GTPases: new insights into their functions from in vivo studies. Nature Reviews Molecular Cell Biology *9*, 690–701.

Hepler, P.K., and Callaham, D.A. (1987). Free calcium increases during anaphase in stamen hair cells of Tradescantia. J Cell Biol *105*, 2137–2143.

Holland, A.J., and Taylor, S.S. (2006). Cyclin-B1-mediated inhibition of excess separase is required for timely chromosome disjunction. J Cell Sci *119*, 3325–3336.

Houghtaling, B.R., Yang, G., Matov, A., Danuser, G., and Kapoor, T.M. (2009). Op18 reveals the contribution of nonkinetochore microtubules to the dynamic organization of the vertebrate meiotic spindle. Pnas *106*, 15338–15343.

Hu, C.-K., Coughlin, M., and Mitchison, T.J. (2012). Midbody assembly and its regulation during cytokinesis. Mol. Biol. Cell *23*, 1024–1034.

Hylander, B.L., and Summers, R.G. (1982). An ultrastructural immunocytochemical localization of hyalin in the sea urchin egg. Developmental Biology.

Inaba, M., and Yamashita, Y.M. (2012). Asymmetric Stem Cell Division: Precision for Robustness. Cell Stem Cell *11*, 461–469.

Ishiguro, K., and Watanabe, Y. (2007). Chromosome cohesion in mitosis and meiosis. J Cell Sci *120*, 367–369.

Ishiguro, T., Tanaka, K., Sakuno, T., and Watanabe, Y. (2010). Shugoshin|[ndash]|PP2A counteracts casein-kinase-1-dependent cleavage of Rec8 by separase. Nature Cell Biology *12*, 500–506.

Isoda, M., Sako, K., Suzuki, K., Nishino, K., and Nakajo, N. (2011). Dynamic Regulation of Emi2 by Emi2-Bound Cdk1/Plk1/CK1 and PP2A-B56 in Meiotic Arrest of Xenopus Eggs. Developmental Cell.

Izant, J.G. (1983). The role of calcium ions during mitosis. Chromosoma.

J Pines, T.H. (1987). Molecular cloning and characterization of the mRNA for cyclin from sea urchin eggs. The EMBO Journal *6*, 2987.

Johnson, D.I. (1999). Cdc42: An essential Rho-type GTPase controlling eukaryotic cell polarity. Microbiol. Mol. Biol. Rev. *63*, 54–105.

Katis, V.L., Galova, M., Rabitsch, K.P., Gregan, J., and Nasmyth, K. (2004). Maintenance of Cohesin at Centromeres after Meiosis I in Budding Yeast Requires a Kinetochore-Associated Protein Related to MEI-S332. Current Biology *14*, 560–572.

Katis, V.L., Lipp, J.J., Imre, R., Bogdanova, A., Okaz, E., Habermann, B., Mechtler, K., Nasmyth, K., and Zachariae, W. (2010). Rec8 Phosphorylation by Casein Kinase 1 and Cdc7-Dbf4 Kinase Regulates Cohesin Cleavage by Separase during Meiosis. Developmental Cell *18*, 397–409.

Kishimoto, T. (2003). Cell-cycle control during meiotic maturation. Current Opinion in Cell Biology *15*, 654–663.

Kitajima, T.S., Kawashima, S.A., and Watanabe, Y. (2004). The conserved kinetochore protein shugoshin protects centromeric cohesion during meiosis. Nature *427*, 510–517.

Kitajima, T.S., Sakuno, T., Ishiguro, K.-I., Iemura, S.-I., Natsume, T., Kawashima, S.A., and Watanabe, Y. (2006). Shugoshin collaborates with protein phosphatase 2A to protect cohesin. Nature *441*, 46–52.

Knott, J.G., Gardner, A.J., Madgwick, S., and Jones, K.T. (2006). Calmodulin-dependent

protein kinase II triggers mouse egg activation and embryo development in the absence of Ca 2+ oscillations. Developmental ….

Kofron, M. (2002). Plakoglobin is required for maintenance of the cortical actin skeleton in early Xenopus embryos and for cdc42-mediated wound healing. J Cell Biol *158*, 695–708.

Kudo, N.R., Wassmann, K., Anger, M., Schuh, M., Wirth, K.G., Xu, H., Helmhart, W., Kudo, H., Mckay, M., Maro, B., et al. (2006). Resolution of Chiasmata in Oocytes Requires Separase-Mediated Proteolysis. Cell *126*, 135–146.

Laporte, D., Coffman, V.C., Lee, I.-J., and Wu, J.-Q. (2011). Assembly and architecture of precursor nodes during fission yeast cytokinesis. J Cell Biol *192*, 1005–1021.

Lara-Gonzalez, P., Westhorpe, F.G., and Taylor, S.S. (2012). The Spindle Assembly Checkpoint. Current Biology *22*, R966–R980.

Larman, M.G., Saunders, C.M., Carroll, J., Lai, F.A., and Swann, K. (2004). Cell cycle-dependent Ca2+ oscillations in mouse embryos are regulated by nuclear targeting of PLCzeta. J Cell Sci *117*, 2513–2521.

Leblanc, J., Zhang, X., McKee, D., Wang, Z.B., Li, R., Ma, C., Sun, Q.Y., and Liu, X.J. (2011). The small GTPase Cdc42 promotes membrane protrusion during polar body emission via ARP2-nucleated actin polymerization. Mol. Hum. Reprod. *17*, 305–316.

Lee, H.H., Elia, N., Ghirlando, R., and Lippincott-Schwartz, J. (2008a). Midbody targeting of the ESCRT machinery by a noncanonical coiled coil in CEP55. Science.

Lee, J., Kitajima, T.S., Tanno, Y., Yoshida, K., Morita, T., Miyano, T., Miyake, M., and Watanabe, Y. (2008b). Unified mode of centromeric protection by shugoshin in mammalian oocytes and somatic cells. Nature Cell Biology *10*, 42–52.

Li, Z., Aizenman, C.D., and Cline, H.T. (2002). Regulation of Rho GTPases by Crosstalk and Neuronal Activity In Vivo. Neuron *33*, 741–750.

Llano, E., Gómez, R., and Gutiérrez-Caballero, C. (2008). Shugoshin-2 is essential for the completion of meiosis but not for mitotic cell division in mice. Genes Dev. *22*, 2400–2413.

Loeb, J. (1899). On the nature of the process of fertilization and the artificial production of normal larvae (plutei) from the unfertilized eggs of the sea urchin. American Journal of Physiology *3*, 135–138.

Lohka, M.J. (1988). Purification of maturation-promoting factor, an intracellular regulator of early mitotic events. Proc. Natl. Acad. Sci. U.S.a. *85*, 3009–3013.

Lorca, T., Cruzalegui, F.H., Fesquet, D., Cavadore, J.-C., ry, J.M.E., Means, A., and e, M.D.E. (1993). Calmodulin-dependent protein kinase II mediates inactivation of MPF and CSF upon fertilization of Xenopus eggs. , Published Online: 18 November 1993; | Doi:10.1038/366270a0 *366*, 270–273.

Lutz, L.B., Kim, B., Jahani, D., and Hammes, S.R. (2000). G Protein βγ Subunits Inhibit Nongenomic Progesterone-induced Signaling and Maturation in Xenopus laevis Oocytes EVIDENCE FOR A RELEASE OF INHIBITION MECHANISM FOR CELL CYCLE PROGRESSION. J. Biol. Chem. *275*, 41512–41520.

Ma, C., Benink, H.A., Cheng, D., Montplaisir, V., Wang, L., Xi, Y., Zheng, P.-P., Bement, W.M., and Liu, X.J. (2006). Cdc42 Activation Couples Spindle Positioning to First Polar Body Formation in Oocyte Maturation. Current Biology *16*, 214–220.

Madgwick, S., Levasseur, M., and Jones, K.T. (2005). Calmodulin-dependent protein kinase II, and not protein kinase C, is sufficient for triggering cell-cycle resumption in mammalian eggs. J Cell Sci.

Mank, M., and Griesbeck, O. (2008). Genetically Encoded Calcium Indicators. Chem. Rev. *108*, 1550–1564.

Marston, A.L., Tham, W.-H., Shah, H., and Amon, A. (2004). A Genome-Wide Screen Identifies Genes Required for Centromeric Cohesion. Science *303*, 1367–1370.

Masui, Y., and Markert, C.L. (1971). Cytoplasmic control of nuclear behavior during meiotic maturation of frog oocytes. Journal of Experimental Zoology.

Mattila, P.K., and Lappalainen, P. (2008). Filopodia: molecular architecture and cellular functions. Nature Reviews Molecular Cell Biology *9*, 446–454.

Miao, Y.-L., Stein, P., Jefferson, W.N., Padilla-Banks, E., and Williams, C.J. (2012). Calcium influx-mediated signaling is required for complete mouse egg activation. Pnas *109*, 4169–4174.

Miller, A.L., Fluck, R.A., McLaughlin, J.A., and Jaffe, L.F. (1993). Calcium buffer injections inhibit cytokinesis in Xenopus eggs. J Cell Sci *106 (Pt 2)*, 523–534.

Miller, A.L. (2011). The contractile ring. Current Biology *21*, R976–R978.

Miyazaki, S.-I., and Igusa, Y. (1981). Fertilization potential in golden hamster eggs consists of recurring hyperpolarizations. , Published Online: 18 November 1993; | Doi:10.1038/366270a0 *290*, 702–704.

Morita, E., Sandrin, V., Chung, H.Y., Morham, S.G., Gygi, S.P., Rodesch, C.K., and Sundquist, W.I. (2007). Human ESCRT and ALIX proteins interact with proteins of the midbody and function in cytokinesis. The EMBO Journal *26*, 4215–4227.

Mozingo, N.M., and Chandler, D.E. (1991). Evidence for the existence of two assembly domains within the sea urchin fertilization envelope. Developmental Biology *146*, 148–157.

Mullins, J., and Biesele, J.J. (1977). Terminal phase of cytokinesis in D-98S cells. J Cell Biol *73*, 672–684.

Musacchio, A., and Salmon, E.D. (2007). The spindle-assembly checkpoint in space and time. Nature Reviews Molecular Cell Biology *8*, 379–393.

Muto, A., Kume, S., Inoue, T., Okano, H., and Mikoshiba, K. (1996). Calcium waves along the cleavage furrows in cleavage-stage Xenopus embryos and its inhibition by heparin. J Cell Biol *135*, 181–190.

Na, J., and Zernicka-Goetz, M. (2006). Asymmetric Positioning and Organization of the Meiotic Spindle of Mouse Oocytes Requires CDC42 Function. Current Biology *16*, 1249–1254.

Nebreda, A.R., Gannon, J.V., and Hunt, T. (1995). Newly synthesized protein(s) must associate with p34cdc2 to activate MAP kinase and MPF during progesterone-induced maturation of Xenopus oocytes. The EMBO Journal *14*, 5597–5607.

Nebreda, A.R., and Ferby, I. (2000). Regulation of the meiotic cell cycle in oocytes. Current Opinion in Cell Biology *12*, 666–675.

Noguchi, T., and Mabuchi, I. (2002). Localized Calcium Signals along the Cleavage Furrow of theXenopus Egg Are Not Involved in Cytokinesis. Mol. Biol. Cell.

Nuccitelli, R., Yim, D.L., and Smart, T. (1993). The Sperm-Induced Ca 2+ Wave Following Fertilization of the Xenopus Egg Requires the Production of Ins (1, 4, 5) P 3. Developmental Biology.

Oancea, E., and Meyer, T. (1998). Protein kinase C as a molecular machine for decoding calcium and diacylglycerol signals. Cell.

Ohan, N., Agazie, Y., Cummings, C., Booth, R., Bayaa, M., and Liu, X.J. (1999). RHO-associated protein kinase alpha potentiates insulin-induced MAP kinase activation in Xenopus oocytes. J Cell Sci *112*, 2177–2184.

Ohi, R., Burbank, K., Liu, Q., and Mitchison, T.J. (2007). Nonredundant Functions of Kinesin-13s during Meiotic Spindle Assembly. Current Biology *17*, 953–959.

Orth, M., Mayer, B., Rehm, K., Rothweiler, U., Heidmann, D., Holak, T.A., and Stemmann, O. (2011). Shugoshin is a Mad1/Cdc20-like interactor of Mad2. The EMBO Journal *30*, 2868–2880.

Parisi, S. (1999). Rec8p, a meiotic recombination and sister chromatid cohesion phosphoprotein of the Rad21p family conserved from fission yeast to humans. Mol. Cell. Biol. *19*, 3515–3528.

Parry, H., McDougall, A., and Whitaker, M. (2005). Microdomains bounded by endoplasmic reticulum segregate cell cycle calcium transients in syncytial Drosophila embryos. J Cell Biol.

Peter, M., Castro, A., Lorca, T., Le Peuch, C., Magnaghi-Jaulin, L., e, M.D.E., and eacute, J.-

C.L. (2001). The APC is dispensable for first meiotic anaphase in Xenopus oocytes. Nature Cell Biology *3*, 83–87.

Peters, J.M. (2006). The anaphase promoting complex/cyclosome: a machine designed to destroy. Nature Reviews Molecular Cell Biology.

Piekny, A.J., and Maddox, A.S. (2010). The myriad roles of Anillin during cytokinesis. Seminars in Cell & Developmental Biology.

Pielak, R.M., Gaysinskaya, V.A., and Cohen, W.D. (2004). Formation and function of the polar body contractile ring in Spisula. Developmental Biology *269*, 421–432.

Pincus, G. (1939). The comparative behavior of mammalian eggs in vivo and in vitro. IV. The development of fertilized and artificially activated rabbit eggs. Journal of Experimental Zoology *82*, 85–129.

Pines, J. (2006). Mitosis: a matter of getting rid of the right protein at the right time. Trends in Cell Biology *16*, 55–63.

Poenie, M., Alderton, J., Steinhardt, R., and Tsien, R. (1986). Calcium rises abruptly and briefly throughout the cell at the onset of anaphase. Science *233*, 886–889.

Poenie, M., Alderton, J., Tsien, R.Y., and Steinhardt, R.A. (1985). Changes of free calcium levels with stages of the cell division cycle. Nature *315*, 147–149.

Polanski, Z. (2012). Spindle assembly checkpoint regulation of chromosome segregation in mammalian oocytes. Reproduction, Fertility and Development *25*, 472–483.

Pollard, T.D., and Wu, J.-Q. (2010). Understanding cytokinesis: lessons from fission yeast. Nature Reviews Molecular Cell Biology *11*, 149–155.

Rabitsch, K.P., Gregan, J., Schleiffer, A., Javerzat, J.-P., Eisenhaber, F., and Nasmyth, K. (2004). Two Fission Yeast Homologs of Drosophila Mei-S332 Are Required for Chromosome Segregation during Meiosis I and II. Current Biology *14*, 287–301.

Rappaport, R., and Rappaport, B.N. (1974). Establishment of cleavage furrows by the mitotic spindle. Journal of Experimental Zoology *189*, 189–196.

Ratan, R.R., and Shelanski, M.L. (1986). Transition from metaphase to anaphase is accompanied by local changes in cytoplasmic free calcium in Pt K2 kidney epithelial cells.

Rieder, C.L., Cole, R.W., Khodjakov, A., and Sluder, G. (1995). The checkpoint delaying anaphase in response to chromosome monoorientation is mediated by an inhibitory signal produced by unattached kinetochores. J Cell Biol *130*, 941–948.

Rieder, C.L., Schultz, A., Cole, R., and Sluder, G. (1994). Anaphase onset in vertebrate somatic cells is controlled by a checkpoint that monitors sister kinetochore attachment to the spindle. J Cell Biol *127*, 1301–1310.

Rivera, T., and Losada, A. (2009). Shugoshin regulates cohesion by driving relocalization of PP2A in Xenopus extracts. Chromosoma *118*, 223–233.

Rivera, T., Ghenoiu, C., guez-Corsino, M.R.I., Mochida, S., Funabiki, H., and Losada, A. (2012). Xenopus Shugoshin 2 regulates the spindle assembly pathway mediated by the chromosomal passenger complex. The EMBO Journal *31*, 1467–1479.

Roy, L.M., Swenson, K.I., Walker, D.H., Gabrielli, B.G., Li, R.S., Piwnica-Worms, H., and Maller, J.L. (1991). Activation of p34cdc2 kinase by cyclin A. J Cell Biol *113*, 507–514.

Rumpf, C., Cipak, L., Dudas, A., Benko, Z., Pozgajova, M., Riedel, C.G., Ammerer, G., Mechtler, K., and Gregan, J. (2010). Casein kinase 1 is required for efficient removal of Rec8 during meiosis I. Cell Cycle *9*, 2655–2660.

Sagata, N. (1996). Meiotic metaphase arrest in animal oocytes: its mechanisms and biological significance. Trends in Cell Biology *6*, 22–28.

Saunders, C.M., Larman, M.G., Parrington, J., Cox, L.J., Royse, J., Blayney, L.M., Swann, K., and Lai, F.A. (2002). PLC zeta: a sperm-specific trigger of Ca(2+) oscillations in eggs and embryo development. Development *129*, 3533–3544.

Saurin, A.T., Durgan, J., Cameron, A.J., Faisal, A., Marber, M.S., and Parker, P.J. (2008). The regulated assembly of a PKC epsilon complex controls the completion of cytokinesis. Nature Cell Biology *10*, 891–901.

Schmidt, A., Duncan, P.I., Rauh, N.R., and Sauer, G. (2005). Xenopus polo-like kinase Plx1 regulates XErp1, a novel inhibitor of APC/C activity. Genes & ….

Shao, H., Li, R., Ma, C., Chen, E., and Liu, X.J. (2013). Xenopus oocyte meiosis lacks spindle assembly checkpoint control. J Cell Biol *201*, 191–200.

Shao, H., Ma, C., Zhang, X., Li, R., Miller, A.L., Bement, W.M., and Liu, X.J. (2012). Aurora B regulates spindle bipolarity in meiosis in vertebrate oocytes. Cell Cycle *11*, 2672–2680.

Sheng, Y., Tiberi, M., Booth, R.A., Ma, C., and Liu, X.J. (2001). Regulation of Xenopus oocyte meiosis arrest by G protein βγ subunits. Current Biology *11*, 405–416.

Shoji, S., Yoshida, N., Amanai, M., Ohgishi, M., Fukui, T., Fujimoto, S., Nakano, Y., Kajikawa, E., and Perry, A.C.F. (2006). Mammalian Emi2 mediates cytostatic arrest and transduces the signal for meiotic exit via Cdc20. The EMBO Journal *25*, 834–845.

Snow, P., and Nuccitelli, R. (1993). Calcium buffer injections delay cleavage in Xenopus laevis blastomeres. J Cell Biol *122*, 387–394.

Sokac, A.M., Co, C., Taunton, J., and Bement, W. (2003). Cdc42-dependent actin polymerization during compensatory endocytosis in Xenopus eggs. Nature Cell Biology *5*, 727–732.

Speksnijder, J.E., Miller, A.L., Weisenseel, M.H., Chen, T.H., and Jaffe, L.F. (1989). Calcium buffer injections block fucoid egg development by facilitating calcium diffusion. Proc. Natl. Acad. Sci. U.S.a. *86*, 6607–6611.

Sun, L., and Machaca, K. (2004). Ca(2+)(cyt) negatively regulates the initiation of oocyte maturation. J Cell Biol *165*, 63–75.

Sun, S.-C., Wang, Z.-B., Xu, Y.-N., Lee, S.-E., Cui, X.-S., and Kim, N.-H. (2011). Arp2/3 Complex Regulates Asymmetric Division and Cytokinesis in Mouse Oocytes. PLoS ONE *6*, e18392.

Swann, K., and Ozil, J.-P. (1994). Dynamics of the Calcium Signal That Triggers Mammalian Egg Activation. In International Review of Cytology, (Elsevier), pp. 183–222.

Swenson, K.I., Farrell, K.M., and Ruderman, J.V. (1986). The clam embryo protein cyclin A induces entry into M phase and the resumption of meiosis in Xenopus oocytes. Cell *47*, 861–870.

Taieb, F.E., Taieb, F.E., Gross, S.D., Gross, S.D., Lewellyn, A.L., and Maller, J.L. (2001). Activation of the anaphase-promoting complex and degradation of cyclin B is not required for progression from Meiosis I to II in Xenopus oocytes. Current Biology *11*, 508–513.

Tarkowski, A.K., WITKOWSKA, A., and NOWICKA, J. (1970). Experimental Parthenogenesis in the Mouse. , Published Online: 18 November 1993; | Doi:10.1038/366270a0 *226*, 162–165.

Thibault, C. (1949). L'oeuf des mammiferes: son development parthenogenetique. Annls Sci Nat *11*, 133–219.

Tombes, R.M., Simerly, C., Borisy, G.G., and Schatten, G. (1992). Meiosis, egg activation, and nuclear envelope breakdown are differentially reliant on Ca2+, whereas germinal vesicle breakdown is Ca2+ independent in the mouse oocyte. J Cell Biol *117*, 799–811.

Tung, J.J., and Jackson, P.K. (2005). Emi1 class of proteins regulate entry into meiosis and the meiosis I to meiosis II transition in Xenopus oocytes. Cell Cycle.

Tung, J.J., Hansen, D.V., Ban, K.H., Loktev, A.V., Summers, M.K., Adler, J.R., III, and Jackson, P.K. (2005). A role for the anaphase-promoting complex inhibitor Emi2/XErp1, a homolog of early mitotic inhibitor 1, in cytostatic factor arrest of Xenopus eggs. Proc. Natl. Acad. Sci. U.S.a. *102*, 4318–4323.

Tunquist, B.J., and Maller, J.L. (2003). Under arrest: cytostatic factor (CSF)-mediated metaphase arrest in vertebrate eggs. Genes Dev. *17*, 683–710.

Tunquist, B.J., Eyers, P.A., Chen, L.G., Lewellyn, A.L., and Maller, J.L. (2003). Spindle checkpoint proteins Mad1 and Mad2 are required for cytostatic factor-mediated metaphase arrest. J Cell Biol *163*, 1231–1242.

Vacquier, V.D., Tegner, M.J., and Epel, D. (1973). Protease released from sea urchin eggs at fertilization alters the vitelline layer and aids in preventing polyspermy. Experimental Cell Research *80*, 111–119.

Vavylonis, D., Wu, J.-Q., O'Shaughnessy, B., and Pollard, T.D. (2008). Assembly mechanism of the contractile ring for cytokinesis by fission yeast. Science *319*, 97–100.

Wagner, J., Fall, C.P., Hong, F., Sims, C.E., Allbritton, N.L., Fontanilla, R.A., Moraru, I.I., Loew, L.M., and Nuccitelli, R. (2004). A wave of IP3 production accompanies the fertilization Ca2+ wave in the egg of the frog, Xenopus laevis: theoretical and experimental support. Cell Calcium *35*, 433–447.

Wang, J. (2003). A G protein-coupled receptor kinase induces Xenopus oocyte maturation. J. Biol. Chem. *278*, 15809–15814.

Wang, J., and Liu, X.J. (2004). Progesterone inhibits protein kinase A (PKA) in Xenopus oocytes: demonstration of endogenous PKA activities using an expressed substrate. J Cell Sci *117*, 5107–5116.

Wang, Z.-B., Jiang, Z.-Z., Zhang, Q.-H., Hu, M.-W., Huang, L., Ou, X.-H., Guo, L., Ouyang, Y.-C., Hou, Y., Brakebusch, C., et al. (2013). Specific deletion of Cdc42 does not affect meiotic spindle organization/migration and homologous chromosome segregation, but disrupts polarity establishment and cytokinesis in mouse oocyte. Mol. Biol. Cell mbc.E13–03–0123.

Wassmann, K. (2013). Sister chromatid segregation in meiosis II: Deprotection through phosphorylation. Cell Cycle *12*, 1352–1359.

Watanabe, Y. (2005). Shugoshin: guardian spirit at the centromere. Current Opinion in Cell Biology *17*, 590–595.

Wilding, M., Wright, E.M., Patel, R., Ellis-Davies, G., and Whitaker, M. (1996). Local perinuclear calcium signals associated with mitosis-entry in early sea urchin embryos. J Cell Biol *135*, 191–199.

Xu, H., Beasley, M.D., Warren, W.D., van der Horst, G.T.J., and McKay, M.J. (2005). Absence of Mouse REC8 Cohesin Promotes Synapsis of Sister Chromatids in Meiosis. Developmental Cell *8*, 949–961.

Yang, G., Cameron, L.A., Maddox, P.S., Salmon, E.D., and Danuser, G. (2008). Regional variation of microtubule flux reveals microtubule organization in the metaphase meiotic spindle. J Cell Biol *182*, 631–639.

Yu, H.-Y.E., and Bement, W.M. (2007). Control of local actin assembly by membrane fusion-dependent compartment mixing. Nature Cell Biology *9*, 149–159.

Zhang, X., Ma, C., Miller, A.L., Katbi, H.A., Bement, W.M., and Liu, X.J. (2008). Polar Body Emission Requires a RhoA Contractile Ring and Cdc42-Mediated Membrane

Protrusion. Developmental Cell *15*, 386–400.

Zou, H., McGarry, T.J., Bernal, T., and Kirschner, M.W. (1999). Identification of a vertebrate sister-chromatid separation inhibitor involved in transformation and tumorigenesis. Science *285*, 418–422.

CURRICULUM VITAE

Education

Sept 2008- Dec 2013	PhD in Biochemistry University of Ottawa, Department of Biochemistry, Microbiology and Immunology "Calcium Signaling during Polar Body Emission in the *Xenopus laevis* Oocyte"
Sept 2004- June 2008	B.Sc. with specialization in Biochemistry University of Ottawa

Awards

May 2010- Dec 2013	Admission Scholarship, University of Ottawa
Sept 2007-May 2008	Dean's Honour List, University of Ottawa

Publications

2014	Leblanc, J.; Li, R.; Bement, W.; Liu, J. "A calcium transient is required for polar body abscission". (to be submitted soon)
2011	Leblanc, J. et al. "The small GTPase Cdc42 promotes membrane protrusion during polar body emission via ARP2-nucleated actin polymerization". Mol. Hum. Reprod. 17(5). 305-316.

Experience

Aug-Sept 2012	Peer review of manuscripts for the journal "Molecular Human Reproduction"

Presentations

1) University of Ottawa - Faculty of Medicine- Biochemistry, Microbiology and Immunology Department- Graduate Student Seminar Symposium- March 11th 2013
2) Ottawa Hospital Research Institute- Work In Progress Seminar- Reproduction Section- January 16th 2013
3) Ottawa Hospital Research Institute Research Day (poster)- November 15th 2012

4) University of Ottawa - Faculty of Medicine- Biochemistry, Microbiology and Immunology Department- Graduate Student Poster Day- May 17th 2012
5) Ottawa Hospital Research Institute- Work In Progress Seminar- Reproduction Section- April 18th 2012
6) Ottawa Hospital Research Institute Research Day (poster)- November 18th 2010
7) Ottawa Hospital Research Institute- Work In Progress Seminar- Reproduction Section- April 14th 2010
8) University of Ottawa - Faculty of Medicine- Biochemistry, Microbiology and Immunology Department- Graduate Student Seminar Symposium- February 17th 2010
9) Ottawa Hospital Research Institute- Reproductive Biology Workshop (poster)- 2009
10) University of Ottawa - Faculty of Medicine- Biochemistry, Microbiology and Immunology Department- Graduate Student Poster Day- May 21st 2009
11) Ottawa Hospital Research Institute- Work In Progress Seminar- Reproduction Section- December 17th 2008
12) Ottawa Hospital Research Institute- Ottawa Hospital Research Institute Research Day (poster)- 2008